THE

LONDON, EDINBURGH, AND DUBLIN

PHILOSOPHICAL MAGAZINE

AND

JOURNAL OF SCIENCE.

[SEVENTH SERIES.]

JUNE 1934.

XCII. *Streamline and Turbulent Flow in Open Channels.*

By J. ALLEN, *M.Sc., Assoc. M.Inst.C.E., of the University, Manchester* *.

1. INTRODUCTION.

THE equation of flow in an open channel is generally assumed to be

$$\frac{dh}{dl} = \frac{v}{g} \cdot \frac{dv}{dl} + \frac{f \cdot v^2}{2g} \cdot \frac{1}{m},$$

where h=depth of stream,

l=length,

v=mean velocity at a given cross-section,

m=hydraulic mean depth at a given cross-section (*i. e.*, area of cross-section divided by wetted perimeter),

f=a coefficient.

Many experimenters have suggested formulæ to express the variation of the coefficient, f, or of C in Chezy's equation for uniform flow, $v = C\sqrt{mi}$, where $C^2 = \frac{2g}{f}$, with the slope i, the dimensions of the channel, and the condition of its surface.

* Communicated by Prof. A. H. Gibson, D.Sc., M.Inst.C.E., M.I.Mech.E.

Their formulæ in general have no rational basis, although it is true that certain of them are used and found to be adequate, in suitable circumstances, in engineering practice.

There is, for example, the expression due to Bazin, viz.,

$$C=\frac{157{\cdot}6}{1+\frac{N}{\sqrt{m}}},$$

where N varies with the character of the surface and in which foot units are employed.

Again, Ganguillet and Kutter attempted to connect the resistance with the slope as well as with the nature of the surfaces in their formula

$$C=\frac{41{\cdot}6+\frac{{\cdot}00281}{i}+\frac{1{\cdot}8112}{N}}{1+\left(41{\cdot}6+\frac{{\cdot}00281}{i}\right)\frac{N}{\sqrt{m}}}\text{ in foot units,}$$

while others, such as Thrupp *, Fidler †, and Barnes ‡, have offered "exponential formulæ" for uniform flow which, in effect, assume that $v=\alpha\,.\,m^{\beta}i^{\gamma}$, instead of the simple Chezy equation, $v=C\sqrt{mi}$. Thrupp also made β a function of m, and all three have treated α, β, γ as dependent on the nature of the surfaces.

No doubt the difficulty of accurately measuring the friction losses in channels has retarded the progress of researches towards placing the phenomenon on a more rational basis, as has been to a large extent established, with the aid of the principle of dynamical similarity, in pipe-flow.

Again, such investigations as have been previously undertaken have usually been on channels of large dimensions §, and in the range of turbulent flow. The increasing tendency to adopt the method of model experiments as a means of investigating large-scale problems

* Trans. Soc. of Engineers, 1887, p. 224.

† 'Calculations in Hydraulic Engineering,' vol. ii. p. 67.

‡ 'Hydraulic Flow Reviewed,' p. 11.

§ Certain of Darcy and Bazin's experiments, however, were performed on a channel only 3·94 inches wide. The results, together with other of their classic tests, reported in 'Recherches Hydrauliques,' 1865, are discussed in Section 5 *c* (i.) of the present paper.

in engineering appears to demand research on the loss of head due to friction in the flow of water along channels of *small* cross-section.

Moreover, so far as the author is aware there is an absence of reliable data regarding the critical velocity in open channels, the tacit assumption being often made that such critical velocity would occur at approximately the same value of $\frac{vm}{\nu}$ (ν being the kinematic viscosity of the fluid) as in pipe-flow.

2. Apparatus and Method of Procedure.

The present experiments were carried out with the apparatus shown in fig. 1, a length of 32·18 inches

Fig. 1.

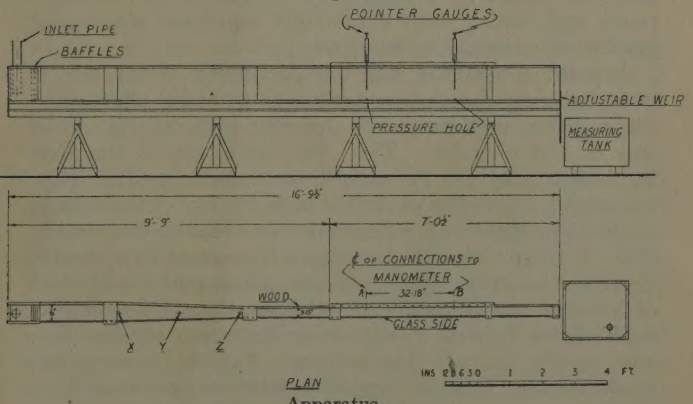

Apparatus.

(81·7 cm.) of a rectangular channel approximately 3·15* inches (8·00 cm.) wide being utilized as the portion for measurement of resistance.

One side was made of planed pine-wood painted white, the other of plate-glass. The bed was of planed pine-wood saturated with paraffin-wax. In this state therefore the channel was as smooth as it could reasonably be made.

* Owing to taking the apparatus to pieces and reassembling for various conditions of test the width varied slightly in different tests; repeated measurements were made by means of callipers to determine its magnitude for any given test.

The bed was first made as level as practicable with the aid of a spirit-level ; its actual slope in any experiment was determined by means of calibrated pointer gauges fitted with vernier scales reading to $\pm$·0025″, these being read in contact with a static water surface and with the bed in turn. The bed-slope never exceeded 0·02 inch in the 32·18 inches gauge-length. Water was supplied under a sensibly constant head from an elevated tank.

For measurement of the depth of the water at the upstream gauge-point, A, the pointer gauge was used ; the depth at B was calculated from the known difference in bed-level together with the observed fall in the water surface.

The depth could be readily adjusted by means of a rectangular weir-plate at the outlet end of the channel, and the discharge obtained by collecting in calibrated tanks and timing with a carefully regulated stop-watch graduated in tenths of a second.

A point considered was the possibility of the loss of head between the chosen gauge-points being affected by the position and shape of the weir-plate at the outlet end of the channel. This was investigated therefore by substituting for the simple rectangular weir a plate containing a number of drilled holes. Any of these holes could be plugged with corks, and it was readily practicable, with a given rate of discharge, to maintain a desired depth of water at the upstream gauge-point with each of various arrangements of holes in the outlet-plate or with water flowing partly over the crest of the plate and partly through the orifices. Typical observations made in this manner, under widely varying conditions at the outlet, gave (within the range of depth and velocity of any of the experiments quoted in this paper) sensibly the same value of the loss of head between the two gauge-points, and it was therefore decided to control the upstream depth simply by a rectangular weir-plate.

The water temperature was measured by means of a calibrated mercury thermometer placed near the inlet, and this temperature used to obtain the kinematic viscosity of the water according to the data given in ' Hydraulics and its Applications ' by Prof. A. H. Gibson (third edition).

No attempt was made to control the water temperature ; thus in the experiments of Series 1 *a* to be discussed later,

the limits of the flowing water temperature were 7·8 and 15·6° C., due to seasonal changes.

Measurements of the fall in the water surface were made by means of a differential pressure-gauge, having toluene * as its upper fluid and its limbs connected to holes in the side of the channel.

This gauge was place on a plane inclined at an angle, α, to the horizontal, determined by means of a tested inclinometer. The plane used was the table of a travelling vernier microscope reading to 0·01 millimetre, and the temperature of the gauge was read directly on a mercury thermometer in contact with it at the time of observing the position of the menisci in the limbs of the gauge.

The magnification of such a gauge is

$$\frac{1}{(\rho-\sigma)\sin\alpha},$$

where ρ is the specific gravity of water and σ of toluene at the given temperature. If α is 8·4°, as commonly adopted in these tests, and $(\rho-\sigma)$ is 0·125, as assumed for a temperature of 50° F., the magnification becomes 54·7 : 1†.

Special precautions were taken in using the differential gauge. The gauge was kept scrupulously clean and great care was observed to expel any air from the flexible connexions between the gauge and the channel. The connexions in the channel were made flush with the side and were drilled approximately $\frac{1}{4}$ inch above the bed.

The difference of pressure registered by the differential gauge would only represent the fall in level of the water surface between the two gauge-points if there were no acceleration perpendicular to the orifice.

A typical set of observations repeated with three pressure holes in the bed at A and B, equally spaced transversely across the channel and connected together before coupling to the limbs of the inclined toluene gauge, gave results agreeing with those obtained with single pressure holes in the side. Accordingly the simpler arrangement of connecting the gauge to the side of the channel in the manner described above was used throughout the investigation.

* The toluene was faintly coloured with dissolved dye, to facilitate readings.

† The values adopted for ρ and σ were obtained from International Critical Tables, vol. iii.

It was found that, in taking the reading of the loss of head for any discharge, approximately 40 minutes was necessary to allow the menisci to take up their final position. For every test up to $\frac{vm}{\nu}=2750$ the static reading of the gauge was taken both before and after the discharge reading, the procedure being equivalent to treating each set of readings by itself as regards the static readings before and after the experiment. Above $\frac{vm}{\nu}=2750$ such differences as were observed in the static readings would have no appreciable effect upon the determination of the frictional resistance.

Such variations as occurred from time to time in the static difference between the two limbs (usually of the order of 0·150 cm.) were attributed to slight changes in the clamping of the gauge to its table at various times, resulting in different *transverse* inclinations, and to temperature and total pressure variations in the gauge.

Furthermore it was found that, provided the gauge was clean and leakage eliminated, the movements of the menisci from their static positions were very nearly the same, indicating that the bore of the tube and the shape of the menisci were sensibly constant. Whenever the movements were not identical within the limits of interpretation of the vernier or the menisci showed signs of not moving freely the gauge was removed and cleaned.

The smallest loss of head measured in this way in any of the tests was $0{\cdot}0018_2$ mm., giving a reading of some 0·10 mm. on the differential gauge. This was at $\frac{vm}{\nu}=220$ for $m=0{\cdot}104$ feet, or 3·17 cm.

In working out the value of f, or $\frac{2\mathrm{R}}{\rho v^2}$,

where R = resistance per unit area of wall surface,

ρ = density of water,

the velocity at A (v_A) was first calculated from the measured discharge, width and depth as shown on the pointer. Next v_B, using the measured width at B, together with the level of the bed relative to A and the observed loss of head. The term $\frac{v_B^2-v_A^2}{2g}$ gave the loss of head

due to acceleration *, which was subtracted from the observed loss of head, δh, while the average of m_A and m_B was used for m, and $\frac{v_A^2+v_B^2}{2}$ for $\bar{v}^2$ in

$$f=\frac{\left(\delta h-\frac{v_B^2-v_A^2}{2g}\right)2gm}{lv^2}.$$

3. Summary of Conditions under which Experiments were Performed.

Three main series of tests have been carried out—the first with the channel in its smooth state as described in Section 2, the second with the bed roughened, and the third with both the bed and the sides of the channel roughened.

The method adopted for roughening the surface was the application of a coat of white paint intermixed with Leighton Buzzard sand. This sand had been screened through a 20-mesh sieve (nominal opening 0·0336 inch) and retained on a 30-mesh sieve (nominal opening 0·0232 inch). The bed so roughened was 0·03 inch higher than the uncoated bed, while the effective width of the channel with roughened sides was taken to be that with smooth sides less 0·06 inch.

Great care was observed to provide as even a distribution of roughness as possible, and a clear space of the original smooth side was left round the pressure holes.

Each of the three main series was performed over a certain range of $\frac{vm}{\nu}$ found to include the critical value, with three different entry conditions, as detailed below :—

(*a*) With the simple convergent entrance as shown in fig. 1.

* It is here assumed that at a given section the kinetic energy is $\frac{A\rho v^3}{2g}$ (per second), where A is the area and v the mean velocity, instead of $\int\frac{\rho u^3 dA}{2g}$, where u is the velocity of the stream through an element δA.

In Appendix A it is shown that the error in the estimate of f, due to this assumption, does not exceed 1·5 per cent. in the worst case in the present experiments.

(*b*) With a number of helical coils standing with their axes vertical in the approach channel between the points labelled X and Y in fig. 1.

(*c*) With additional obstructions introduced at the point Z (see fig. 1).

The experiments are accordingly referred to as :—

Series 1 *a*.—Smooth sides, smooth bed.

,, 1 *b*.—Smooth sides, smooth bed, with obstructions in the approach channel to promote eddy formation.

,, 1 *c*.—Smooth sides, smooth bed, with additional obstructions in approach channel.

Series 2 *a*.—As Series 1 *a*, but with smooth sides, rough bed.

,, 2 *b*.— ,, ,, 1 *b*, ,, ,, ,, ,, ,,

,, 2 *c*.— ,, ,, 1 *c*, ,, ,, ,, ,, ,,

Series 3 *a*.—As Series 1 *a*, but with rough sides, rough bed.

,, 3 *b*.— ,, ,, 1 *b*, ,, ,, ,, ,, ,, ,,

,, 3 *c*.— ,, ,, 1 *c*, ,, ,, ,, ,, ,, ,,

4. Method of Exhibiting Results.

The principal results of the experiments are summarized in the following diagrams (figs. 2–10) :—

Fig. 2.

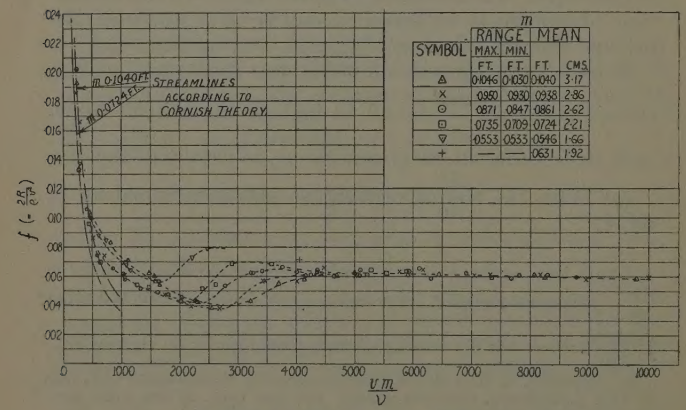

Series 1 *a*, *f* plotted against *vm*/*ν*.

Fig. 3.

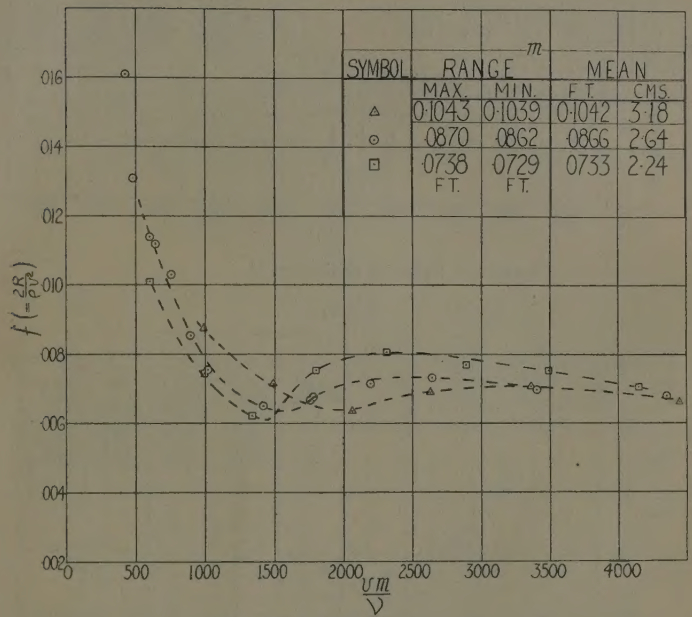

Series 1 *b*, *f* plotted against *vm*/*v*.

Fig. 4.

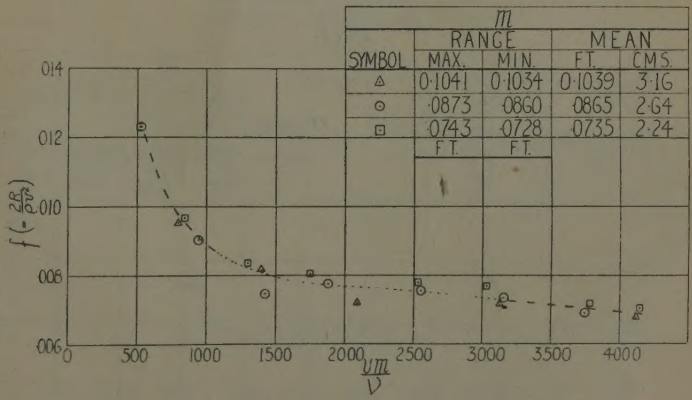

Series 1 *c*, *f* plotted against *vm*/*v*.

Fig. 5.

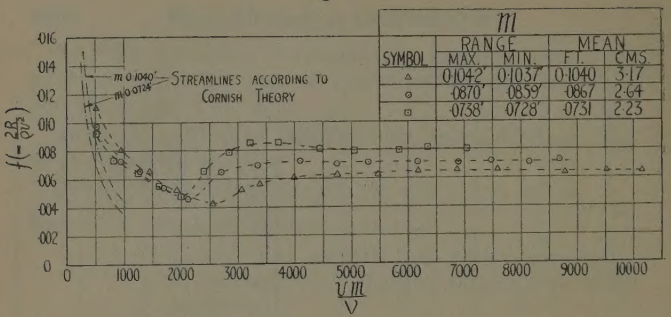

Series 2 *a*, *f* plotted against *vm*/*ν*.

Fig. 6.

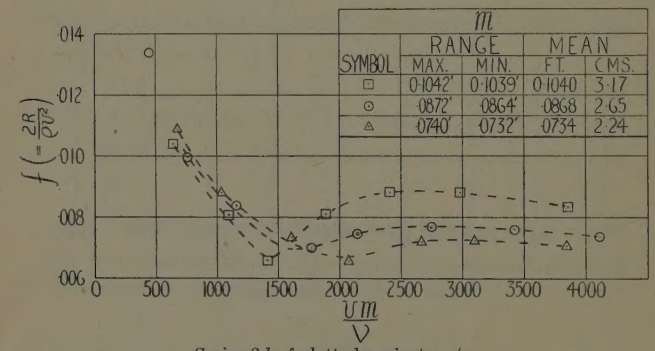

Series 2 *b*, *f* plotted against *vm*/*ν*.

Fig. 7.

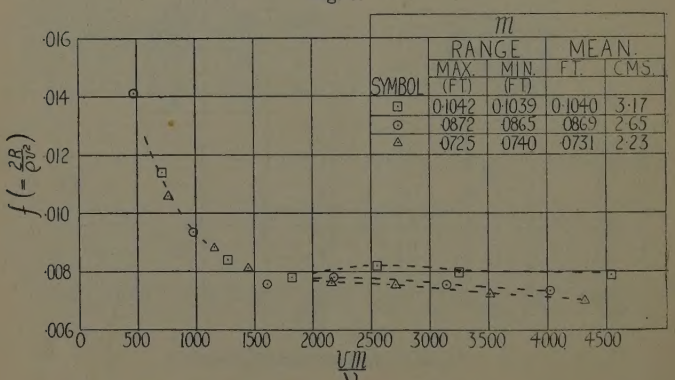

Series 2 *c*, *f* plotted against *vm*/*ν*.

Fig. 8.

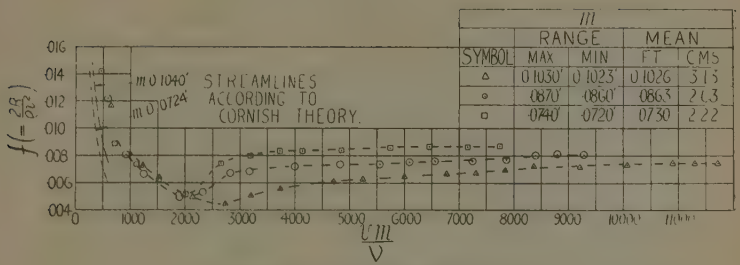

Series 3 *a*, *f* plotted against vm/ν.

Fig. 9.

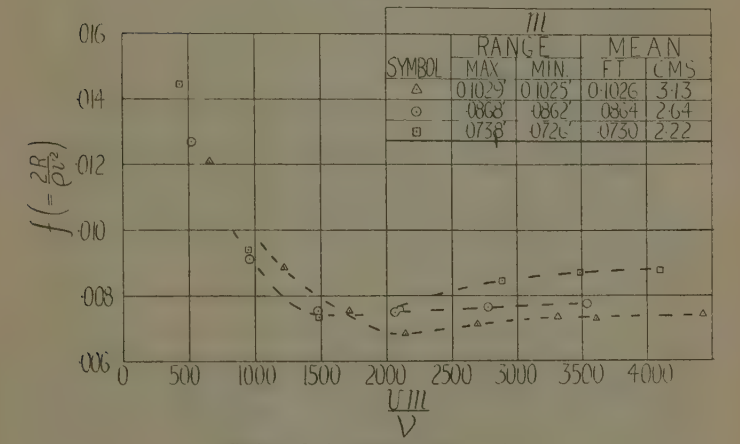

Series 3 *b*, *f* plotted against vm/ν.

Fig. 10.

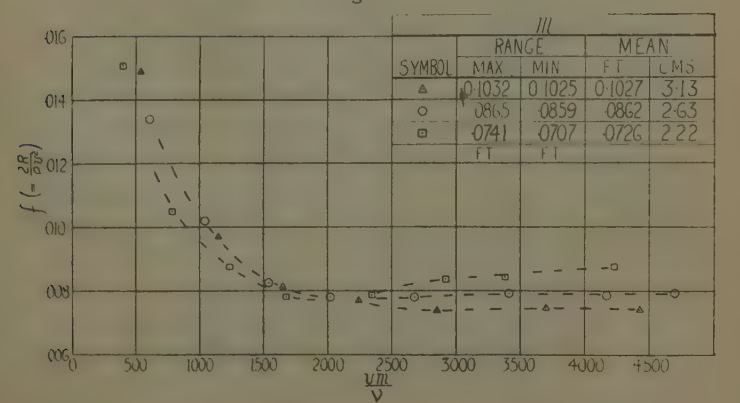

Series 3 *c*, *f* plotted against vm/ν.

Reference to these, as well as to other diagrams illustrating special features of the results, will be made in the discussion forming the body of the paper.

The method of plotting direct values instead of logarithms has been adopted as showing the results of the present investigation more graphically—*i. e.*, to avoid the "telescoping" of the values which apply to the region of turbulent flow.

Owing to the large number of observations made tables of detailed results are omitted, but a typical observation sheet is given in Appendix B.

5. Discussion of Results.

(A) *Critical Velocity.*

(i.) *With the Simple Convergent Approach Channel.*

Examination of figs. 2, 5, and 8 shows that the minimum value of f occurs at different values of $\frac{vm}{\nu}$ for different hydraulic mean depths, as summarized in Tables I., II., and III. below :—

Table I.

Series 1 *a*.

m. feet.	*m*. cm.	Minimum f occurs at vm/ν.
0·1040	3·17	2800
·0938	2·86	2700
·0861	2·62	2400
·0724	2·21	2150
·0546	1·66	1700

Table II.

Series 2 *a*.

m. feet.	*m*. cm.	Minimum f occurs at vm/ν.
0·1040	3·17	2600
·0867	2·64	2150
·0731	2·23	2000

TABLE III.

Series 3 *a*.

m.		Minimum *f* occurs at
feet.	cm.	vm/ν.
0·1026	3·13	2600
·0863	2·63	2000
·0730	2·22	1880

The critical velocities implied by these tables must, however, be regarded as "higher" critical velocities, since the convergent form of the approach channel reduces the tendency to the creation of eddies in the stream entering the experimental portion. The stabilizing influence of the approach channel, indeed, increases with increasing depth of the stream, for the convergence, defined as the ratio of the hydraulic mean depths at the entrance and exit of the approach channel, increases. This latter effect is borne out by the observed rise in the critical value of $\frac{vm}{\nu}$ as the stream is deepened.

The transition from approximate laminar flow to turbulence, then, is seen to depend essentially upon the entry conditions, as, indeed, has been demonstrated for pipe-flow by many investigators, notably Davies and White * (who found it to be the case up to a ratio of 54 : 1 of length of approach to depth of pipe) and Schiller †.

Again, Ekman ‡, using Reynolds's original form of pipe apparatus, found it possible by careful reduction of inlet disturbance to maintain a colour band at values of Reynolds's number three to four times as great as found by Reynolds himself, while Gibson § has measured the relatively high critical velocities in flow through converging tubes.

A recent investigation by Engel ‖, using a "venturi flume," is of great interest also in connexion with the

* Proc. Roy. Soc. A, cxix. p. 95 (1928).
† *Z. f. ang. Math. u. Mech.* 1921, p. 436.
‡ *Arkiv. Mat. Astron. och Fysik*, Bd. vi. (1910).
§ Proc. Roy. Soc. A, lxxxiii. p. 376 (1910).
‖ 'The Engineer,' April 21, 1933, p. 392.

present tests. He notes that " in spite of the Reynolds' numbers in the channel upstream of the venturi flume being more than ten times the critical value, the coefficients of discharge plotted against the Reynolds' number show the typical characteristic of the laminar range," and this he attributes to the convergent mouth of the venturi.

Another feature of the results summarized in Tables I., II., and III. is the lowering of the corresponding " higher " critical values of $\frac{vm}{\nu}$ by roughening the bed and sides of the channel.

(ii.) *Examination of the Flow by means of Colour Bands.*

The flow has been studied visually by means of a fine stream of aniline dye issuing from a glass capillary tube of outside diameter approximately 1/16 inch bent to the shape of an L, with the horizontal limb parallel to the axis of the channel.

With the tube situated halfway along the convergent approach channel and at one-quarter depth of the channel, for $m = 0{\cdot}107$ feet, it was possible to maintain an unbroken thread throughout up to a value of $\frac{vm}{\nu} = 1750$, although at all but very low velocities the thread was undulating or oscillating in a vertical plane with a general tendency to droop towards half-depth. At 1980 $\frac{vm}{\nu}$ the first signs of " corkscrew " motion or " scrawl " were observed. With a smaller depth, giving $m = 0{\cdot}0308$ feet, the " scrawl " or eddy breakdown was first observed at $\frac{vm}{\nu} = 1100$. These observations, while providing an interesting and important confirmation of the change of flow within the region of the transition curve determined by loss of head, would in all probability indicate an artificially low point of breakdown, as it was found extremely difficult to eliminate external vibrations.

(iii.) *Critical Velocity with Eddy Formation in the Approach Channel.*

These experiments were designed to determine the " lower " or true critical velocity, and it will be seen

from fig. 3 that the first obstructions to be introduced in the approach channel for the purpose of inducing eddies in the channel with smooth sides and smooth bed have the effect of reducing the apparent critical $\frac{vm}{\nu}$ to about 2000 in the case of $m=0{\cdot}1042$ feet, to 1600 for $m=0{\cdot}0866$ feet and to 1450 for $m=0{\cdot}0733$ feet. Correspondingly the maximum "f" following "transition" is raised, although once turbulent flow is established the conditions of series 1 *b* rapidly revert towards those of series 1 *a*. Again, in the critical region, the points plotted on fig. 3 are seen to be approaching more closely to one curve than those of fig. 2.

With additional obstructions as used for the tests of series 1 *c* all the points are brought within a fairly close band (see fig. 4), and there is no well-defined critical point in the accepted sense. The conditions are comparable in general effect with those of Davies and White's thin rectangular pipes, series 8 and 9 *.

It is of interest to note that the curve in fig. 4 does not rise as high as for m 0·0733 feet in series 1 *b* (fig. 3), an effect which reappears in the tests with roughened bed.

The whole results of series 1 *a*, *b*, and *c* indicate that the true "lower critical velocity" is in the region of $\frac{vm}{\nu}=1400$, while inspection of figs. 6, 7, and 9, 10 shows that this conclusion also applies very closely to the channel with roughened bed or with roughened bed and sides.

Now the value of 1400 for the "lower" critical $\frac{vm}{\nu}$ is some 2·4 times as great as that obtained by Stanton and Pannell † for smooth circular pipes. Similarly it is approximately 2·4 times as great as that determined by Cornish ‡ in his experiments with rectangular pipes, and about 1·9 times the value given by Davies and White § for rectangular pipes in which the width is large compared with the depth.

Some such conclusion would be anticipated from

* Proc. Roy. Soc. A, cxix. p. 97 (1928).
† Phil. Trans. Roy. Soc. A, ccxiv. p. 199 (1914).
‡ Proc. Roy. Soc. A, cxx. fig. 2, p. 694 (1928).
§ Proc. Roy. Soc. A, cxix. p. 95 (1928).

Reynolds' view *, viz., that free (exposed to air) surfaces promote or favour stability.

(B) *The Equation of Laminar Flow.*

The equation of laminar flow for open channels has been calculated by Cornish † on the assumption that the velocity gradient at the surface, perpendicular to the surface, is zero.

His equation, with the numerical substitutions appropriate to the present tests, shows that

$$\text{if} \qquad \frac{f}{2} = \frac{R}{\rho \cdot v^2} = K \cdot \frac{\nu}{vm},$$

K has the value 2·24 for $m =$ ·1040 feet.
2·06 ,, ,, = ·0938 ,,
1·92 ,, ,, = ·0861 ,,
1·79 ,, ,, = ·0724 ,,
1·80 ,, ,, = ·0546 ,,

The corresponding curves for $m = 0{\cdot}1040$ and $m = 0{\cdot}0724$ feet have been indicated on fig. 2, from which it will be seen that there is reasonable agreement with the observed values for $\frac{vm}{\nu}$ up to about 300.

The subsequent departure from the Cornish lines is not in its earlier stages due to the formation of eddies, but to one or more of the following effects :—

(*a*) The possibility that the filament of maximum velocity is not situated in the surface. This is certainly the case for fairly high velocities and big depths, when, as shown by pitometer readings, it may occur at 0·3 of the depth, below the surface, but there is no evidence to show how far the phenomenon persists as the discharge is decreased.

Using Cornish's notation for a rectangular pipe, of width $2a$ and depth $2b$,

$$w = -\frac{32\tau b^2}{\pi^3}\left\{\frac{\cosh(\pi x/2b)}{\cosh(\pi a/2b)}\cos\frac{\pi y}{2b} - \frac{1}{3^3}\frac{\cosh(3\pi x/2b)}{\cosh(3\pi a/2b)}\cos\frac{3\pi y}{2b} + \ldots\ldots\right\} + \tau(b^2 - y^2).$$

* Proc. Roy. Inst. of Great Britain, 1884.
† *Loc. cit.*

Assuming now the flow in an open rectangular channel to be the same for a given pressure drop as that in a rectangular pipe between $y=-b$ and $y=0{\cdot}429\,b$ (so as to have the maximum w at ·30 depth *),

$$Q=\int_{y=-b}^{y=+{\cdot}429b}\int_{x=-a}^{x=+a} w.\,dx\,.\,dy,$$

or

$$Q=2\left[-\frac{32\tau b^2}{3}\left\{(2b/\pi)^2\tanh(\pi a/2b)\sin(\pi y/2b)\right.\right.$$
$$\left.-\frac{1}{3^3}(2b/3\pi)^2\tanh(3\pi a/2b)\sin(3\pi y/2b)+\ldots\right\}$$
$$\left.+\tau a\left(b^2y-\frac{y^3}{3}\right)\right]_{y=-b}^{y=+0{\cdot}429b}.$$

Evaluating this in the case of $2a=8{\cdot}00$ cm., $1{\cdot}429b=15{\cdot}5$ cm.†, shows that $Q=-\frac{565}{\mu}\frac{dp}{dz}$, or the quantity flowing is 48·6 per cent. of that in a whole pipe of depth 31·0 cm., and, incidentally, 79 per cent. of that in a whole pipe of depth $2b=21{\cdot}7$ cm.

The equation of laminar flow for the given channel, when m is 0·1040 feet, would therefore be

$$\frac{R}{\rho\,.\,v^2}=2{\cdot}30\frac{\nu}{vm}\quad\text{instead of}\quad\frac{R}{\rho\,.\,v^2}=2{\cdot}24\frac{\nu}{vm}$$

as stated previously. With lower depths, however, the disparity is greater. Thus for $m=0{\cdot}0861$ feet K becomes 2·16 instead of 1·92, and for $m=0{\cdot}0546$ feet 2·69 instead of 1·80.

In connexion with the depression of the filament of maximum velocity Prof. A. H. Gibson has described the phenomenon of transverse currents in the flow‡ (see fig. 11). Now this effect implies that any point in the surface other than on the axis or centre-line may have a transverse or lateral component of velocity. This has been traced in the present channel at values of $\frac{vm}{\nu}$ as low as

* In other words, the upper limit of integration has been chosen because $\frac{0{\cdot}429}{1{\cdot}429}=0{\cdot}300$.

† In a channel of width 8·00 cm., depth 15·5 cm., $m=0{\cdot}1041$ feet.

‡ Proc. Roy. Soc. A, lxxxii. pp. 144–159 (1909).

1000 by observing the drift of aluminium dust on the water-surface. A typical case is shown in fig. 12. The tendency, already referred to, of colour bands to droop from one-quarter to one-half depth further confirms the existence of transverse currents. In other words the flow is not truly laminar although streamline.

(*b*) It has been previously remarked, in discussing the examination of the flow by means of colour bands,

Fig. 11.

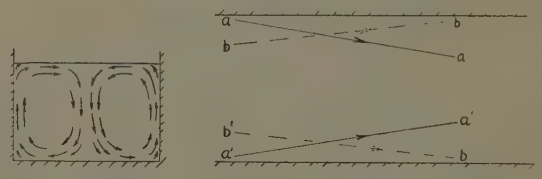

Transverse currents in channel flow.
(After Gibson, Proc. Roy. Soc. A, lxxxii. pp. 149–159 (1909),)

Fig. 12.

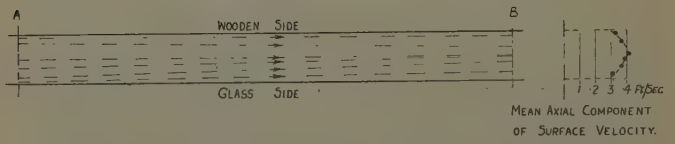

Plan of channel, showlng drift of aluminium dust on surface of water.
$m = 0{\cdot}1022$ ft., $vm/\nu = 2860$.

that at certain low velocities the thread of dye was observed to sway or oscillate in a vertical plane. A similar effect is described by Piercy, Hooper, and Winny *, although in connexion with flow through pipes with cores. They suggest that this oscillation must be damped, together with inlet disturbances, before the resistance to rectilinear flow will agree with the theoretical laminar law.

* "Viscous Flow through Pipes with Cores," Phil. Mag. xv. no. 99, p. 673 (March 1933).

(C). *Turbulent Flow.*

(i.) *Series* 1 *a, b, c. Smooth Sides and Smooth Bed.*

The smooth curves passed through the points plotted in fig. 2 have been re-plotted logarithmically in fig. 13 *, on which also are shown the "main" curve of Davies and White's tests, a portion of the bounding curves of Stanton and Pannell for smooth circular pipes, and lines of laminar flow in open channels deduced from Cornish's theory.

Fig. 13.

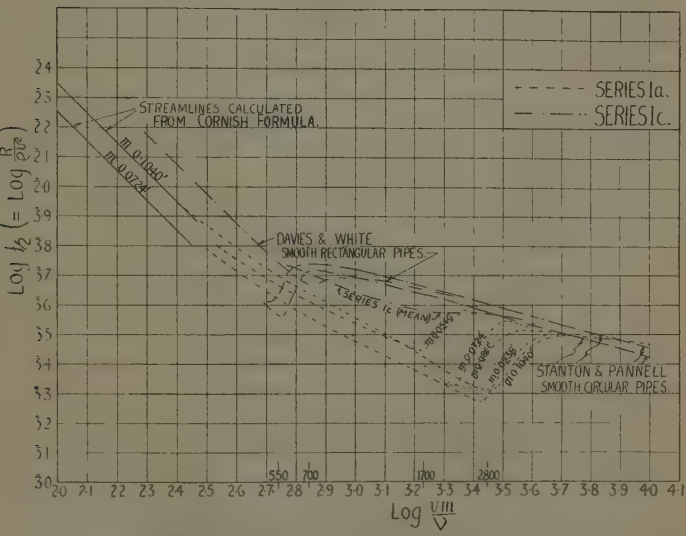

Fig. 2 replotted logarithmically.

From the results of Davies and White it appears that in rectangular pipe-flow the turbulent line may be less inclined to the horizontal than in circular pipe-flow; in the channel tests it is definitely less inclined, and, in fact, crosses the Stanton and Pannell band at $\frac{vm}{\nu}$ = approximately 6900, or $\frac{R}{\rho . v^2} = 0{\cdot}00305$.

* The ordinate now used is $\frac{R}{\rho . v^2}$, or $\frac{f}{2}$.

It might at this stage be observed that, since the values of f lie on one curve if plotted against $\frac{vm}{\nu}$ after turbulent flow is established, it is quite impossible to apply a formula of the Bazin type,

$$C = \frac{157{\cdot}6}{1 + \frac{N}{\sqrt{m}}},$$

which regards f as a function of m but not of v or ν. If, however, the mean square root of m over the range of the present tests be taken as 0·279, and f as 0·00585 (as applicable for $\frac{vm}{\nu} = 10{,}000$), then the value of Bazin's N becomes 0·135, as compared with his stated value of 0·109 for smooth cement or planed timber, and 0·290 for unplaned timber or slightly tuberculated iron.

Adopting the value 0·135 for N would give the following values for f :—

TABLE IV.

m (feet).	f.
0·1040	0·00519
·0861	·00550
·0724	·00585
·0546	·00644

A detailed examination of Darcy and Bazin's original papers * has, however, revealed that four series of experiments were carried out with what they describe as smooth open channels, viz. :—

Series 2.—Rectangular, pure cement, 5·94 ft. wide, slope 0·0049.

Series 24.—Semicircular, pure cement, diameter 4·1 ft., slope 0·0015.

Series 28.—Rectangular, carefully planed wood, 0·328 ft. wide, slope 0·0047.

Series 29.—Ditto, but slope 0·0152.

* ' Recherches Hydrauliques ' (Paris, Imprimerie Impériale, 1865).

There is also a Series 25, similar to 24, except that the wall was of cement mixed with one-third very fine sand.

The results of these tests have accordingly been plotted in fig. 14, together with the general line of the present tests, Stanton and Pannell's average line, and results quoted by Fidler in his 'Calculations in Hydraulic Engineering,' for

Sudbury Culvert*—hard smooth brick, pointed in cement (tests by Fteley and Stearns); also

Roquefavour Aqueduct*—smooth brick with floor of cement (tests by Darcy).

Fig. 14.

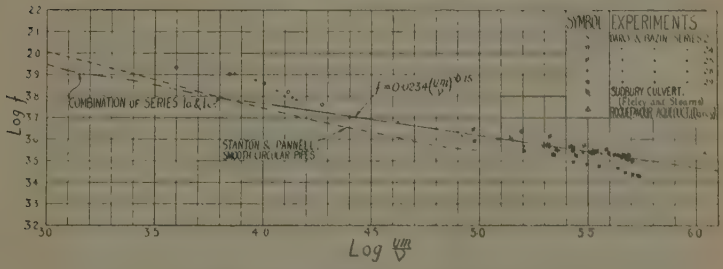

Present results + Darcy and Bazin's, etc.

Series 28 and 29 of Darcy and Bazin must, however, be regarded with considerable doubt, for the following reasons :—

(*a*) The slope of their channel was by no means constant throughout its length. In Series 28 it varied from 0·003 to 0·0065, as compared with the assumed mean of 0·0047.

(*b*) The depth of water differed considerably from point to point. Thus, in Series 28, experiment 7, it varied from 0·057 metre to 0·070, while the assumed depth, apparently based on an average of many profile readings neglecting two at the entry and one near the exit, was 0·0656 metre. In other words there was a variation of 0·512 inch in an average of 2·58 inches, due to wave

* In plotting these the water temperature has been assumed to be 10° C. or 50° F.

disturbance caused by the submerged orifice supplying water to the channel.

Again, in Series 29, experiment 5, the depth varied by 0·118 inch, while the assumed mean was only 1·61 inches.

Now the plotted value of f for $\frac{vm}{\nu}=1840$, from Series 28, experiment 1, is 0·0111. This is from their stated figures, in which they have used a depth of 0·0109 metre. The depth actually varied between 0·009 and 0·013, and it is of interest to note that 0·009 would reduce f to 0·0064.

(*c*) For these particular tests the method of measurement of depth by depth gauges could not in any case justify confidence.

(*d*) Owing to the pronounced disturbance the resistance would necessarily appear high.

(*e*) The flow was assumed uniform, but it appears that if the drop in the water surface over a length of 10 feet had been 0·158 feet, as compared with the 0·152 drop in bed-level, the results of Series 29 would agree reasonably with the present tests.

The same objections do not apply to any such great extent in the other series, owing to the bigger depths, longer lengths of channel, and more uniform slope, and accordingly it appears justifiable to regard the results from them as an extension of the present tests.

In this connexion, however, it must be noted that there is considerable evidence in Darcy and Bazin's work to show that the resistance in semicircular channels is less than in rectangular, even with the sides made of similar material; this applies not only to their "smooth" sided, but also to unplaned.

Having regard to this, the line whose equation is

$$f=0{\cdot}0234\left(\frac{vm}{\nu}\right)^{-0{\cdot}15}$$

may be taken to represent the resistance in open rectangular channels over a wide range, with probably considerable accuracy, although at the higher values of $\frac{vm}{\nu}$, and also in the region following the critical, there are indications that the line is not so steep.

These effects are similar to those in pipe-flow, although the approximate equation then is

$$f = 0{\cdot}08\left(\frac{vd}{\nu}\right)^{-0{\cdot}25} * \quad \text{or} \quad 0{\cdot}056\left(\frac{vm}{\nu}\right)^{-0{\cdot}25}.$$

The formula $f = 0{\cdot}0234\left(\frac{vm}{\nu}\right)^{-0{\cdot}15}$ implies that

$$\frac{dh}{dl} = i = \frac{0{\cdot}000364 v^{1{\cdot}85}\nu^{0{\cdot}15}}{m^{1{\cdot}15}}$$

or

$$v = \frac{72{\cdot}2 m^{0{\cdot}621} i^{0{\cdot}54}}{\nu^{0{\cdot}081}}$$

in ft.-lb.-sec. units.

(ii.) *Series 2 a, b, c. Smooth Sides, Rough Bed.*

The observations show that now, for $\frac{vm}{\nu}$ greater than 5000, f is sensibly constant for a given m, indicating that the flow is fully turbulent in the sense that the resistance is proportional to the square of the velocity.

If N in Bazin's expression

$$C = \sqrt{\frac{2g}{f}} = \frac{157{\cdot}6}{1 + \frac{N}{\sqrt{m}}}$$

be taken as 0·195, the following results are obtained :—

TABLE V.

m (feet).	Calculated f.	Measured f.	Calculated C.	Measured C.
0·1040	0·00664	0·00640	98·4	100·5
·0867	·00725	·00710	94·1	95·1
·0731	·00769	·00800	91·5	89·6

There is therefore a close agreement between the observed values and those calculated, using N = 0·195, although, as was shown in discussing Series 1 *a*, an expression of this type cannot be used when both sides and bed of channel are smooth.

* Davies and White, "A Review of Flow in Pipes and Channels," 'Engineering,' July–August, 1929.

(iii.) *Series* 3 *a*, *b*, *c*. *Rough Sides, Rough Bed.*

Reference to fig. 8 shows that after the transition the curves slope upward slightly, although there is every indication that they are becoming horizontal.

Eddy formation, due to obstructions in the approach channel, has the effect of reducing the upward slope of the curves over the range of $\frac{vm}{\nu}=2500$ to 4000, so that the values of "f" approach their apparent final magnitudes more rapidly (see figs. 9 and 10).

Incidentally, owing to higher water temperature it has been possible, in Series 3 *a*, to continue the observations to a somewhat higher magnitude of $\frac{vm}{\nu}$.

If N in Bazin's expression

$$C=\sqrt{\frac{2g}{f}}=\frac{157{\cdot}6}{1+\frac{N}{\sqrt{m}}}$$

be taken now as 0·225, the following are obtained :—

TABLE VI.

m (feet).	Calculated C.	Measured C*.	Calculated f.	Measured f*.
0·1026	92·6	93·0	0·00748	0·00745
·0863	89·3	89·2	·00807	·00810
·0730	86·0	86·3	·00870	·00865

The agreement between calculated and measured values is thus seen to be even closer than when the bed of the channel is roughened but the sides left smooth.

6. OBSERVATIONS OF VELOCITY DISTRIBUTION.

In the course of the investigation a number of observations were made (at values of $\frac{vm}{\nu}$ greater than 2700) by means of a carefully calibrated pitometer of the velocities at a section midway between the gauge-points A and B.

* These are the values which the curves of fig. 8 ultimately reach at the high values of vm/ν.

The pitometer was connected to a differential gauge having toluene as its upper fluid.

The results showed a general tendency for the depths of mean and maximum velocity along the vertical axis, measured below the surface, and expressed as a proportion of the total depth of the stream, to decrease as the depth of water was reduced for a given discharge.

In stream-gauging it is commonly assumed that the mean velocity occurs at 0·6 of the depth, except in shallow streams, when the mean is sometimes obtained by taking the average of the velocities at 0·2 and 0·8 of the depth.

The following Table shows that the latter method gives a very reasonable approximation over the range considered :—

TABLE VII.

Depth (inches).	Q (cu. ft./sec.)	v_{mean} from curve* (ft. per sec.).	$\frac{v \text{ at } \cdot 2d + v \text{ at } \cdot 8d}{2}$ (ft. per sec.).	Per cent. error. +	Per cent. error. −
3·40	0·067	0·95	0·97	2·0	..
2·90	·0900	1·50	1·50	nil.	..
†6·50	·0470	0·365	0·365	nil.	..
†4·06	,,	0·530	0·540	1·9	..
3·09	,,	0·760	0·755	..	0·7
2·21	,,	0·980	0·980	nil.	..
2·25	·0720	1·55	1·52	..	2·0

On the other hand the maximum error in taking the mean velocity as that measured at 0·6 depth is 8·2 per cent. and the average 4·2 per cent., the value obtained being too high.

The observations were made with smooth sides and rough bed.

A significant feature, as shown by the typical curves of fig. 15, is the high velocity close to the bed of the stream.

7. SIMILARITY OF CHANNELS.

Considering *uniform* flow ‡ in a full-size channel and its model, let the suffix 1 refer to the natural channel and the suffix 2 to the model.

* By planimetry of curve of velocity distribution.

† Curves shown in fig. 15.

‡ In uniform flow $\frac{dv}{dl}$ is zero, and $\frac{dh}{dl}$ then $= i = \frac{f \cdot v^2}{2gm}$, or, in the Chezy form, $v = C\sqrt{mi}$.

(i.) If the flow in each is turbulent and within the range to which the formula $f=\lambda\left(\frac{vm}{\nu}\right)^{\alpha}$ is applicable, then, for similarity,

$$\left(\frac{v_2}{v_1}\right)^{2+\alpha}=\left(\frac{m_1}{m_2}\right)^{\alpha-1}\cdot\frac{i_2}{i_1}\cdot\left(\frac{\nu_2}{\nu_1}\right)^{\alpha}.$$

Fig. 15.

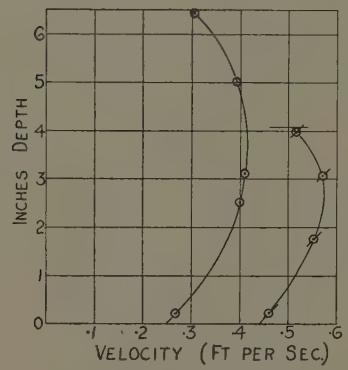

Typical pitometer readings of velocity in axial plane of channel.

In the particular case of geometrically similar channels (having the same horizontal and vertical scale ratios $1:x$),

$$i_1=i_2,$$

$$m_1=x\,.\,m_2,$$

and the corresponding velocity for operation of the model will be given by

$$\left(\frac{v_2}{v_1}\right)^{2+\alpha}=x^{\alpha-1}\cdot\left(\frac{\nu_2}{\nu_1}\right)^{\alpha}.$$

According to the present investigation α is approximately $-0{\cdot}15$ over a wide range, in which case

$$\left(\frac{v_2}{v_1}\right)^{1{\cdot}85}\text{ must}=x^{-1{\cdot}15}\cdot\left(\frac{\nu_2}{\nu_1}\right)^{-0{\cdot}15}.$$

(ii.) If, however, the sides and bed of the channels are rough and the flow again turbulent f may be constant for a stated m and given by Bazin's expression

$$C=\sqrt{\frac{2g}{f}}=\frac{157{\cdot}6}{1+\frac{N}{\sqrt{m}}}.$$

Supposing the horizontal scale of the model to be $1:x$ and the vertical $1:y$,

$$v_2 \text{ will be chosen} = \frac{v_1}{\sqrt{y}},$$

and x will have to be such that

$$\frac{1+\frac{N_2}{\sqrt{m_2}}}{1+\frac{N_1}{\sqrt{m_1}}}=\sqrt{\frac{m_2}{m_1}\cdot x}.$$

An example of model investigation in which this equality was found to hold is provided by the upper reaches of the Severn Tidal Model *, when it is assumed, as must be sensibly true in such a case where the bed is composed of sand not very different from that of the estuary and where the river has so many bends, that $N_1=N_2$.

On the other hand, if there is no distortion of scale and x therefore is equal to y,

$$\frac{N_2}{N_1} \text{ must } =\frac{1}{\sqrt{x}}, \text{ if } \frac{v_2}{v_1}=\frac{1}{\sqrt{x}} \text{ and } i_2=i_1.$$

This, in a small-scale model, would be an impossible condition, and it would be necessary instead either to have

$$\frac{i_2}{i_1}=\left(\frac{1+\frac{N_2}{\sqrt{m_2}}}{1+\frac{N_1}{\sqrt{xm_2}}}\right)^2\cdot\frac{1}{x},$$

* 'Construction and Operation of a Tidal Model of the Severn Estuary.' Two Reports by Prof. A. H. Gibson; H.M. Stationery Office, 63–78–2, p. 63 (1933).

or to ensure that $i_2 = i_1$, by making

$$\frac{v_2}{v_1} = \frac{1 + \frac{N_1}{\sqrt{xm_2}}}{1 + \frac{N_2}{\sqrt{xm_2}}} \cdot \sqrt{\frac{1}{x}}.$$

8. Summary.

(*a*) The true lower critical velocity in an open channel is given approximately by $\frac{vm}{\nu} = 1400$. This value is independent of the roughness of the walls and bed of the channel.

(*b*) The observed loss of head agrees very closely with the theoretical loss of head on the assumption of true laminar flow for values of $\frac{vm}{\nu}$ up to about 300. Then follows a range in which the flow is not turbulent, but there is, superimposed on the laminar flow, a series of transverse currents which increases the loss of head.

(*c*) In the turbulent range values of f for different velocities and hydraulic mean depths lie on one curve, when plotted against $\frac{vm}{\nu}$, provided the bed and sides of the channel are smooth. Continuing the curve to join the results of other investigators obtained with smooth channels at higher Reynolds numbers indicates that over a wide range

$$f = 0{\cdot}0234\left(\frac{vm}{\nu}\right)^{-0{\cdot}15},$$

or

$$i = \frac{0{\cdot}000364\, v^{1{\cdot}85}\nu^{0{\cdot}15}}{m^{1{\cdot}15}},$$

or

$$v = \frac{72{\cdot}2 m^{0{\cdot}621} i^{0{\cdot}54}}{\nu^{0{\cdot}081}},$$

approximately. } using ft.-lb.-sec. units.

(*d*) For smooth sides and a rough bed Bazin's formula for turbulent flow,

$$C = \frac{157{\cdot}6}{1 + \frac{N}{\sqrt{m}}},$$

in foot units, applies quite reasonably, N having the value 0·195 for the roughness used in the present tests.

(*e*) For rough sides and a rough bed of the kind used the formula

$$C = \frac{157{\cdot}6}{1 + \frac{N}{\sqrt{m}}}$$

fits the observed results with remarkable accuracy, N being then 0·225.

(*f*) Over the range of pitometer measurements made a close approximation to the mean velocity in a vertical is obtained by averaging the velocities at 0·2 and 0·8 of the depth.

The investigation described in this paper has been carried out in the Whitworth Engineering Laboratory at Manchester University, and the author wishes to record his thanks to the Director, Professor A. H. Gibson, D.Sc., for the facilities provided and the interest he has taken in the work, and to Professor D. R. Hartree, F.R.S., for helpful criticism.

The author would also express his high appreciation of the painstaking and enthusiastic assistance given to him in the taking of the observations and the calculation of results by Mr. A. C. Hall, M.Sc., Osborne Reynolds Fellow, and Mr. M. K. Sein, M.Sc., the former throughout, and the latter in a large part of, the experimental work.

Appendix A.

Concerning the term $\frac{V_B^2 - V_A^2}{2g}$.

It has been assumed that the kinetic head at a section is $\frac{v^2}{2g}$, where v is the mean velocity. The error due to this has been estimated in a particular case thus :—

Referring to fig. 16, the velocity distribution in a vertical section is obtained from actual measurement, the depth

in the case considered being 2·90 inches, mean velocity 1·38 ft. per sec., and (to show the scale) the surface velocity at the centre of the stream 1·48 ft. per sec.

The kinetic head is

$$\frac{\iint \frac{\rho u^3}{2g}\, dx\, dy}{\iint \rho u\, dx\, dy}.$$

Fig. 16.

VELOCITY DISTRIBUTION IN VERTICAL AXIAL PLANE.

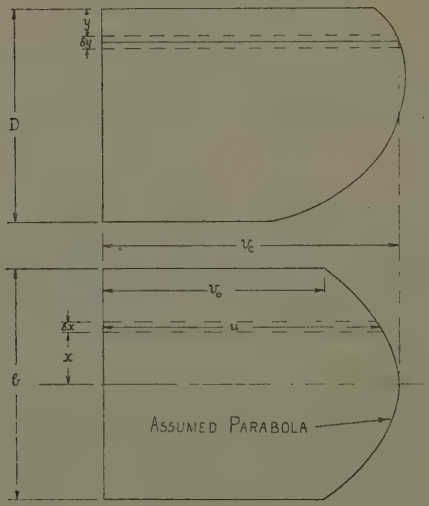

SECTIONAL PLAN OF VELOCITY DISTRIBUTION.

Illustrating Appendix A.

Similarly,

$$v = \frac{\iint \rho u\, dx\, dy}{b D \rho}.$$

These integrals have been evaluated in the case considered by assuming the velocity curve in plan to be a parabola, in which $v_0 = 0{\cdot}75\ v_c$, and by summing arith-

metically the magnitudes of $\delta y \int \frac{\rho u^3}{2g} dx$ and $\delta y \int \rho u \, dx$ for small strips δy.

In this way a value 1·40 ft. per sec. was obtained for v, as compared with the measured 1·38, showing that the assumption of the parabola was substantially correct.

Moreover, it appears from the calculations that, in the example chosen,

$$\frac{\iint \frac{\rho u^3}{2g} dx\, dy}{\iint \rho u \, dx\, dy} = 1{\cdot}03 \frac{v^2}{2g}, \quad = \epsilon \frac{v^2}{2g}, \quad \text{say,}$$

v being taken as 1·40 ft. per sec. as deduced from

$$\frac{\iint \rho u \, dx\, dy}{b \mathrm{D} \rho}.$$

On the simple basis of $\frac{v_B^2 - v_A^2}{2g}$ instead of $1{\cdot}03 \left(\frac{v_B^2 - v_A^2}{2g}\right)$ therefore it appears that f would have been estimated 1·5 per cent. too high.

But in no case has a value been relied upon for such a relatively high magnitude (9520) of $\frac{vm}{\nu}$, except for the biggest m's, when the effect of $\frac{v_B^2 - v_A^2}{2g}$ would in any event be proportionately less.

On the other hand, the vertical distribution of velocity in the present investigation was obtained with rough bed and smooth sides; with both sides and bed roughened, and consequently still less uniform distribution of velocity, ϵ would have been higher than 1·03, so that, on the whole, it is established that the error in estimating f, due to the discrepancy in the term $\frac{v_B^2 - v_A^2}{2g}$, may at worst have been of the order of 1·5 per cent.

It is of interest to note that ϵ was estimated by Darcy and Bazin *, typical values being 1·038 for a semicircular channel of unplaned wood, 1·052 for a rectangular channel of unplaned wood, 1·025 for a semicircular channel in pure cement.

* 'Recherches Hydrauliques,' 1865, p. 258.

Appendix B.

Typical Sheet of Observations.

Series 1 *a*, mean $m = 0{\cdot}0546$ feet.

Q (cusecs.).	Temperature (°F.). Water.	Gauge.	Corrected difference on gauge (cm.).	δH. in.	ft.	Depth (inches). A.	B.
·00163(5)	55	58	·073	·000545	·0000454	1·13	1·15
·00273(5)	55·5	58	·150	·00112	·0000933	1·14	1·16
·00359(5)	56	58	·229	·00171	·000142	1·13	1·148
·00425	56·2	57	·308	·00229	·000191	1·13	1·148
·00587	56	57	·499	·00371	·000309	1·12	1·136
·00640	56·2	54	·558	·00411	·000343	1·14	1·156
·00698	53·5	48	·671	·00483	·000402	1·125	1·140
·00970	53·5	49	1·190	·00860	·000717	1·115	1·126
·0135(5)	52·0	48·5	3·230	·0233	·00194	1·12	1·116
·0166	47·0	48·5	5·742	·0414	·00345	1·12	1·100

Q (cusecs.).	Velocity (ft./sec.). A.	B.	m (feet).	$\delta H - \frac{V_B^2 - V_A^2}{2g}$ (feet).	$\frac{vm}{\nu}$.	f.
·00163(5)	·0663	·0661	·0549	·0000460	277	0·0137
·00273(5)	·109(6)	·109(6)	·0553	·0000933	466	·0103
·00359(5)	·145(5)	·145(5)	·0549	·000142	621	·00882
·00425	·172	·172	·0549	·000191	733	·00850
·00587	·239(5)	·240	·0546	·000306	1015	·00696
·00640	·256(5)	·257	·0552	·000338	1105	·00678
·00698	·283(5)	·284(5)	·0547	·000396	1160	·00643
·00970	·398	·400	·0543	·000691	1630	·00565
·0135(5)	·553	·563(5)	·0542	·00175	2205	·00730
·0166	·677(5)	·700(5)	·0533	·00295	2480	·00791

Inclination of gauge 8°–30′.
Bed at B 0·02 inch lower than A.
Mean width at A 3·15 inches.
Mean width at B 3·10 inches.
Distance between A and B 32·18 inches.

XCIII. *Raman Effect for Water in Different States.* *By* I. Ramakrishna Rao, *M.A., Ph.D., Andhra University, Waltair, India.**

1. *Introduction.*

MANY workers have studied the Raman spectrum of water in different states. The first systematic investigation was by the author †. Therein it was found that both ice and water gave three sets of bands, at $\lambda\lambda$ 4170, 4680, and 5105 Å.U. respectively, corresponding to exciting mercury lines at $\lambda\lambda$ 3650, 4047, and 4358 Å.U. The positions of these bands were not identical for ice and water. The former was found to give sharper bands, and their shift from the original exciting line was less than for water. The mean infra-red absorptions corresponding to the bands for ice and water were 3·1 μ and 2·99 μ respectively.

The above work was done with an instrument of very small dispersion, so that the structure of the band in either case could not be studied at all.

Working with a spectrograph of larger dispersion, Kohlrausch and Dadieu ‡ found that these bands were not single, but double, and they observed the same sets of bands as the author reported in the work referred to above. To determine if these bands in the different regions of the spectrum correspond to the same infra-red frequency, the author § investigated the Raman spectrum for water in the visible as well as the ultra-violet parts of the spectrum. Eleven bands were obtained due to eleven strong exciting mercury lines. The shift of each band from the corresponding original line was found, within the limits of accuracy of determining the position of the maximum of intensity of the band, to be the same for all the bands. Thus there cannot be any doubt as to the origin of these bands. They all correspond to one and the same infra-red frequency of water.

A more thorough investigation with water, ice, and solutions of electrolytes was made by Ganesan and

* Communicated by the Author.
† Ind. Jour. Phys. iii. p. 131 (1928).
‡ *Naturwiss.* xvii. p. 627 (1929).
§ 'Nature,' cxxiii. p. 87 (1929).

Venkateswaran *. They obtained with water three bands, each of which consisted of three components gradually shading into one another, the central one being the brightest These corresponded to infra-red wave-lengths at $2{\cdot}77\,\mu$, $2{\cdot}90\,\mu$, and $3{\cdot}13\,\mu$ respectively. They recorded observing two more faint bands corresponding to $4{\cdot}25\,\mu$ and $1{\cdot}82\,\mu$. For ice they got the former three bands distinctly resolved from one another, and their shifts from the exciting lines were attributed to $2{\cdot}82\,\mu$, $2{\cdot}95\,\mu$, and $3{\cdot}13\,\mu$. Their work with nitric acid has shown equally sharp bands.

Krishnan † has obtained, with selenite crystal, bands which were in the same position as for ice, and equally sharp.

Working with concentrated solutions of electrolytes and with water at different temperatures, the author obtained results which were briefly reported previously ‡. It was found that with increasing concentration of the electrolyte (nitric acid in the case reported), the three bands which merged into one another became sharper until, in very strong solutions, there appeared only two sharply resolved bands. With increasing temperature of water the band which was unresolved became sharper and shifted more and more from the exciting line. The interesting part of the observation lay not in the sharpening of the bands, but in the change in the distribution of their intensity.

Gerlach § recorded a similar observation with solutions of strong electrolytes.

Pringsheim and Schlivitch || also observed the same phenomenon with a solution of lithium chloride and with change of temperature.

Meyer ¶ interpreted the bands at $\lambda\lambda$ 4167 and 4678 Å.U. as belonging not to two different exciting mercury lines, but to two different characteristic frequencies of two different modifications of the water-molecule. But in a later communication ** this view was contradicted by him. In this he described his work with water at high temperatures also. He found the sharpening of the water-bands

* Ind. Journ. Phys. iv. p. 236 (1929).
† 'Nature,' cxxii. p. 477 (1928).
‡ 'Nature,' cxxv. p. 600 (1930).
§ *Naturwiss.* xviii. p. 68 (1930).
|| *Zeit. f. Phys.* lx. p. 581 (1930).
¶ *Phys. Zeit.* xxx. p. 170 (1929).
** *Phys. Zeit.* xxxi. p. 509 (1930).

with increase of temperature, and attributed this to change of water-molecules from the associated to the unassociated state. He also mentioned a difference in the intensity changes with temperature of the above two water-bands which could not be noticed by the author.

Nisi * worked with a number of crystals containing water of crystallization. His results indicate that, in general, water in this state gives rise to one diffuse band for which the mean Raman frequency is $\delta\nu = 3420$ cm.$^{-1}$. But for some crystals which have a low degree of symmetry other bands are observed.

Recently Daure and Kastler † found that water-vapour gives a sharp Raman line with $\delta\nu = 3655$ cm.$^{-1}$ in contrast to the diffuse bands in water and ice.

With all the work that has so far been done on this substance it has not been possible to decide what is the cause of such large variations in the structure of the water-band in its various states. The purpose of the present paper is to describe certain additional results in the light of which it is found possible to explain the above variations.

2. *Infra-red Vibration Frequencies of the H_2O Molecule.*

The large dipole moment of water indicates that the model of the molecule is not straight wherein the oxygen atom is situated midway between the two hydrogens in the same straight line, but that the three atoms form the corners of an isosceles triangle in which the oxygen is at the vertex, the hydrogen atoms being at the two ends of the base. Another evidence for the non-linear structure of the H_2O molecule is the existence, in the fine structure of its rotation-vibration bands, of three series ‡, with frequency differences equal to 18, 24, and 57 cm.$^{-1}$, corresponding to principal moments of inertia: $A = 3{\cdot}07 \cdot 10^{-40}$, $B = 2{\cdot}31 \cdot 10^{-40}$, and $C = 0{\cdot}97 \cdot 10^{-40}$ gram/cm.^{2}

Different authors have suggested different dimensions for such a model of the H_2O molecule. By assuming a certain force of mutual attraction between the atoms (Hund postulates the fifth power), it is possible to calculate the characteristic frequencies for any particular model.

* Jap. Jour. Physics, vii. p. 30 (1931).
† *Comptes Rendus*, cxcii. p. 1721 (1931).
‡ With, *Zeit. f. Phys.* xxviii. p. 249 (1924).

Taking the molecule to be of the type represented in fig. 1, the dimensions given by different authors are collected in Table I., with the characteristic frequencies corresponding to each.

Fig. 1.

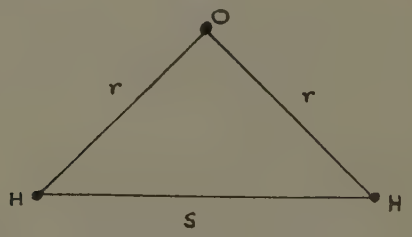

Shape of the H_2O molecule.

TABLE I.

Dimensions and Characteristic Frequencies of the H_2O Molecule.

Author.	Value of $r10^8$ cm.	Value of $s10^8$ cm.	Value of angle at O.	Frequencies in cm.$^{-1}$. ν_1.	ν_2.	ν_3.
Eucken *	1·030	1·696	110° 56′	5250	1210	4760
Hund †	1·038	1·10	64° 6′	6100	3000	5800
Mecke ‡	0·86	1·28	96°	—	—	—

In the first two models there are three possible characteristic frequencies of the molecule. It is difficult to choose between them on account of the large uncertainty in this method of calculating frequencies.

From the experimental values of the structure of the infra-red absorption bands of water-vapour, Hettner § concludes that by assuming two of the observed lines, $\lambda = 6{\cdot}26$ and $2{\cdot}66\,\mu$, as corresponding to the fundamental frequencies of the molecules, all the observed infra-red absorption frequencies of water-vapour can be represented as combinations of these.

* Eucken, *Jahrb. d. Radioact.* xvi. p. 361 (1920).
† Hund, *Zeit. f. Phys.* xxxi. p. 81 (1925).
‡ Mecke, *Phys. Zeit.* xxx. p. 907 (1929).
§ Hettner, *Zeit. f. Phys.* i. p. 345 (1920).

The following is the analysis suggested by him to explain all the observed absorption bands of water-vapour.

TABLE II.

Absorption Wave-lengths of Water-vapour.

Combination.	λ (calculated) in μ.	λ (observed) in μ.	
		Hettner.	Sleator and Phelps.
Fundamentals ν_1	—	6·26	6·2673
Fundamentals ν_2	—	2·66	2·6720
$2\nu_1$	3·1337	3·19	3·1087
$\nu_1+\nu_2$	1·8733	1·87	1·8700
$2\nu_2$	1·3360	1·37	1·3821
$3\nu_1$	2·09	2·00	—
$2\nu_1+\nu_2$	1·44	1·46	—
$\nu_1+2\nu_2$	1·10	1·13	—
$3\nu_2$	0·89	—	—
$4\nu_1$	1·55	—	—
$3\nu_1+\nu_2$	1·17	1·16	—
$2\nu_1+2\nu_2$	0·94	0·94	—
$\nu_1+3\nu_2$	0·79	0·77	—
$4\nu_2$	0·67	0·69	—

But if the triangular form of the molecule is to be adopted, as is required by its strongly dipole nature, there should be three fundamental frequencies as against two that are found by Hettner to be sufficient to explain the infra-red absorption bands. This discrepancy has been explained by Hund on the assumption that one of the frequencies ν_1 or ν_2 in Table I. is only weakly active. Since an inactive frequency can give rise to active combinations, it appears probable that the two higher frequencies may be very nearly equal, thus leading actually to only two fundamental frequencies.

This is what Mecke * actually obtains. From the two known fundamental frequencies corresponding to wave-lengths 2·66 and 6·26 μ, arrived at by Hettner, he obtains

* *Phys. Zeit.* xxx. p. 907 (1929).

a third fundamental frequency of value $\lambda_3 = 2{\cdot}33\,\mu$. The forms of vibration proposed by Mecke are given below (fig. 2).

Fig. 2.

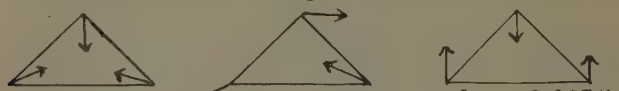

Vibrations of the H_2O molecule.

Thus the fundamental absorption bands of water-vapour appear to be at $2{\cdot}66$ and $6{\cdot}26\,\mu$.

The study of the absorption in the liquid state, however, leads to different values of the fundamental frequencies. All the absorption bands of water are explained by Ellis * as being different combinations of two fundamental frequencies, as will be clear from the following table given by him :—

TABLE III.

Absorption Bands of Water.

λ (observed) in μ.	Combination.	λ (calculated) in μ.	Combination.	λ (calculated) in μ.	Combination.	λ (calculated) in μ.
6·1	ν_1	..	—	—	—	—
4·7	—	—	—	—	—	—
2·97	$2\nu_1$	3·05	ν_2	—	—	—
1·98	$3\nu_1$	2·03	—	—	$\nu_1+\nu_2$	1·96
1·46	$4\nu_1$	1·52	$2\nu_2$	1·45	$2\nu_1+\nu_2$	1·48
1·18	$5\nu_1$	1·22	—	—	$\nu_1+2\nu_2$	1·17
0·98	$6\nu_1$	1·02	$3\nu_2$	0·97	$2\nu_1+2\nu_2$	0·98
0·85	$7\nu_1$	0·88	—	—	$\nu_1+3\nu_2$	0·85
0·75	$8\nu_1$	0·77	$4\nu_2$	0·73	$2\nu_1+3\nu_2$	0·73
0·63	$9\nu_1$ / $10\nu_1$	0·68 / 0·61	—	—	—	—
0·55	$11\nu_1$	0·55	$5\nu_2$	0·58	—	—

Excepting the band at $4{\cdot}7\,\mu$, all others have been explained on the assumption that $6{\cdot}1$ and $2{\cdot}97\,\mu$ are the fundamental frequencies. Ellis attributes the $4{\cdot}7\,\mu$ band

* Phil. Mag. iii. p. 618 (1927).

to 0–0 vibration in a double molecule $(H_2O)_2$ formed in water due to association. The absence of this band in the absorption of water-vapour is taken as an evidence for this view. Water shows two strong reflexion maxima at $3{\cdot}0\,\mu$ and $6{\cdot}3\,\mu$ and a weak one at $4{\cdot}5\,\mu$. Perhaps the third is another fundamental vibration of the H_2O molecule. At 3 and $6\,\mu$ there is also anomalous dispersion, indicating that these are the fundamental bands for water.

Plyler * found for ice-absorption bands at mean positions 0·80, 0·91, 1·04, and $1{\cdot}27\,\mu$, which are displaced towards the longer wave-lengths with respect to those for water. The $4{\cdot}7\,\mu$ band, which is weak in water, increased in intensity for ice. If this band is to be attributed to associated molecules, its increase in intensity in ice indicates the formation of a larger number of associated molecules in this state.

3. *Results from Raman Spectra.*

Water-vapour.—Daure and Kastler † obtained a single sharp Raman line with $\delta\nu = 3655$ cm^{-1}. This line obviously corresponds to the infra-red fundamental absorption at $2{\cdot}66\,\mu$, which gives, for the frequency of the molecule, 3759 cm.$^{-1}$. The disagreement between the two values may be due to the inaccuracy in measuring infra-red wave-lengths.

Water.—There is difference of opinion as regards the structure of the Raman band for water with mean $\delta\nu = 3435$ cm.$^{-1}$. While the author and the Raman school of workers maintain that it consists of three components, the German school regard it as consisting of only two components. This difference of opinion has arisen on account of the fact that water, unlike most other substances thus far investigated, gives rise to a broad diffuse band extending over about 300 cm.$^{-1}$. On account of this it is necessary that the exciting line should be isolated and unaccompanied by any line in its neighbourhood within 300 cm.$^{-1}$ on either side of it, so that the band excited by the latter is not superposed over that excited by the main line; and this band should fall in a region entirely free from any mercury lines which are likely to be superposed over it. None of the lines

* Journ. Opt. Soc. America, vol. xi. p. 545 (1924).
† *Comptes Rendus*, cxcii. p. 1721 (1931).

in the spectrum of the mercury arc satisfies the above two conditions except the feeble one at 2894 Å.U.

Fig. 3, given here, is the microphotometric curve of the Raman band of water (marked by a bracket) formed at about 3214 λ excited by the 2894 λ of the mercury arc.

There is really one maximum in the band; but the general structure indicates that there are two more maxima (indicated by arrows), unresolved from the central one, which seem to exist on either side of it. Since it is not possible to locate their positions, it is difficult to assign the exact wave-lengths to which they correspond.

In the entire Raman spectrum of water * in the visible and ultra-violet regions there are, altogether, eleven Raman bands, corresponding to eleven strong exciting mercury lines. Each of these bands appears to consist

Fig. 3.

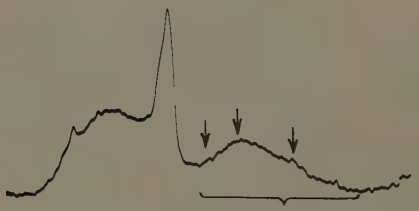

Microphotometric curve of the Raman band of water excited by the 2894 Å.U. Hg line.

of three components, which gradually diffuse into one another. The central component is of maximum intensity and is unsymmetrical with respect to the other two. It is nearer the band with the greatest shift from the exciting mercury line. Since, with visual micrometer measurements, it is difficult to locate the position of the maxima of intensity, microphotometric records of the whole spectrum were taken, from which the positions of the maxima were easily located and their wave-lengths determined. Though visually the band appears to consist of three components, even the microphotometer could not distinctly resolve them. The results of the wave-length measurements of the intense bands are given in

* *Loc. cit.*

Table IV. For each band the wave-lengths of the two ends and the central maxima are indicated in the table.

The first and second columns in the table contain the wave-lengths of the exciting mercury lines and their wave-numbers respectively. In the third and fourth columns are given the same values for the Raman bands accompanying them. The fifth column contains the wave-number differences of the numbers in the second and fourth columns. The infra-red wave-lengths corresponding to these differences are represented in column 6.

TABLE IV.

λ_{Hg} in A.U.	ν_{Hg} in cm.$^{-1}$.	λ_R in A.U.	ν_R in cm.$^{-1}$.	$\delta\nu$ in cm.$^{-1}$.	$\lambda_{infra\text{-}red}$ in μ.
		2750	36353	3083	3·24
2535–37	39436–05	2780	35961	3459	2·89
		2795	35768	3637	2·75
		3176	31477	3067	3·26
2894	34544	3214	31105	3439	2·91
		3236	30893	3651	2·74
		3268	30591	3103	3·22
2967	33694	3301	30285	3409	2·93
		3325	30139	3555	2·76
3022	33081	3368	29683	3398	2·94
		3452	28960	3021	3·31
3126–32	31981–19	3507	28506	3444	2·90
		3532	28305	3614	2·77
		4124	24241	3148	3·18
3663–50	27389–292	4172	23963	3399	2·95
		4232	23623	3669	2·73
		4623	21622	3083	3·24
4047	2470	4697	21282	3423	2·92
		4746	21065	3640	2·75

It is evident from the table that the maximum is not symmetrically situated with respect to the whole band. The mean values of the three positions of the band are 3·24 μ, 2·92 μ, and 2·75 μ.

The infra-red absorption band of water has its maximum at 2·97 μ, given in Table III. This compares well with the maximum 2·92$\pm$·03 μ obtained in the Raman spectrum of water. The agreement between the two indicates that it is the same vibration that gives rise to the Raman band as that which brings about infra-red absorption.

The infra-red absorption band of water-vapour shows the rotational structure, which is absent in that for water. The latter shows a diffuse band with a single maximum at 2·97 μ. The Raman band, however, appears to consist of three components. Table V. gives the Raman frequencies of the maxima obtained by different authors.

TABLE V.

Structure of the Raman Band of Water.

Author.	Frequencies of the components in cm.$^{-1}$.		
Ramkrisnha Rao *	3208	3419	3582
Genesan-Venkateswaran †	3193	3453	3609
Nisi ‡.....	3206	3456	3578
Specchia §	3260	3405	3560
Mean.....	3217	3433	3582

The mean frequencies of the three components are 3217, 3433, 3582 cm.$^{-1}$, which correspond to infra-red absorption at 3·11, 2·91, 2·79 μ respectively. The fundamental absorptions in the infra-red are at 6·1 and 2·97 μ, as will be seen from Table III. The latter agrees fairly well with the value 2·91 μ obtained from the Raman spectrum.

Ice.—The preliminary work with ice by the author || was made with an instrument of small dispersion. Therein was found an unresolved band which was much sharper than that of water. The maximum was at 3·10 μ, compared with 2·99 μ for water.

With a view to compare the Raman spectrum of H_2O in different states, the author repeated the work with ice with a Fuess spectrograph which has a sufficiently large dispersion. The positions of the maxima were determined from microphotometric records, and the wave-lengths thus calculated. The Raman spectrum of ice showed only

* 'Nature,' cxxiv. p. 762 (1929); Proc. Roy. Soc. cxxvii p. 279 (1930); 'Nature,' cxxv. p. 600 (1930).
† Ind. Journ. Phys. iv. p. 281 (1929).
‡ Jap. Journ. Phys. v. p. 119 (1929).
§ Cim. vii. p. 388 (1930.)
|| Ind. Journ. Phys. iii. p. 131 (1928).

two components in the band. The third component reported by Ganesan-Venkateswaran is not found; also the band with $\delta\nu = 5393$ observed by them is absent in the spectrum obtained by the author. The values of $\delta\nu$ obtained for the band excited by the 4047 line of the mercury arc are 3321 and 3196 cm.$^{-1}$. The values for the bands excited by the 3650 group of lines are not given, as these are not excited by a single line, but are the result of superposition of the bands excited by the three components of this group.

Water of Crystallization.—Krishnan *, working with selenite, found three diffuse bands with Raman frequencies

TABLE VI.

Raman Bands due to Water of Crystallization.

Substance.	$\delta\nu$ in cm.$^{-1}$.		
Li_2SO_4, H_2O	—	3438	—
Na_2SO_4, IOH_2O	—	3438	—
$AlK(SO_4)_2\ 12H_2O$	—	3384	—
$MgSO_4, 7H_2O$	3227	3445	—
$CdSO_4, \frac{8}{3}H_2O$	—	3423	—
$CaSO_4, 2H_2O$.....	—	3404	3497
$CuSO_4, 5H_2O$	3211	3377	3494
$Na_2S_2O_3, 5H_2O$.....	3337	3414	—
$C_4H_4O_6\ KNa, 4H_2O$	3303	3405	—
H_2O (liquid)	3195	3437	—

equal to 3240, 3396, 3494 cm.$^{-2}$. Schaefer and Matossi reported having observed with the same substance only two bands at 3396 and 3494 cm.$^{-1}$; but the most systematic work on water of crystallization was done by Nisi †. Table VI. contains his results with a number of crystals containing water of crystallization.

His results indicate that, in general, water of crystallization gives rise to one diffuse band whose mean $\delta\nu = 3420$ cm.$^{-1}$; but in the case of crystals which show a low degree of symmetry other bands are obtained. The mean values of the three bands thus obtained are 3210,

* Ind. Journ. Phys. iv. p. 131 (1929).
† Jap. Journ. Phys. vii. p. 30 (1931).

3416, and 3495 cm.$^{-1}$ respectively, compared with 3240, 3396, and 3494 cm.$^{-1}$ obtained by Krishnan for gypsum.

Coblentz * investigated the infra-red absorption of a large number of substances containing water of crystallization. In gypsum he obtained absorption maxima at 6 μ, 4·75 μ, 3 μ, 1·9 μ, and 1·5 μ. Schaefer and Schubert† observed similar maxima for some alums and double sulphates. Table VII. contains their results.

The mean frequencies obtained from Raman effect for water of crystallization are 3210, 3416, 3495 cm.$^{-1}$.

TABLE VII.

Infra-red Absorption Bands of Water of Crystallization.

Substance.	λ_1 in μ.	λ_2 in μ.	λ_3 in μ.	λ_4 in μ.
Ammonium alum	3·03	3·495	6·05	6·27
Sodium alum	3·01	3·51	6·09	6·32
Potassium alum	3·015	3·51	—	—
Rubidium alum	3·03	3·52	—	—
Thallium alum	3·07	3·50	6·10	6·27
Amm.-chrom.-alum	3·07	3·60	6·02	6·33
Rubidium-chrom.-alum ..	3·04	3·60	—	—
Amm.-iron-alum	3·15	3·65	—	—
Mean wave-length	3·05	3·55	6·06	6·30
Mean frequency in cm.$^{-1}$.	3279	2817	1650	1587

4. *Comparison of Frequencies in the Different States.*

Table VIII. contains a summary of the results obtained for the characteristic frequencies of the water-molecule in the vapour liquid and solid states and in the state of crystallization.

In the table the dashed frequencies are from Raman spectra and the undashed from the infra-red absorption; corresponding values from the above two sets of data are given side by side. The infra-red absorption wave-lengths in μ are given below each of the frequencies.

An examination of the table reveals that the infra-red absorption at about 6·26 μ, which is assumed by Hettner

* 'Investigations in the Infra-red,' iii. p. 19 (1906).
† *Ann. d. Phys.* p. 339 (1916).

to be one of the two fundamental frequencies of the H_2O molecule, has absolutely no corresponding Raman band in any of its states. Ice has been investigated by Plyler in the infra-red only up to $1{\cdot}27\,\mu$. Hence the presence of its absorption band at $2{\cdot}6\,\mu$ has not been indicated in the above table, as it has not been so far investigated. The infra-red absorption at about $3\,\mu$, however, has its corresponding Raman band in all the different states of H_2O.

TABLE VIII.

Infra-red and Raman Frequencies, in cm.$^{-1}$, of H_2O in Different States.

	ν_1.	ν_1'.	ν_2.	ν_2'.	ν_3.	ν_3'.	ν_4.	ν_4'.
Water-vapour ..	1597	—	—	—	—	—	3759	3655
	(6·26)	—	—	—	—	—	(2·66)	(2·74)
Water (liquid)...	1639	—	—	3217	3367	3433	—	3582
	(6·1)	—	—	(3·11)	(2·97)	(2·91)	—	(2·79)
Ice	—	—	—	3196	—	3321	—	—
	—	—	—	(3·13)	—	(3·01)	—	—
Water of crystallization.	1650	—	3279	3210	—	3416	—	—
	(6·06)	—	(3·05)	(3·12)	—	(2·93)	—	—
	1587	—	—	—	—	3495	—	—
	(6·30)	—	—	—	—	(2·86)	—	—

A glance at fig. 2 shows that of the three possible fundamental frequencies for the H_2O molecule, the one corresponding to $\lambda_3=2{\cdot}325\,\mu$ is absent both in the infra-red absorption as well as in the Raman spectrum. Of the other two, $\lambda_1=6{\cdot}26\,\mu$ is present only in the infra-red spectrum. The third, $\lambda_2=2{\cdot}66\,\mu$, is present in both the types of spectra.

At a first glance at the Raman frequencies for water one may explain the component $\delta\nu=3217$ cm.$^{-1}$ ($3{\cdot}11\,\mu$) as being the first overtone of the $6{\cdot}26\,\mu$ band. But one serious objection against such an assignment is the absence of the Raman band corresponding to the fundamental itself, *i. e.*, the $6{\cdot}26\,\mu$ band. It is difficult to conceive how an overtone of any frequency can be present in the

Raman spectrum without the fundamental making its appearance. Another objection against supposing the 3·13 μ component of the Raman water-band as being the overtone of the 6·26 μ band is the absence of the corresponding band in the water-vapour spectrum taken by Daure-Kastler. The latter substance shows only one sharp Raman line, 2·74 μ, which, within limits of experimental error, corresponds to the infra-red absorption band of water-vapour at 2·66 μ.

The form of vibration for the 6·26 μ band from fig. 2 indicates that it is symmetrical, involving very little change in the electric moment of the molecule. The 2·66 μ vibration, however, is unsymmetrical, and, therefore, involves a considerable change in the electric moment of the molecule. This interpretation is supported by the fact that the absorption at 2·66 μ is much greater than at 6·26 μ. The former can, therefore, be treated as an active frequency, while the latter is very nearly inactive.

Though there are cases where inactive vibrations give rise to very strong Raman lines (*e. g.*, the NO_3 line with $\delta\nu = 1049$ cm.$^{-1}$) without any corresponding infra-red absorption, and, conversely, there are active vibrations with strong infra-red absorption without the corresponding Raman line, we may have, in the case of water, a nearly inactive frequency (6·26 μ), being entirely absent in the Raman spectrum.

Whatever may be the cause of the absence of the Raman band corresponding to 6·26 μ infra-red absorption, the above argument entirely excludes the assignment of any of the Raman bands at about 3·10 μ as being the overtone of the above band. Hence all the Raman frequencies obtained for water must be attributed to the vibration giving rise to the 2·7 μ line in the vapour state.

But a comparison of these frequencies in the various states of H_2O shows that there is a large difference in them from one state to another. While there is in the Raman spectrum of water-vapour a sharp line with $\delta\nu = 3655$ cm.$^{-1}$, water gives rise to a very diffuse band, apparently showing three components with $\delta\nu = 3217$, 3433, and 3582 cm.$^{-1}$ which are not resolved from one another. Only the third frequency, $\delta\nu = 3582$, has any relation to that with $\delta\nu = 3655$ for water-vapour. The appearance of the other two bands, therefore, requires an explanation.

A further change in the structure of the H_2O spectrum is obtained in the transition from water to ice, which shows only two bands, with mean frequencies 3196, 3321 cm.$^{-1}$ respectively. Ice, therefore, does not show any band with $\delta\nu = 3655$ cm.$^{-1}$. This change also remains to be explained.

The change in frequency from the vapour to the liquid state is also found in the infra-red absorption, as is evident from Table VIII. If all the Raman frequencies are to be attributed to one and the same fundamental vibration of the H_2O molecule, the above changes must be due to alteration in the structure of the H_2O molecule itself on passing from the vapour to the liquid and from the liquid to the solid state.

5. *Explanation of Changes in Frequencies with Change of State of Water.*

The only substance that has so far been investigated for Raman effect in all the three states is H_2O. Other substances have been studied in the gaseous and liquid states. While some substances show appreciable change in frequency due to change of state, there are others whose frequencies remain practically unchanged, due to the transition. Surprisingly, all the former set of substances happen to be polar, while the others are non-polar.

The following tables (IX. and X.) give the frequencies of both types of substances in the gaseous and liquid states.

While the non-polar substances show very little change of frequency with change of state (in most cases of the order of magnitude of error in wave-length determination), the polar molecules undergo a definite change. This may be due to two causes. In the gaseous state the molecules are at great distances from one another, so that there is no possibility of any mutual action influencing their vibration frequencies. Hence the frequency in the gaseous state can be taken to be that natural to the molecule. On changing to the liquid state, however, the molecules come so close to one another that the vibrations of one molecule are influenced by the presence of the neighbouring ones, thus bringing about a change in the absorption frequency of the molecule.

This influence is larger in the case of polar molecules, where the electric field due to the neighbouring molecules modifies the vibration to a greater extent than in the case of non-polar substances, for which there is no electric

TABLE IX *.

Frequencies of Non-polar Substances in the Liquid and Gaseous States.

Substance.	Frequencies in cm.$^{-1}$.		
	ν_{gas}.	ν quid.	$\nu_{gas}-\nu_{liquid}$.
Hydrogen	4162	4149	13
Nitrogen	2331	2330	1
Oxygen	1555	1552	3
Methane	2915	2909	6
,, ...	—	2953	—
,, ...	—	2999	—
,, ...	3022	3023	−1
,, ...	3072	3071	1
Ethylene	1342	1340	2
,, ...	1623	1620	3
,, ...	2880	—	—
,, ...	—	3000	—
,, ...	3019	—	—
,, ...	—	3080	—
,, ...	3240	—	—
,, ...	3272	—	—
Acetylene	1979	1960	19
,, ...	—	3320	—
Nitrous oxide	1282	1281·5	·5
,, ...	—	2223·5	—

* The frequencies in Tables IX. and X. are taken from K. F. W. Kohlrausch, "Smekal-Raman Effect," pp. 126 and 127.

field. This may, therefore, be one of the reasons for the large change in the frequency of polar molecules on going from the gaseous to the liquid state.

Another, and perhaps a more important, cause of the change may be due to polymerization of polar molecules in the liquid state. Due to this, each molecule does not

exist as single, as in the gaseous state, but combines with one or more of the neighbouring molecules, forming complexes. In such a case the vibration is influenced to a much greater extent, as the attached molecules are permanently in combination with it, bringing about a change in the disposition of its constituent atoms. A natural consequence of this is the large frequency change which is observed for these substances.

Water, which comes last in the table, is known to be a strongly polar molecule. Hence the causes that bring about the frequency change from gaseous to liquid state

TABLE X.

Frequencies of Polar Molecules in the Liquid and Gaseous States.

Substance.	Frequencies in cm.$^{-1}$.		
	ν_{gas}.	ν_{liquid}.	$\nu_{gas}-\nu_{liquid}$.
Hydrogen chloride	2886	2800	86
Hydrogen bromide	2558	2487	71
Hydrogen sulphide	2615	2578	37
Sulphide dioxide	1514	1146 or 1340	368 or 174
Ammonia	3334	3300	34
Water	3655	3217 3433 3582	438 222 73

in other polar substances also give rise to a similar change for the H_2O molecule. But another characteristic of the Raman spectrum of H_2O is that, in addition to the frequency 3655 cm.$^{-1}$ corresponding to the vapour state, two additional frequencies make their appearance in the liquid state. In the case of only sulphur dioxide and ammonia similar new lines appear in the liquid state which have no corresponding frequencies in the vapour state. This must be due to formation of new molecular species.

Change from Liquid to Solid State.—There are data on change of Raman frequency from the gaseous to the liquid state sufficient to permit definite conclusions to be arrived at as to the nature of such a change; but

very few experimental results are available for the transition from the liquid to the solid state. Krishnamurti * obtained with benzophenone a change from 1657 cm.$^{-1}$ to 1650 cm.$^{-1}$ in the Raman frequency on changing from the liquid to the crystalline state. The author, working with sodium nitrate in the crystalline and molten states, found a change of frequency from 1069 cm.$^{-1}$ to 1052^{-1} cm. While in the above two examples the Raman frequency in the solid state is larger than in the liquid, ice, however, shows just the opposite effect, the frequency increasing from the solid to the liquid states, as will be found from Table VIII. The change is also too large to be explained as merely due to change of state.

The shift of the Raman lines of H_2O from the liquid to solid state has been explained by the author † on the assumption that there is association resulting in the formation of double $(H_2O)_2$ and triple $(H_2O)_3$ molecules.

The explanation given is that the three components in the Raman band for water with $\delta\nu=3582$, 3433, and 3217 cm.$^{-1}$ correspond respectively to single, double, and triple molecules of water. The presence of a single Raman line for water-vapour with $\delta\nu=3655$ cm.$^{-1}$ supports this view, as in the vapour state very few double and triple molecules can exist. The existence of three components in the Raman band for the liquid state indicates that all three types of molecules are present in that state. In ice the component corresponding to 3655 cm.$^{-1}$ frequency of the vapour is entirely absent. This is a proof that in the solid state there are no single molecules, or they are too few to be detected by the Raman spectrum.

Preliminary work with Raman spectra of water at different temperatures has shown that there is a change in the distribution of the intensity of the three components with change of temperature. At low temperatures the component with $\delta\nu=3217$ cm.$^{-1}$ is more conspicuous, diminishing in intensity with increasing temperature. The central component $\delta\nu=3433$ cm.$^{-1}$ does not suffer any appreciable change, whereas the third component, with $\delta\nu=3582$ cm.$^{-1}$, increases in intensity with increasing temperature. These phenomena find a natural explanation in the changes in the proportion of the single, double,

* 'Nature,' cxxv. p. 463 (1930).
† Proc. Roy. Soc. xcxx. p. 496 (1931).

and triple molecules with temperatures. While at higher temperatures the single molecules are larger in number, at lower temperatures the triple molecules predominate, the double molecules, however, being nearly constant in number.

Water of Crystallization.—The two bands with $\delta\nu = 3210$ and 3416 appearing in the Raman spectra of crystals containing water of crystallization remain to be explained. They appear to correspond to the 3217 and 3433 bands of water attributed to the $(H_2O)_3$ and $(H_2O)_2$ molecules respectively. If the above explanation of these two bands is tenable, one may assume that water of crystallization exists as double and triple molecules. On referring to Table VI. it is found that substances that give rise to the band 3227, which is attributed to the triple molecules, contain more than three H_2O molecules, indicating thereby the possibility of the formation of triple molecules. Another evidence for this view is that crystals containing less than three molecules do not give rise to this band.

One exception to the above rule is the lithium-sulphate crystal, which contains only one molecule of water, but yet gives rise to the 3438 band, due to the $(H_2O)_2$ molecules. The formation of double molecules of water is not possible, and the position of the band does not indicate that the water-molecules exist as independent, as in that case they ought to give rise to the 3582 band corresponding to single molecules.

The only explanation possible for this substance is that the influence of the neighbouring $LiSO_4$ molecules on the frequency of H_2O is the same as that of another H_2O molecule in combination with it. Perhaps this may be taken as an alternative explanation of both the bands. The 3416 band of water of crystallization may arise out of the frequency of single molecules of water as influenced by the neighbouring molecules, either H_2O or otherwise; but this seems to be more far-fetched than the previous explanation.

6. *Other Evidences for the Polymerization of Water.*

The above hypothesis, that water does not consist of simple H_2O molecules, but is constituted of complicated ones like $(H_2O)_2$ or $(H_2O)_3$, is not a new one. As early as

1891 Vernon *, from a comparison of the boiling-points of water with those of the corresponding hydrides of sulphur (H_2S), selenium (H_2Se), and tellurium (H_2Te), found that the value for water is anomalous compared with those of the others. While the boiling-points for the latter three compounds are $-60°$, $-42°$, and $0°$ respectively, that for water is $100°$, whereas on extrapolating the above values for the hydride of oxygen it ought to be $-207°$. From this anomaly Vernon concluded that the molecule of water is very complex, which fact makes it different from the hydrides of the other elements of the same group.

P. Walden †, on similar grounds, argued that the substitution of oxygen by sulphur raises the boiling-points of the ethyl and methyl compounds by about 60°, and if a similar difference should manifest itself in the hydrogen compounds, water should boil at $-120°$. But the fact that it boils at a much higher temperature was taken by Walden as an indication of the complex structure of the water-molecule.

Walker ‡, on the one hand, and Jones and his co-workers § on the other, found that the freezing-points of solutions of water in many other solvents are different from what are required by the assumption that it consists of the simple H_2O molecules. Much earlier than any of these workers, Thomson || concluded that water has a molecular weight corresponding to the double molecule $(H_2O)_2$, as he found that the heat developed during the hydration of some salts agrees with the assumption that the water combines very often as pairs of molecules.

A very systematic investigation of the problem of association of water seems to have been undertaken by Sutherland ¶. From careful measurements of the variation of density of water with temperature, he came to the conclusion that water consists mainly of the $(H_2O)_2$ molecules, whereas in ice the $(H_2O)_3$ molecules predominate. He actually calculated the proportions of the two types of molecules in water at different temperatures. He

* Phil. Mag. xxxi. p. 387 (1891).
† *Zeit. Phys. Chem.* lxvi. p. 385 (1909).
‡ *Zeit. Phys. Chem.* v. p. 193 (1909).
§ Amer. Chem. Journ. xxx. p. 193 (1903).
|| Der. xviii. p. 1088 (1885).
¶ Phil. Mag. l. p. 460 (1900).

suggested for these molecular aggregates the following graphic formulæ :—

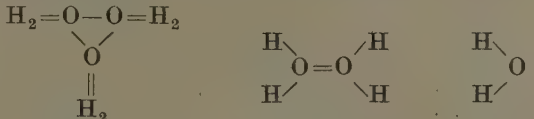

Triple. Double. Single.

Many other people have given support to the above hypothesis from various other physical properties of water.

E. Bose * measured the density of saturated water-vapour at different temperatures, and came to the conclusion that the density is greater than is required by the molecular formula H_2O and less for $(H_2O)_2$. He explained this on the hypothesis that water-vapour contains not only single, but a small proportion of double molecules also.

All the above results confirm the assumption that water contains double and triple molecules also. This hypothesis is supported by the study of the Raman band for water.

7. *Summary.*

1. The shape and dimensions of the H_2O molecules are discussed and the vibration frequencies obtained from them correlated with the infra-red absorption frequencies.

2. Results from Raman spectra of H_2O in different states are compared with the infra-red data. It is concluded that in the former there is only one band at about 3μ as against two at $2{\cdot}66$ and $6{\cdot}26\mu$ that are obtained in infra-red absorption.

3. A comparison is made between the Raman frequencies of H_2O in different states. The changes could not be explained as due merely to change of state. They are explained as arising from new molecular aggregates formed, due to association of single into double and triple molecules with change from vapour to liquid and solid states.

4. Other evidences for this theory of molecular association in H_2O are also discussed.

Note added in proof.—In a recent communication (Proc. Roy. Soc. cxli. p. 545 (1933)) Sutherland suggested that it

* *Zeit. Electrochemie*, xiv. p. 269 (1908).

is sufficient to assume that there are only two kinds of molecules, viz , H_2O and $(H_2O)_2$, the latter giving rise to the 3200 cm.$^{-1}$ component, and that the other two components arise out of a doubling of the H_2O frequency due to resonance degeneracy. But, since the rotational structure of the water bands has not been completely analysed, it is difficult to say how far the conditions necessary for such a degeneracy are fulfilled by the water molecule. Also the observed variations with temperature of the intensity distribution of the water band are not easily explained on Sutherland's hypothesis.

XCIV. *On the Operational Treatment of certain Mechanical and Electrical Problems.* *By* Arnold N. Lowan *.

BY means of the Laplace transformation any physical problem characterized by a partial differential equation, the solution of which must satisfy prescribed initial and boundary conditions, can formally be transformed into a boundary problem for an ordinary differential equation. From the solution of the latter problem that of the original problem may be obtained by the inversion of the Laplace transformation.

This method has previously been applied to the problem of the cooling of a radioactive sphere †. As is well known, the differential equation which governs the process of heat conduction is of parabolic type. The development in the present paper is illustrative of the class of physical problems characterized by a partial differential equation of hyperbolic or elliptic type.

Section I.—*Forced Vibration of a String with Variable Cross-section in a Medium of Constant Damping Coefficient.*

Let $p(x)$=cross-sectional area$\times$modulus of elasticity; δ=mass per unit length; r=damping coefficient; and $P(x, t)$=applied force per unit length. Then the dis-

* Communicated by the Author.

† Phys. Rev. Nov. 1, 1933. This paper will be referred to as A. N. L.

placement $u(x, t)$ must satisfy the following differential equation, initial and boundary conditions:

$$\frac{\partial}{\partial x}\left(p\frac{\partial u}{\partial x}\right)-r\frac{\partial u}{\partial t}=\delta\frac{\partial^2 u}{\partial t^2}-\mathrm{P}(x,t),\quad t>0, \quad . \quad . \quad (1)$$

$$\lim_{t\to 0}u(x,t)-f(x)=\lim_{t\to 0}\frac{\partial}{\partial t}u(x,t)-g(x)=0, \quad . \quad (2\text{–}3)$$

$$\frac{\partial u}{\partial x}-h_0 u=0, \qquad x=0, \quad . \quad . \quad . \quad . \quad . \quad (4)$$

$$\frac{\partial u}{\partial x}+h_1 u=0, \qquad x=a \quad . \quad . \quad . \quad . \quad . \quad (5)$$

(if we consider the general case of elastically bound ends).

Let us make the substitution:

$$u(x,t)=f(x)+e^{-\alpha t}v(x,t), \quad . \quad . \quad . \quad . \quad (6)$$

where $\alpha=\frac{1}{2}\frac{r}{\delta}$. It is then readily seen that $v(x, t)$ must satisfy the following equations:

$$\frac{\partial}{\partial x}\left(p\frac{\partial v}{\partial x}\right)-\delta\frac{\partial^2 v}{\partial t^2}+\alpha^2 v=e^{\alpha t}\frac{\partial}{\partial x}\{pf'(x)\}-e^{\alpha t}\mathrm{P}(x,t), \quad t>0,$$

$$. \quad . \quad . \quad (7)$$

$$\lim_{t\to 0}v(x,t)=\lim_{t\to 0}\frac{\partial}{\partial t}v(x,t)-g(x)=0, \quad . \quad (8\text{–}9)$$

$$\frac{\partial v}{\partial x}-h_0 v=0, \qquad x=0, \quad . \quad . \quad . \quad . \quad . \quad (10)$$

$$\frac{\partial v}{\partial x}+h_1 v=0, \qquad x=a, \quad . \quad . \quad . \quad . \quad . \quad (11)$$

provided $f(x)$ satisfies the boundary conditions (4) and (5). As in A. N. L., let us define

$$y(x,\lambda)=\mathrm{L}\{v(x,t)\}=\int_0^\infty e^{-\lambda t}v(x,t)\,dt, \quad . \quad . \quad (12)$$

$$\mathrm{Q}(x,\lambda)=\mathrm{L}\{\mathrm{P}(x,t)\}. \quad . \quad . \quad . \quad . \quad . \quad . \quad . \quad . \quad (13)$$

Consider the expressions:

$$\left.\begin{aligned}\mathrm{L}\left\{\frac{\partial v}{\partial t}\right\}&=\int_0^\infty e^{-\lambda t}\frac{\partial}{\partial t}v(x,t)\,dt;\\ \mathrm{L}\left\{\frac{\partial^2 v}{\partial t^2}\right\}&=\int_0^\infty e^{-\lambda t}\frac{\partial^2}{\partial t^2}v(x,t)\,dt.\end{aligned}\right\} \quad . \quad . \quad (14)$$

If the integrals in the second members are once (respectively twice) integrated by parts, we obtain the identities:

$$\mathrm{L}\left\{\frac{\partial v}{\partial t}\right\} = \lambda y(x,\lambda) - v(x,0) = \lambda(x,\lambda), \quad . \quad . \quad . \quad (15)$$

$$\mathrm{L}\left\{\frac{\partial^2 v}{\partial t^2}\right\} = \lambda^2 y(x,\lambda) - \lambda v(x,0) - \left\{\frac{\partial}{\partial t} v(x,t)\right\}_{t=0} \quad (16)$$

$$= \lambda^2 y(x,\lambda) - g(x).$$

If we operate on (7), (10), and (11) by the operator L, defined by (14), then in view of (16) it is readily seen that the function $y(x,\lambda)$ must satisfy the system of equations:

$$\frac{\partial}{\partial x}\left(p\frac{\partial y}{\partial x}\right) + (a^2 - \delta\lambda^2)y = -\delta g(x) - \frac{1}{\lambda - a} q(x) - \mathrm{Q}(x,\lambda), \quad (17)$$

$$\frac{\partial y}{\partial x} - h_0 y = 0, \qquad x = 0, \quad . \quad . \quad . \quad . \quad (18)$$

$$\frac{\partial y}{\partial x} + h_1 y = 0, \qquad x = a, \quad . \quad . \quad . \quad . \quad (19)$$

where

$$q(x) = \frac{\partial}{\partial x}\{pf'(x)\}.$$

The solution of this system may be written in the form

$$y(x,\lambda) = \int_0^a \mathrm{G}(x,\xi,\lambda)\left\{\delta g(\xi) + \frac{1}{\lambda - a} q(\xi) + \mathrm{Q}(\xi,\lambda)\right\} d\xi,$$

$$. \quad . \quad . \quad (20)$$

where $\mathrm{G}(x,\xi,\lambda)$ is the Green function corresponding to the homogeneous differential equation

$$\frac{\partial}{\partial x}\left(p\frac{\partial y}{\partial x}\right) + (a^2 - \delta\lambda^2)y = 0, \quad . \quad . \quad . \quad . \quad (21)$$

in conjunction with the boundary conditions (18) and (19).

From (20), by inversion of the Laplace transformation

and making use of the theorem of Borel *, we ultimately get

$$v(x,t) = \int_0^a \delta g(\xi)\Gamma(x,\xi,t)\,d\xi + \int_0^a q(\xi)\,d\xi \int_0^t \Gamma(x,\xi,t-\eta)e^{a\eta}\,d\eta + \int_0^a d\xi \int_0^t \mathrm{P}(\xi,\eta)e^{a\eta}\Gamma(x,\xi,t-\eta)\,d\eta, \quad (22)$$

where

$$\Gamma(x,\xi,t) = \mathrm{L}^{-1}\{\mathrm{G}(x,\xi,\lambda)\}. \quad (23)$$

If we designate by λ_n the characteristic values of the system (21), (18), (19), and by y_n the corresponding normalized characteristic functions, it is well known that

$$\mathrm{G}(x,\xi,\lambda) = \sum_{n=1}^{\infty} \frac{y_n(x)y_n(\xi)}{\lambda_n^3+\lambda^2}, \quad (24)$$

where the second member is uniformly convergent in the interval $0-a$ under consideration. From (24) we obtain at once

$$\Gamma(x,\xi,t) = \sum_{n=1}^{\infty} \frac{\sin\lambda_n t}{\lambda_n} y_n(x)y_n(\xi). \quad (25)$$

In view of (25), (22) becomes

$$\begin{aligned} v(x,t) &= \sum_{n=1}^{\infty} \frac{\sin\lambda_n t}{\lambda_n} y_n(x) \int_0^a \delta g(\xi)y_n(\xi)\,d\xi \\ &\quad + \sum_{n=1}^{\infty} \frac{y_n(x)}{\lambda_n} \int_0^a q(\xi)y_n(\xi)\,d\xi \int_0^t e^{a\eta}\sin\lambda_n(t-\eta)\,d\eta \\ &\quad + \sum_{n=1}^{\infty} \frac{y_n(x)}{\lambda_n} \int_0^a y_n(\xi)\left\{\int_0^t \mathrm{P}(\xi,\eta)e^{a\eta}\sin\lambda_n(t-\eta)\,d\eta\right\} d\xi \\ &= \mathrm{S}_1+\mathrm{S}_2+\mathrm{S}_3 \quad \text{(say)}. \quad (26) \end{aligned}$$

The second infinite sum in (26) may be written in the form

$$\begin{aligned} \mathrm{S}_2 &= e^{at} \sum_{n=1}^{\infty} \frac{y_n(x)}{\lambda_n^2+a^2} \int_0^a q(\xi)y_n(\xi)\,d\xi \\ &\quad - \sum_{n=1}^{\infty} \frac{y_n(x)}{\lambda_n^2+a^2}\left(\frac{a}{\lambda_n}\sin\lambda_n t+\cos\lambda_n t\right)\int_0^a q(\xi)y_n(\xi)\,d\xi. \quad (27) \end{aligned}$$

* See formula (9), A. N. L.

Also, in view of the differential equation and the boundary conditions satisfied by y_n, we ultimately get

$$\int_0^a q(\xi)y_n(\xi)\,d\xi = -(\lambda_n^2+\alpha^2)\int_0^a \delta f(\xi)y_n(\xi)\,d\xi. \quad . \quad (28)$$

Thus (27) becomes

$$S_2 = -e^{\alpha t}\sum_{n=1}^{\infty} y_n(x)\int_0^a \delta f(\xi)y_n(\xi)\,d\xi$$

$$+\sum_{n=1}^{\infty}\left(\frac{a}{\lambda_n}\sin\lambda_n t+\cos\lambda_n t\right)y_n(x)\int_0^a \delta f(\xi)y_n(\xi)\,d\xi. \quad (27')$$

If we assume that $f(x)$ is piecewise continuous and twice differentiable, it is clear that the first term in (27′) is identically $=-e^{\alpha t}f(x)$. Therefore, in view of (6), (26), and (27′), our desired solution becomes

$u(x, t)$

$$= e^{-\alpha t}\sum_{n=1}^{\infty}\frac{\sin\lambda_n t}{\lambda_n}y_n(x)\left\{\int_0^a \delta g(\xi)y_n(\xi)\,d\xi+\int_0^a a\delta f(\xi)y_n(\xi)\,d\xi\right\}$$

$$+e^{-\alpha t}\sum_{n=1}^{\infty} y_n(x)\cos\lambda_n t\int_0^a \delta f(\xi)y_n(\xi)\,d\xi$$

$$+e^{-\alpha t}\sum_{n=1}^{\infty}\frac{y_n(x)}{\lambda_n}\int_0^a y_n(\xi)\left\{\int_0^t e^{\alpha\eta}\mathrm{P}(\xi,\eta)\sin\lambda_n(t-\eta)\,d\eta\right\}d\xi.$$

$$. \quad . \quad . \quad (28)$$

This is the complete solution of the system (1) to (5). For $\mathrm{P}(x, t)\equiv 0$ (28) yields a well-known result *.

Section II.—*Forced Vibration of a Non-uniformly Loaded String in Vacuum.*

Assuming that the string carries a number of concentrated loads $m_1, m_2, \ldots m_s$ at the points of abscissæ $a_1, a_2, \ldots a_s$, the displacement $u(x, t)$ must satisfy the equations:

$$\mathrm{P}\frac{\partial^2 u}{dx^2} = \delta\frac{\partial^2 u}{\partial t^2}-\mathrm{P}(x, t), \qquad t>0, \quad . \quad . \quad (1)$$

$$\lim_{t\to 0} u(x, t)-f(x) = \lim_{t\to 0}\frac{\partial}{\partial t}u(x, t) = 0, \quad . \quad . \quad . \quad . \quad . \quad (2\text{–}3)$$

* Riemann-Weber, 'Differenzialgleichungen der Physik,' vol. i. chap. xviii.; vol. ii. chap. xix. (1927).

$$u(a_i-0,t)=u(a_i+0,t), \qquad i=1,2,\ldots s, \quad (4)$$

$$m_i\left(\frac{\partial^2 u}{\partial t^2}\right)_{x=a_i}=p\left|\frac{\partial}{\partial x}u(x,t)\right|_{x=a_i-0}^{x=a_i+0}, \quad i=1,2,\ldots s, \quad (5)$$

$$\frac{\partial u}{\partial x}-h_0 u=0, \qquad x=0, \quad . \quad . \quad . \quad . \quad . \quad . \quad . \quad . \quad (6)$$

$$\frac{\partial u}{\partial x}+h_1 u=0, \qquad x=a, \quad . \quad . \quad . \quad . \quad . \quad . \quad . \quad . \quad (7)$$

where we have assumed that the velocity vanishes at $t=0$ for all points of the string. Further, we assume that $f(x)$ satisfies the conditions of Section I., has a continuous first derivative in the interval $0-a$, and satisfies the boundary conditions (6) and (7).

Let us make again the substitution

$$u(x,t)=f(x)+v(x,t); \quad . \quad . \quad . \quad . \quad . \quad . \quad (8)$$

then the function $v(x,t)$ must satisfy the equations

$$p\frac{\partial^2 v}{\partial x^2}=\delta\frac{\partial^2 v}{\partial t^2}-pf''(x)-\mathrm{P}(x,t), \quad t>0, \quad . \quad . \quad (1')$$

$$\operatorname*{Lim}_{t\to 0} v(x,t)=\operatorname*{Lim}_{t\to 0}\frac{\partial}{\partial t}v(x,t)=0, \quad . \quad . \quad . \quad . \quad . \quad . \quad (2'\text{–}3')$$

$$v(a_i-0,t)=v(a_i+0,t), \qquad i=1,2,\ldots s, \quad (4')$$

$$m_i\left(\frac{\partial^2 v}{\partial t^2}\right)_{x=a_i}=p\left|\frac{\partial}{\partial x}v(x,t)\right|_{x=a_i-0}^{x=a_i+0}, \quad i=1,2,\ldots s, \quad (5')$$

$$\frac{\partial v}{\partial x}-h_0 v=0, \qquad x=0, \quad . \quad . \quad . \quad . \quad . \quad . \quad . \quad . \quad (6')$$

$$\frac{\partial v}{\partial x}+h_1 v=0, \qquad x=a. \quad . \quad . \quad . \quad . \quad . \quad . \quad . \quad (7')$$

If we define, in the usual manner,

$$y(x,\lambda)=\mathrm{L}\{v(x,t)\} \quad \text{and} \quad \mathrm{Q}(x,\lambda)=\mathrm{L}\{\mathrm{P}(x,t)\},$$

then the function $y(x,\lambda)$ must satisfy the equations

$$py''=\delta\lambda^2 y-pf''(x).\frac{1}{\lambda}-\mathrm{Q}(x,\lambda), \quad . \quad . \quad . \quad (9)$$

$$y(a_i-0)=y(a_i+0), \qquad i=1,2,\ldots s, \quad (10)$$

$$m_i\lambda^2 y(a_i) = p\left|\frac{\partial y}{\partial x}\right|_{a_i-0}^{ai+0}, \quad i=1, 2, \ldots s, \quad (11)$$

$$y'(0) - h_0 y(0) = 0, \quad . \quad . \quad . \quad . \quad . \quad (12)$$

$$y'(a) + h_1 y(a) = 0. \quad . \quad . \quad . \quad . \quad . \quad (13)$$

The system (9) to (13) differs from the system (17) to (19) in Sect. I. in that it involves the additional boundary conditions (11) which contain the arbitrary parameter λ. Let $G(x, \xi, \lambda)$ be the Green function defined as the solution of the homogeneous differential equation

$$py''(x) - \delta\lambda^2 y(x) = 0, \quad . \quad . \quad . \quad . \quad . \quad (14)$$

satisfying the boundary conditions (10) to (13), and the usual discontinuity condition

$$\frac{\partial}{\partial x} G(x, \xi, \lambda)\left|\frac{\xi+0}{\xi-0}\right. = -\frac{1}{p}. \quad . \quad . \quad . \quad . \quad . \quad (15)$$

Then we may write the solution of the system (7) to (13) in the form

$$y(x, \lambda) = \int_0^a G(x, \xi, \lambda)\left\{\frac{p}{\lambda} f''(\xi) + Q(\xi, \lambda)\right\} d\xi, \quad . \quad (16)$$

as can be verified by direct substitution. Furthermore, it has been shown * that the expansion

$$G(x, \xi, \lambda) = \sum_{n=1}^{\infty} \frac{y_n(x) y_n(\xi)}{\lambda_n^2 + \lambda^2} \quad . \quad . \quad . \quad (17)$$

is valid, provided the y_n's satisfy the loaded orthogonality and normalizing conditions

$$\int_0^a \delta y_m(\xi) y_n(\xi)\, d\xi + \sum_{i=1}^{s} m_i y_n(a_i) y_m(a_i) = \begin{cases} 0 \text{ if } m \neq n, \\ 1 \text{ if } m = n. \end{cases} \quad . \quad (18)$$

In view of (8) and (18) we obtain from (16), by the usual process of inversion of the Laplace Transformation and with the aid of Borel's theorem, previously mentioned,

$$u(x, t) = f(x) + p \sum_{n=1}^{\infty} \frac{y_n(x)}{\lambda_n} \int_0^a f''(\xi) y_n(\xi)\, d\xi \int_0^t \sin \lambda_n (t-\eta)\, d\eta$$

$$+ \sum_{n=1}^{\infty} \frac{y_n(x)}{\lambda_n} \int_0^a y_n(\xi)\, d\xi \int_0^t P(\xi, \eta) \sin \lambda_n (t-\eta)\, d\eta,$$

* J. Teichmann, 'Mechanische Probleme die auf belastete Integralgleichungen fuhren,' Dissertation (Breslau, 1919).

where the summation is extended over the characteristic values of the system (14), (10), (11), (12), and (13), and the corresponding characteristic functions normalized in accordance with (18). This is the complete solution of the system (1) to (7).

Section III.—*Electrical Oscillations in Transmission Lines.*

It is well known that when electromagnetic disturbances are propagated along a cable or a transmission line the current i and the voltage p may be expressed in the form

$$i=-\mathrm{C}\frac{\partial \mathrm{W}}{\partial t}, \quad p=\frac{\partial \mathrm{W}}{\partial x}, \quad . \quad . \quad . \quad . \quad (1)$$

provided $\mathrm{W}(x,t)$ satisfies the telegraphic differential equation

$$\frac{\partial^2 \mathrm{W}}{\partial x^2}=\omega \mathrm{C}\frac{\partial \mathrm{W}}{\partial t}+\mathrm{LC}\frac{\partial^2 \mathrm{W}}{\partial t^2}, \quad . \quad . \quad . \quad . \quad (2)$$

where ω=ohmic resistance per unit length, C=capacity per unit length, and L=self-inductance per unit length.

Solutions of (2) for the case of an infinitely long cable were given by Poincaré*, Boussinesq †, Picard ‡, Heaviside §, and Wiener ‖.

For the case of the finite cable whose ends are connected to specified circuits approximate solutions were obtained by K. W. Wagner ¶, the approximation consisting in assuming that the damping coefficient is negligibly small compared to the frequencies of the constituent oscillations, or, what amounts to the same thing, that the velocity of propagation of the oscillations is independent of wave-length.

By means of the method employed in the previous sections it is possible to derive exact solutions for a large number of practical problems encountered in the study of the electromagnetic disturbunces in transmission lines and

* *Comptes Rendus*, cxvii. p. 1072 (1893).
† *Comptes Rendus*, cxviii. p. 162 (1894),
‡ *Comptes Rendus*, cxviii. p. 16 (1894).
§ Phil. Mag. (1888) and Coll. Papers.
‖ "Theory of Transient Oscillations in Electrical Networks and Transmission Lines," Trans. A. I. E. E. 1919.
¶ 'Electromagnetische Ausgleichsvorgänge in Kabeln' (Leipzig, 1908).

their electrical behaviour under the influence of atmospheric electricity.

The method will be illustrated by the following problem:—

Consider the case of a long transmission line open at both ends. When struck by lightning the line acquires a charge $q(x)$, corresponding to which there is a potential difference distribution $\phi(x) = \frac{1}{C} q(x)$. For a short period of time the line will be the seat of electrical oscillations, a steady state being ultimately reached when the charge is distributed uniformly, and, therefore, the potential difference is

$$E = \frac{1}{a} \int_0^a \phi(x)\, dx.$$

It is clear that the current and the voltage during the interval of time before a steady state has been reached must satisfy the following initial and boundary conditions:

$$\lim_{t \to 0} i(x,t) = -C \lim_{t \to 0} \frac{\partial}{\partial t} W(x,t) = 0, \quad . \quad . \quad (3)$$

$$\lim_{t \to 0} p(x,t) = \lim_{t \to 0} \frac{\partial}{\partial x} W(x,t) = \phi(x), \quad . \quad . \quad . \quad (4)$$

$$i(o,t) = -C \frac{\partial}{\partial t} W(o,t) = 0, \quad . \quad . \quad . \quad . \quad (5)$$

$$i(a,t) = -C \frac{\partial}{\partial t} W(a,t) = 0. \quad . \quad . \quad . \quad . \quad (6)$$

To solve the system (1) to (6) let us make the substitution

$$W(x,t) = v(x) + e^{-\alpha t} u(x,t), \quad . \quad . \quad . \quad . \quad (7)$$

where

$$\alpha = \frac{1}{2} \frac{\omega}{L} \quad \text{and} \quad v(x) = \int_0^x \phi(x)\, dx.$$

The function $u(x,t)$ must then satisfy the following equations:

$$\frac{\partial^2 u}{\partial x^2} + \alpha^2 LC u = LC \frac{\partial^2 u}{\partial t^2} - e^{\alpha t} v''(x), \quad . \quad . \quad . \quad (8)$$

$$\lim_{t\to 0} u(x,t) = \lim_{t\to 0} \frac{\partial}{\partial t} u(x,t) = 0, \quad . \quad . \quad (9\text{–}10)$$

$$\frac{\partial u}{\partial t} - \alpha u = 0, \qquad x = 0, \quad . \quad . \quad . \quad . \quad . \quad (11)$$

$$\frac{\partial u}{\partial t} - \alpha u = 0, \qquad x = a. \quad . \quad . \quad . \quad . \quad (12)$$

If we subject the system (8–12) to the Laplace Transformation, and make use of the identities ((15)–(16), Sect. I.) and of (9–10), it is readily seen that the function $y(x,\lambda) = \mathrm{L}\{u(x,t)\}$ must satisfy the system of equations

$$y''(x) + (\alpha^2 - \lambda^2)\mathrm{L}Cy = -\frac{1}{\lambda - \alpha}\phi'(x), \quad . \quad . \quad (13)$$

$$y(0) = y(a) = 0, \quad . \quad . \quad . \quad . \quad . \quad (14\text{–}15)$$

the solution of which is

$$y(x,\lambda) = \int_0^a \mathrm{G}(x,\xi,\lambda)\phi'(\xi)\frac{1}{\lambda - \alpha}\,d\xi, \quad . \quad . \quad (16)$$

where $\mathrm{G}(x,\xi,\lambda)$ is the Green function defined in the usual manner.

From (16), by the process of inverisonof the Laplace Transformation, we ultimately get

$$u(x,t) = \sum_{n=1}^{\infty} \frac{y_n(x)}{\lambda_n} \cdot \int_0^a \phi'(\xi) y_n(\xi)\,d\xi \cdot \int_0^t e^{\alpha\eta} \sin \lambda_n (t-\eta)\,d\eta$$

$$= e^{\alpha t} \sum_{n=1}^{\infty} \frac{y_n(x)}{\lambda_n^2 + \alpha^2} \int_0^a \phi'(\xi) y_n(\xi)\,d\xi$$

$$- \sum_{n=1}^{\infty} \frac{y_n(x)}{\lambda_n^2 + \alpha^2}\left(\frac{\alpha}{\lambda_n}\sin \lambda_n t + \cos \lambda_n t\right) \int_0^a \phi'(\xi) y_n(\xi)\,d\xi.$$

. . . (17)

Making use of the identities

$$v(x) = \int_0^x \phi(x)\,dx = \sum_{n=1}^{\infty} y_n(x) \int_0^a \mathrm{L}Cv(\xi) y_n(\xi)\,d\xi, \quad (18)$$

$$\int_0^a v''(\xi) y_n(\xi)\,d\xi = -v(a) y_n'(a) - (\lambda_n^2 + \alpha^2) \int_0^a \mathrm{L}Cv(\xi) y_n(\xi)\,a\xi,$$

. . . (19)

$$\sum_{n=1}^{\infty} \frac{y_n(x) y_n'(a)}{\lambda_n^2 + \alpha^2} = \left|\frac{\partial}{\partial \xi}\mathrm{G}(x,\xi,\lambda)\right|_{\xi = a,\ \lambda^2 + \alpha^2 = 0} = -\frac{x}{a} \quad (20)$$

(indeed, for $\lambda_n^2+\alpha^2=0$, G reduces to $\frac{x}{a}(a-\xi)$), our solution (7) ultimately becomes

$$W(x,t)=\frac{x}{a}v(a)+e^{-\alpha t}\sum_{n=1}^{\infty}\left(\frac{\alpha}{\lambda_n}\sin\lambda_n t+\cos\lambda_n t\right)y_n(x)$$
$$\left\{\frac{y_n'(a)v(a)}{\lambda_n^2+\alpha^2}+\mathrm{LC}\int_0^a v(\xi)y_n(\xi)\,d\xi\right\}, \quad . \quad . \quad (21)$$

where the summation extends over the characteristic values of the system

$$y''+(\alpha^2+\lambda^2)\mathrm{LC}y=0, \quad . \quad . \quad . \quad . \quad . \quad (22)$$
$$y(0)=y(a)=0, \quad . \quad . \quad . \quad (23\text{–}24)$$

and the corresponding characteristic functions normalized in accordance with

$$\int_0^a \mathrm{LC}\{y_n(\xi)\}^2\,d\xi=1. \quad . \quad . \quad . \quad . \quad . \quad (25)$$

In (1) and (21) we have the complete solution of our problem.

It may be remarked that

$$\lim_{t\to\infty}p(x,t)=\frac{1}{a}v(a)=\frac{1}{a}\int_0^a\phi(x)\,dx=\mathrm{E},$$

this being in agreement with the above statement regarding the steady state.

XCV. *Electrometric Measurement of Röntgen Energy.* *By* N. Waterman *and* H. Limburg, *Laboratory of the Antoni van Leeuwenhoekhuis, Amsterdam* *.

[Plates XXII. & XXIII.]

In a communication in the *Biochemische Zeitschrift* we indicated a method by which it is possible to measure the emitted Röntgen energy by the change of the so-called redox-potential in reversible and probably irreversible chemical systems.

The experiments described in that communication showed that the potential difference between a platinum

* Communicated by the Authors.

electrode and a solution of, *e. g.*, methylene-blue in which it was dipped changed in a rather complicated manner under the influence of Röntgen rays : an initial rather rapid change of the potential difference is followed by a slower change, which to a first approximation is independent of the concentration of the dissolved substance. The first rapid change was called the " electrode effect."

More careful analysis of the phenomena has shown us that the changes of the potential difference in the first moments after starting the irradiation are completely governed by the energy of the Röntgen rays acting on the system. Inversely it must be possible, as we already supposed in our former communication, to measure the intensity of the irradiation by the initial change of potential in suitable systems *. We believe that the following data fully justify this assumption.

Technical.

The determinations were made with a half-cell consisting of a platinum electrode, dipping into a 0·01 per cent. solution of methylene-blue in a phosphate buffer of P_H 6·8. Although this half-cell may be coupled with, *e. g.*, a calomel-electrode, it appeared to be more simple to combine it with an identical half-element, both enclosed in a twin electrode vessel as shown by fig. 1.

The well-cleaned electrode vessel with well-cleaned electrodes is carefully filled with the methylene-blue solution in a phosphate solution of P_H6·8, after which the air is completely expelled from the vessel by an oil- or diffusion-pump and the vessel closed by melting off the side-tube. The level of the fluid must be so high as to establish contact between the two parts.

As will be clear the initial electromotive force of the cell must be zero.

The potential difference is measured by a potentiometric † method. After every determination the apparatus must be shaken, to eliminate the polarization arisen from the irradiation. After this polarization is eliminated the measuring can be repeated.

* For the moment we will not dilate further on the possible influence of the wave-length of the Röntgen rays on the phenomena.

† It would be better to use a static method, which we, however, had not at our disposition.

On the photos (Pls. XXII. & XXIII.) the arrangement is shown whereby the irradiated part of the electrode is placed in the centre of the bundle, at a *fixed distance* from the anticathode. For this purpose the entire apparatus is fastened with a screw to the Röntgen apparatus. Parallel with the screw is fixed a screen of lead, which can be withdrawn when the irradiation has to begin. In this way the commencement of the irradiation is known to

Fig. 1.

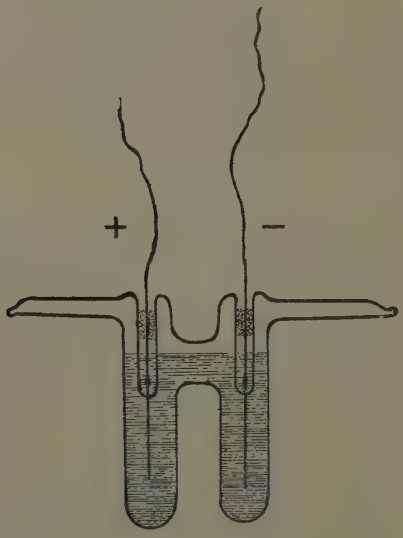

within the value of a second. In quantitative measurements this precaution is necessary, as will be evident by our results. In our arrangement the screen turns on an eccentric, so that from outside the Röntgen room it may be withdrawn by pulling a little cord running on a pulley and returned again to its original position.

Results.

The preliminary conclusions given in our first communication were amply confirmed. As is brought out fully by

the slope of the curves reproduced here (fig. 5) we have to distinguish between a preliminary "electrode effect" strictly dependent on the energy to which the chemical system is subjected and a secondary process which, as we elucidated in our first communication, afterwards continues at a rate as given by the formula of a monomolecular reaction.

Both phases are well represented by the curves. And we may add now to our former conclusions that only the former, the electrode effect, is quantitatively equivalent to the emitted energy, and gives thus the exact figure of this energy. This is proved in a striking

Fig. 5.

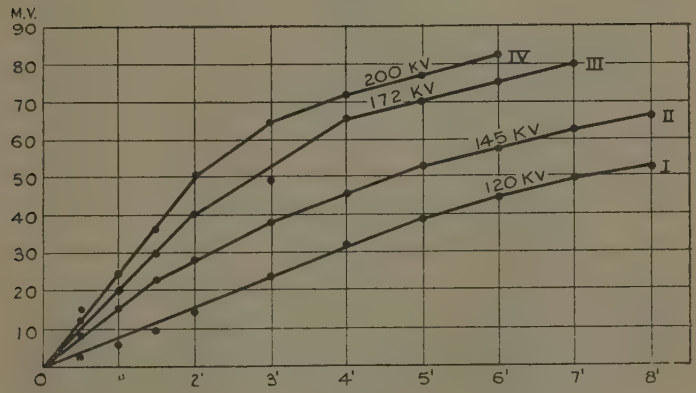

Curve 1.—I. 120 kv.; II. 145 kv.; III. 172 kv.; IV. 200 kv.

way, *in so far as the values of the potential differences at a given moment expressed in millivolts are equivalent to the square values of the kilovoltages*, whereby the rays are generated, with the condition that the glow-current is held constant.

This is well borne out by Table I.

When every precaution has been taken, when the distance to the anticathode is kept strictly constant, and there is no scattering of Röntgen rays, there will be concordance within a limit of 5 per cent. between observation and calculated value.

It may be claimed that this method, which certainly is still capable of improvement, may be regarded as a

simple way of measuring Röntgen-ray emittance. We will not discuss here if such a new method is needed at the present moment, in view of the highly perfectioned ionization methods in use at present. In any case it may be claimed that the method is a cheap one.

The theoretical data, however, seem to us of more importance yet. The method described has been applied

TABLE I.

The Figures indicate the Electromotive force in Millivolts.

(M.A. = 3). The absolute values of the constants are dependent on the individual apparatus.

(1)

Time.	138 kv.	145 kv.	165 kv.	180 kv.
$\frac{1}{4}'$	(4)	4	4	5
$\frac{1}{2}'$	6·5	7·5	8	10
$1'$	11	15	16	20·5
$1\frac{1}{2}'$	16·5	21	24	30
$2'$	21	26·5	31	38
$\frac{\text{mv. } 1'}{(\text{kv.})^2} \cdot 10^4$....	5·8	7·1	5·8	6·3
$\frac{\text{mv. } 2'}{(\text{kv.})^2} \cdot 10^4$....	11·1	12·6	11·4	11·7

(2)

Time.	138 kv.	145 kv.	165 kv.	180 kv.
$\frac{1}{4}'$	..	7	16	(10)
$\frac{1}{2}'$	..	15	18	24
$1'$	..	28	41	51
$1\frac{1}{2}'$	..	46	61	68
$2'$	..	59	76	87
$\frac{\text{mv. } 1'}{(\text{kv.})^2} \cdot 10^4$....	..	13·3	15·1	15·7
$\frac{\text{mv. } 2'}{(\text{kv.})^2} \cdot 10^4$....	..	28·1	27·9	26·9

TABLE I. (*cont.*).

(3)

Time.	120 kv.	145 kv.	137 kv.*	172 kv.	183 kv.	200 kv.
½′	−3	−9	−11	12	−18	−15
½′	6	16	15	20	27	..
1½′	10	23	19·5	29·5	38	36
2′	15	28	24	41	45	51
3′	24	38	31	49	56	65
4′	32	46	35	65	65	72
5′	39	53	39	70	68	77
6′	45	58	43	75	70	83
7′	50	63	47	80	..	..
8′	53	66	..	..	..	..
$\frac{\text{mv. } 2'}{(\text{kv.})^2} \cdot 10^4$ ..	10·4	13·3	12·8	13·8	13·4	12·8
$\frac{\text{mv. } 3'}{(\text{kv.})^2} \cdot 10^4$ ..	16·6	18·1	16·4	16·6	16·7	16·2

* New transformer in the Röntgen apparatus.

TABLE II.

Time.	165 kv.	180 kv.
15″	5·5	..
30″	10·5	13
45″	..	17·5
1′	17	20
1½′	19·5	23
2	23	26
$\frac{\text{mv. } 1'}{(\text{kv.})^2} \cdot 10^4$	6·25	6·17
$\frac{\text{mv. } 2'}{(\text{kv.})^2} \cdot 10^4$	8·45	8·03

so far to the methylene-blue solutions. Other chemical systems, however, may prove equally or even more useful (quinone-hydroquinone etc.). We will merely

give some data concerning the reaction of rongalite-white, the leucoproduct of methylene-blue, as they are so far interesting that they show that the leucoproduct is *oxidized* by the same rays which *reduce* the methylene-blue. Here also the reaction velocity depends quantitatively on the square of the kilovoltage.

It may be remarked that in the rongalite system the electrode effect is of still shorter duration than in methylene blue.

Conclusions.

1. The conclusions arrived at in our communication in the *Biochemische Zeitschrift* are confirmed.
2. The electrochemical effects of Röntgen rays are to be distinguished in two different actions, viz., an "electrode effect" and a secondary process.
3. The "electrode effect" depends quantitatively on the energy which is received by the chemical system, and may serve as the measure of this.
4. A practical form of apparatus for this kind of determinations is described.

Literature.

Waterman, N., and Limburg, H., *Biochemische Zeitschrift*, Bd. cclxiii. Heft. 4/6, p. 400 (1933).

XCVI. *On the Laminar Flow of a Viscous Fluid with Vanishing Viscosity.* *By* H. B. Squire, *Beit Research Fellow**.

I.

THE paradox that a perfect fluid offers no resistance to the steady motion of a body through it is very ancient, and there are two general explanations why the motion of a fluid with small viscosity does not closely resemble that of a perfect fluid. One explanation is that the flow becomes turbulent as the viscosity decreases, so that a finite amount of energy, which must be supplied by external forces, is always being dissipated. The other is that the solutions of the equations for the steady motion

* Communicated by the Author.

of a viscous fluid do not tend, as ν tends to zero, to the functions which are obtained by putting ν equal to zero in the equations before solving them.

It is with the latter viewpoint that this paper is concerned. While it is not so generally held as the former, it is the basis of Oseen's asymptotic theory *, the results of which are in qualitative agreement with experiment. This theory is based on the reduction of the equations to a linear type by the substitution of the undisturbed for the disturbed velocities in certain of the terms. The equations are solved, and ν is then put equal to zero. It is found that the stream-lines do not close up behind the body, but that free stream-lines leave it tangentially and run parallel to the main flow. The pressure distribution is no longer symmetrical before and behind the body and a resistance is offered to the motion.

Zeilon † has extended Oseen's theory and has obtained a pressure distribution round a circular cylinder moving uniformly which is in close agreement with the experimental results. His modifications of Oseen's theory are rather arbitrary and reduce its mathematical interest.

Another conclusion as to the character of fluid flow for vanishing viscosity was reached by Burgers ‡ who used a simplified boundary-layer theory to investigate the flow past a circular cylinder. As usual, an arbitrary function is available which determines the velocity distribution at the outside of the boundary layer; Burgers took this to be the function corresponding to irrotational flow. He found that breakaway occurs at an angular distance of 120° from the front stagnation point. When, however, the coefficient of viscosity tends to zero the solution approaches the solution for irrotational flow and no resistance is offered to the motion.

It is proposed to investigate by Burgers' method the limiting flow past a circular cylinder which would be obtained if the available arbitrary function were successively given values corresponding to potential flow with a free stream-line; this discontinuous flow is uniquely determined when the point of breakaway of the free stream-line is known. By this method we reach a con-

* A full account of this theory is given in Oseen's 'Hydrodynamik' (Leipzig, 1927).

† Appendix II. to Oseen's 'Hydrodynamik.'

‡ *Kon. Ak. Wet. Amst.* xxiii. p. 1082 (1921).

clusion as to the nature of the laminar flow of a fluid with vanishing viscosity which seems less open to objection than Burgers' and Oseen's. The discordance between this conclusion and the experimental results is due to the restriction of the theory to laminar flow.

II.

The fluid is incompressible and motion is restricted to two dimensions. The origin is taken at the centre of the cylinder, and the axis of x is in the direction of the main stream, which has uniform velocity V at infinity.

The equation satisfied by the vorticity ζ is

$$\frac{\partial \zeta}{\partial t}+u\frac{\partial \zeta}{\partial x}+v\frac{\partial \zeta}{\partial y}=\nu\nabla^2\zeta, \quad \ldots \quad (1)$$

where u and v are the component velocities in the directions Ox and Oy respectively. We further limit the analysis to steady motion, for which the first term in (1) vanishes.

This equation is now reduced to a linear form by putting

$$u=\frac{\partial \alpha}{\partial x}, \quad v=\frac{\partial \alpha}{\partial y},$$

where they occur explicitly; α is some undetermined harmonic function having a conjugate harmonic function β. Equation (1) becomes

$$\frac{\partial \alpha}{\partial x}\cdot\frac{\partial \zeta}{\partial x}+\frac{\partial \alpha}{\partial y}\cdot\frac{\partial \zeta}{\partial y}=\nu\nabla^2\zeta. \quad \ldots \quad (2)$$

The coordinates may now be changed from x, y to α, β*. If z stands for $x+iy$, w for $\alpha+i\beta$, we have in the usual notation

$$h^2=\left|\frac{dw}{dz}\right|^2=\left(\frac{\partial \alpha}{\partial x}\right)^2+\left(\frac{\partial \alpha}{\partial y}\right)^2, \quad \ldots \quad (3)$$

and the relations

$$\frac{\partial \alpha}{\partial x}\cdot\frac{\partial}{\partial x}+\frac{\partial \alpha}{\partial y}\cdot\frac{\partial}{\partial y}=h^2\frac{\partial}{\partial \alpha},$$

$$\frac{\partial^2}{\partial x^2}+\frac{\partial^2}{\partial y^2}=h^2\left[\frac{\partial^2}{\partial \alpha^2}+\frac{\partial^2}{\partial \beta^2}\right]$$

* This transformation was first suggested by Boussinesq in his treatment of heat conduction (*Journal de Math.* (6) i. p. 285 (1905)). It was applied by Burgers to the flow of a viscous fluid (*Kon. Ak. Wet. Amst.* xxiii. p. 1082 (1921)). A full account of its use is given in a joint paper by Professor Southwell and the writer (Phil. Trans A, ccxxxii. p. 27 (1933)).

hold. Equation (2) takes the form

$$\frac{\partial \zeta}{\partial \alpha} = \nu \left[\frac{\partial^2}{\partial \alpha^2} + \frac{\partial^2}{\partial \beta^2} \right] \zeta. \quad . \quad . \quad . \quad . \quad (4)$$

We shall now define α and β to be respectively the velocity potential and stream-function of the irrotational flow past the cylinder. They may, however, be discontinuous functions analogous to Kirchhoff's solution * for flow past a flat plate which is perpendicular to the main stream.

We assume that ν is a small quantity, which allows a further modification of equation (4). The effects of viscosity will only be important, as in the Prandtl boundary-layer theory, in a thin layer surrounding the cylinder. Within this layer the velocity rises from zero at the surface of the cylinder to a finite value at the outside of it, which requires that derivatives with respect to β shall be much greater than derivatives with respect to α. Thus we may neglect the term $\frac{\partial^2 \zeta}{\partial \alpha^2}$ in equation (4) in comparison with $\frac{\partial^2 \zeta}{\partial \beta^2}$, and take the governing equation to be

$$\frac{\partial \zeta}{\partial \alpha} = \nu \frac{\partial^2 \zeta}{\partial \beta^2}. \quad . \quad . \quad . \quad . \quad . \quad . \quad (5)$$

The boundary conditions require that there shall be no slipping at the surface of the cylinder and that the motion shall become irrotational at the outside of the boundary layer.

In the (α, β) plane the cylinder stretches on the α-axis from $(\alpha_1, 0)$ to $(\alpha_2, 0)$; the main flow is a uniform stream of velocity V in the direction of α increasing. When the cylinder is a flat plate lying parallel to the stream the (α, β) plane is identical with the (x, y) plane. This case has already been treated in detail by Piercy and Winny † and by Burgers ‡, who has carried out a second approximation.

* *Cf.* Lamb, 'Hydrodynamics,' 5th ed. § 75.
† Proc. Roy. Soc. A, cxl. p. 543 (1933).
‡ *Kon. Ak. Wet. Amst.* xxxiii. p. 605 (1930).

III.

Following Burgers we take for the solution of (5) for $\beta > 0$ (the upper half of the cylinder)

$$\zeta = -\int_{\alpha_1}^{\alpha} d\alpha' . \frac{f(\alpha')}{\sqrt{\pi\nu(\alpha-\alpha')}} . \exp \frac{-\beta^2}{4\nu(\alpha-\alpha')}; \quad . \quad (6)$$

the same expression with the sign changed holds for $\beta < 0$.

We have also

$$\zeta = -\frac{\partial u_s}{\partial n},$$

where u_s is the velocity in the boundary layer parallel to the surface and n is the outward-drawn normal; when the boundary layer is sufficiently thin

$$dn = \frac{d\beta}{h},$$

where h is the velocity of the potential flow. Hence for the velocity in the boundary layer we have

$$u_s = -\int_0^n \zeta \, dn = -\frac{1}{h}\int_0^{\beta} \zeta \, d\beta,$$

$$= \frac{1}{h}\int_{\alpha_1}^{\alpha} d\alpha' . f(\alpha') . \operatorname{erf} \frac{\beta}{\sqrt{4\nu(\alpha-\alpha')}} . \quad . \quad (7)$$

This expression vanishes on the surface of the cylinder $\beta = 0$.

As β increases indefinitely u_s must tend to h, the velocity of the potential flow, whence the relation

$$h^2 = \int_{\alpha_1}^{\alpha} d\alpha' . f(\alpha')$$

must hold, since the error function tends to unity as β tends to infinity. From this we obtain

$$f(\alpha) = \frac{d(h^2)}{d\alpha} . \quad . \quad . \quad . \quad . \quad . \quad . \quad . \quad (8)$$

IV.

We shall apply the above to the investigation of the flow past a circular cylinder. The potential flow is given by

$$\alpha = Vx\left(1+\frac{a^2}{r^2}\right), \quad \beta = Vy\left(1-\frac{a^2}{r^2}\right). \quad . \quad . \quad (9)$$

In the (α, β) plane the stagnation points have coordinates $(-2a\mathrm{V}, 0)$ and $(2a\mathrm{V}, 0)$; at the surface of the cylinder $\beta = 0$

$$h^2 = 4\mathrm{V}^2\left(1 - \frac{\alpha^2}{4a^2\mathrm{V}^2}\right),$$

and hence equation (8) gives for the function $f(\alpha)$, which governs the vorticity distribution,

$$f(\alpha) = -\frac{2a}{a^2}.$$

We have now, from (6), for the vorticity at the surface of the cylinder $\beta = 0$,

$$\zeta = \int_{-2a\mathrm{V}}^{\alpha} \frac{2\alpha\, d\alpha'}{a^2\sqrt{\pi\nu(\alpha - \alpha')}} = \frac{8}{3a^2}\cdot\frac{(a\mathrm{V}-\alpha)(\alpha+2a\mathrm{V})^{\frac{1}{2}}}{(\pi\nu)^{\frac{1}{2}}}.$$

From this we deduce immediately the position of the point of breakaway at which ζ vanishes. This occurs for $\alpha = a\mathrm{V}$, giving $\theta = 120°$, where θ is the angle round the cylinder measured from the front stagnation point.

V.

This is as far as Burgers has carried the analysis, which he has illustrated by diagrams. He concluded that, as the value of Reynolds's number tended to infinity, the flow would more and more closely resemble the ordinary potential flow with the addition of an axial vortex sheet behind the cylinder. But breakaway of the boundary layer always takes place at the same points, and it would only be correct to conclude that the ordinary potential flow is the limit of viscous flow if, on increasing the value of Reynolds's number, the points of breakaway moved towards the rear stagnation point and eventually coincided with it. It is more satisfactory physically to choose a potential function in place of (9) for which breakaway takes place at the points given by our previous solution, and to find the new position of breakaway. This process may then be repeated until a limiting position is obtained. To carry this out we need a knowledge of the discontinuous potentials corresponding to breakaway at different points on the circumference of the circular boundary.

VI.

Levi-Civita * has devised a method for solving problems of discontinuous flow past curved boundaries corresponding to the well-known method for straight boundaries. This has been applied by Brodetsky † and Schmieden ‡ to investigate the flow past a circular cylinder. The former only considered the case for which the curvature of the free stream-line at the point of breakaway is equal to the curvature of the barrier §, while the latter has considered the whole problem in detail

Schmieden has proved that the solution is unique when the breakaway point P is given. As this point P moves along the boundary from the leading stagnation point A no solutions exist until P reaches C, for which $\theta = 55°$, since the free stream-lines may not cut the boundary.

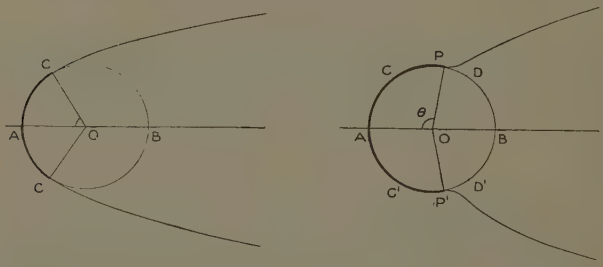

The solution with breakaway at C, for which the curvature of the free stream-line at C is equal to the curvature of the cylinder, is identical with Brodetsky's solution. This is the only case for which the curvature of the free stream-line is not infinite at the breakaway point.

If breakaway takes place between C and D the free stream-line has infinite curvature where it leaves the barrier and one point of inflexion. In every case there is a region of dead water whose width eventually increases parabolically. The stream-line which leaves the cylinder at D, for which $\theta = 120°$, has infinite curvature at D and

* *Rend. Mat. Pal.* xxiii. p. 1 (1907).
† Proc. Roy. Soc. A, cii. p. 542 (1923).
‡ *Ingenieur-Arkiv*, i. p. 104 (1930); iii. p. 356 (1932).
§ Brodetsky states that this makes the problem "real" and of practical use, but it is rather an extra condition which makes the solution unique.

approaches the axis of x asymptotically. For points between D and B, the rear stagnation point, no solutions exist, since a crossing of the free stream-lines would follow, which is inadmissible.

It is necessary for the application of the above potential theory to give a short summary of the Levi-Civita transformation. A full account of this is given in Brodetsky's paper and his notation is adopted here.

The complex variables z and w stand for $x+iy$ and $\alpha+i\beta$ respectively; we introduce also

$$\xi = \frac{dz}{dw} = re^{i\theta},$$

$$\Omega = \log \xi = \log r + i\theta.$$

Further, a new function τ is defined by

$$\sqrt{w} = \left(\tau - \frac{1}{\tau}\right)/2i,$$

from which we have

$$\tau = i\sqrt{w} + \sqrt{(1-w)}.$$

Finally Ω and τ are connected by the relation

$$\Omega = \log \frac{1-\tau}{1+\tau} + A_1\tau + \tfrac{1}{3}A_3\tau^3 + \dots,$$

whence

$$\frac{dw}{dz} = \xi^{-1} = \frac{1+\tau}{1-\tau} \exp[-A_1\tau - \tfrac{1}{3}A_3\tau^3 \dots].$$

Real values of w for which $0 < w < 1$ correspond to the surface of the barrier and real values greater than unity to the free stream-line.

We are only interested in the behaviour of these functions on the surface near the point of breakaway $w=1$, and so we may put

$$w = 1-\epsilon,$$

where ϵ is a small quantity. Then

$$\tau = i + \epsilon^{\frac{1}{2}} - \tfrac{1}{2}i\epsilon + \dots,$$

and

$$\frac{dw}{dz} = \frac{1+i+\epsilon^{\frac{1}{2}}-\frac{1}{2}i\epsilon}{1-i-\epsilon^{\frac{1}{2}}+\frac{1}{2}i\epsilon}\exp[-A_1(i+\epsilon^{\frac{1}{2}})-\tfrac{1}{3}A_3(i+\epsilon^{\frac{1}{2}})^3-\dots],$$

$$=\left(\frac{1+i}{1-i}\right)(1-c_1\epsilon^{\frac{1}{2}}+c_2\epsilon+\dots),$$

where

$$c_1=1+A_1-A_3+A_5-\dots.$$

When $c_1=0$ the curvature of the free stream-line is finite at the point of breakaway; Brodetsky has investigated only the solution satisfying this condition.

VII.

We shall now make use of the above expressions to determine the vorticity distribution round the cylinder when the basic potential flow is discontinuous and of the type described above. For this we need to know the behaviour of h^2 on the surface of the cylinder. We have

$$h^2=\left|\frac{dw}{dz}\right|^2,$$

and hence, near $w=1$,

$$h^2=1-2c_1\epsilon^{\frac{1}{2}}+c_3\epsilon+\dots,$$

where

$$c_3=2c_2+c_1^2.$$

Substituting this in equation (8),

$$f(\alpha)=c_1\epsilon^{-\frac{1}{2}}+c_3=c_1(1-\alpha)^{-\frac{1}{2}}+c_3;$$

for the particular case $c_1=0$, $f(\alpha)$ remains finite as $\alpha\to 1$. The vorticity distribution on the surface of the cylinder $\beta=0$ is

$$\zeta=\int_{\alpha_1}^{\alpha}\frac{d\alpha'}{(\alpha-\alpha')^{\frac{1}{2}}}\left[\frac{c_1}{(1-\alpha')^{\frac{1}{2}}}+c_3\right],$$

and, as $\alpha\to 1$, ζ becomes proportional to $\log(1-\alpha)$ and tends to $-\infty$.

We conclude that the distribution of vorticity, when c_1 does not vanish, begins by being positive and becomes $-\infty$ at the point where the free stream-line of the basic flow leaves the cylinder, and hence that the actual point of breakaway (given by $\zeta=0$) will always lie further upstream than the point of breakaway of the basic flow.

A determination of the position of breakaway by a method of successive approximation will thus give points further and further forward until the limiting position is reached for which the curvature of the free stream-line at the point of breakaway is equal to that of the barrier. Hence the limit of the laminar flow of a viscous fluid past a circular cylinder will be that discontinuous irrotational motion for which the curvature of the free stream-line is finite at the point of breakaway*.

VIII.

The above conclusion is not merely a deduction from modified boundary-layer equation but holds also for the complete boundary-layer theory.

It can be shown that the latter will always give breakaway further upstream than the former. For example, when the pressure distribution outside the boundary layer is the same as for the ordinary potential flow, the complete theory† gives breakaway for $\theta = 110°$, while the modified theory‡ gives $\theta = 120°$. This result is quite general and depends on the particular modification of the complete theory which has been made. This is that the convection of vorticity is taken to be constant throughout the layer instead of falling to zero at the surface of the body, which is what in fact happens. It follows that the fluid is apparently carried farther along the cylinder before breakaway than is actually the case.

Thus the complete boundary-layer theory § will lead to the same conclusion as our modified theory, namely, that as the viscosity tends to zero the flow will tend more and more to approach the type described by Brodetsky, and the resistance will be equal to the value given in his paper.

* If the condition defining the free stream-line were changed a different conclusion would be reached. There is, however, no other condition so satisfactory as that of constant pressure in the wake.

† *Cf.* Falkner and Skan, Phil. Mag. xii. p. 865 (1931).

‡ *Cf.* § III. above.

§ Most solutions of the Prandtl boundary-layer equation have been obtained semi-empirically. The pressure distribution is measured, and it is found that the theory gives correct values for the velocity distribution in the layer. But any deductions of the position of breakaway are meaningless, since this is fixed when the pressure distribution is known. That the point obtained by solution of the equation coincides with the experimental one is useful merely as a verification of the validity of the equation.

The contradiction between this conclusion and the experimental results for very large values of Reynolds's number, which give breakaway on the down-stream side of the cylinder *, is due to the limitation to laminar flow, and shows that a theory of laminar flow will not give results in agreement with those observed. Investigations whose object is to explain the experimental results must deal with the effect of turbulence in the boundary layer and in the wake.

Summary.

The laminar flow of a fluid of small viscosity past a circular cylinder is investigated by means of a modified boundary-layer theory. It is shown that, as the viscosity tends to zero, the motion must approximate to the discontinuous potential flow for which the free stream-line leaves the cylinder with finite curvature. It is further shown that the complete boundary-layer theory would lead to the same conclusion, which does not hold in practice owing to the instability of the laminar flow for large values of Reynolds's number.

XCVII. *Studies in Paramagnetism.*—II. *On the Origin of the term "Δ" in Paramagnetic Salts.* *By* S. Datta, *Ghosh Research Scholar in Physics, Calcutta University* †.

In a previous paper ‡ it has been shown how the magnetic behaviour of ions belonging to the first transition group is remarkably modified owing to the perturbing force of their immediate neighbours, the interaction with which causes a quenching of the orbital magnetic moments of the paramagnetic ions. It has also been mentioned that a second effect of this interaction with neighbouring ions, atoms, or molecules is to cause a deviation from the relation given by Curie for the variation of the susceptibility with temperature, viz., $\chi=c/T$. The experimental results for a large number of paramagnetic salts of the iron group both in solution as well

* *Cf.* Prandtl-Tietjens. 'Hydro-und-Aerodynamik,' ii. p. 113 (Berlin, 1931).

† Communicated by Prof. D. M. Bose.

‡ Phil. Mag. xvii. p. 585 (1934).

as in the solid state are represented well down to a certain critical temperature by the well-known Weiss formula

$$\chi = \frac{c}{T - \Delta},$$

containing the additional term Δ:

Two different types of theory have been developed to account for the origin of the correction term Δ:

(i.) the molecular field theory of Weiss, subsequently modified and further developed by Heisenberg ;

(ii.) as arising out of the distortion of the orbital moment of the magnetic electron in the electric field due to the presence of the surrounding ions, atoms, and molecules. This was first suggested by Cabrera, and later elaborated by Van Vleck, Penny and Schlapp, and others.

The above theories indicate that Δ is independent of the temperature over a large range. Theories have also been developed where it has been assumed that Δ is an empirical constant whose value changes with temperature. In the present paper have been recorded some values of Δ obtained for different types of Co^{++} and Ni^{++} compounds containing the ions in different states of aggregation, viz., in the state of powdered crystals, of hydrated and other complex salts, and in different solutions over a wide range of temperature. As in our experiments the value of Δ was found to remain constant over a fairly wide range of temperature, we will only compare the results of our measurements with the predictions of the first two types of theory, and show how far they are adequate, and try to suggest directions along which the theories have to be modified in order to be made more in accord with the experimental results.

The experimental method and arrangement for the measurement of temperature-variation of susceptibility, from which Δ is determined, have been described in detail in an earlier paper. In the following tables are given the values of Δ for different paramagnetic salts and solutions, together with the ranges of temperature over which measurements have been made and Δ has been found to remain unaltered.

Table I.

Crystal Powders.

Substance.	Δ.	Temp. range.
$CoCl_2$ (anhydrous crystal powder)	+47 *	0° +325° C.
$[Co(H_2O)_6]Cl_2$ (crystal powder)	+ 8	−182° + 33° C.
$[Co(N_2H_4)_2]Cl_2$ (crystal powder).....	+ 9	− 80° + 80° C.
$CoSO_4$ (anhydrous crystal powder).....	−45 †	−196° + 16° C.
$[Co(H_2O)_6]SO_4.H_2O$ (crystal powder) ..	−14 †	−209° + 14° C.
$[Co(N_2H_4)_3]SO_4$ (crystal powder).....	−15	− 80° + 77° C.
$NiCl_2$ (anhydrous crystal powder)	+67 ‡	−210° + 19° C.
$[Ni(H_2O)_6]Cl_2$ (crystal powder)	+24	−182° + 29° C.
$[Ni(N_2H_4)_2]Cl_2$ (crystal powder)	+21	− 80° + 77° C.
$NiSO_4$ (anhydrous crystal powder).....	−79 †	−196° + 16° C.
$[Ni(H_2O)_6]SO_4.H_2O$ (crystal powder) ..	− 3 §	−259° + 17° C.
$[Ni(N_2H_4)_3]SO_4$ (crystal powder)	−40	− 80° + 77° C.

* P. Theodorides. † L. C. Jackson.
‡ H. R. Woltjer. § C. J. Gorter.

Table II.

Solutions.

Substance.	Condition in which measurement is made.	Temp. range.	Δ.
$CoCl_2$..	Anhydrous crystal powder.	....	+47
,,	Hydrated crystal powder	−182° C. + 33° C.*	+ 8
,,	18·3 p.c. solution in dilute HCl (4·5 p.c.).	− 80° C. + 59° C.	+ 5
		+ 59° C. +114° C.	+55
,,	18·5 p.c. solution in concentrated HCl (26 p.c.).	−182° C. − 48° C.	+16
		− 48° C. +113° C.	+50
,,	17·5 p.c. solution in anhydrous ethyl alcohol.	−182° C. − 65° C.	+19
		− 65° C. +100° C.	+45
$NiCl_2$..	Anhydrous crystal powder.	....	+67
,,	Hydrated crystal powder	−182° C. + 29° C.*	+24
,,	22·5 p.c. solution in dilute HCl (7 p.c.).	− 80° C. + 54° C.	+ 5
		+ 54° C. +113° C.	+42
,,	19·4 p.c. solution in concentrated HCl (30 p.c.). ..	− 80° C. + 17° C.	+15
		+ 17° C. +108° C.	+36
,,	22·5 p.c. solution in ethyl alcohol.	−182° C. + 95° C.	+29

* At higher temperatures the salts begin to dissolve in their water of crystallization.

Discussion of Results.

From the tables it is found that the values of Δ are much smaller for powdered crystals of the hydrated and the complex salts than for powdered crystals of the same salts in the anhydrous state, and for the latter salts the value of Δ is fairly large. It is evident that the sign of Δ remains unchanged for the same anion, only the absolute value changing with the state of aggregation in which the cation exists. This view is also largely if not invariably supported by a large amount of data collected by different observers for salts of the iron group of ions in the state of hydrated crystals or concentrated aqueous solutions *, in the latter state the magnitude and sign of Δ being of the same order as in hydrated crystal powders. In the acid or alcohol solutions, however, the value of Δ changes as we pass from one temperature range to the other †; for the lower temperature range the values of Δ are small and of the same order of magnitude as for the hydrated salts, whereas for the upper temperature range the Δ-values are considerably greater, always approaching nearly the value for the corresponding anhydrous salt. The magnetic dilution in each of the solutions, however, remains the same throughout.

We shall first give a brief account of the two types of theories mentioned before, and then proceed to criticize them in the light of the above experimental results.

To explain the properties and behaviour of ferromagnetic substances Weiss [1] assumed the existence of a molecular field νM proportional to the intensity of magnetization M. Later he applied the same conception to explain the empirical modification of Curie's Law, $\chi(T-\Delta)=c$, obeyed by paramagnetic solids and solutions. A large

* We exclude from our discussions the results obtained by Fahlenbrach etc. for very dilute solutions which seem difficult of any theoretical interpretation.

† The $NiCl_2$ solution in ethyl alcohol contained a small quantity of water, as hydrated crystals were dissolved, the anhydrous salt being very little soluble in absolute alcohol. Due to the presence of the water molecules the Ni^{++} ions have a tendency to retain their hydrated complex character in the alcohol solution, and as such its magnetic behaviour is not in conformity with the others, and has to be omitted from the present discussions. This emphasizes the necessity of making the alcohol as well as the salt perfectly free from water when one investigates the magnetic behaviour of such solutions, as the presence of a trace of water would profoundly alter the value of Δ.

amount of experimental facts support the idea of the existence of such a molecular field, but on the classical theory there is difficulty in accounting for the presence of such large fields and for such large values of ν. A satisfactory explanation of the origin of molecular field has been given by Heisenberg [2], who has shown that when in a crystal lattice the atoms, with each of which is associated a conducting electron, interact, then by applying the methods of wave-mechanics the total energy of perturbation is given by $J_E + J_0$, where J_E is the statical energy of mutual action of charged particles as calculated according to classical theory, and J_0 is the energy of interchange interaction, which is due to the fact that no electron is permanently attached to any one nucleus, but any two electrons may interchange their positions with regard to the atomic nuclei. To this interchange interaction energy Heisenberg attributes the origin of the molecular field to which ferromagnetism is due, and his theory also shows that the interchange interaction energy (otherwise called exchange force) between paramagnetic ions or atoms have the effect of introducing a constant Δ, as was empirically done by Weiss, and which corresponds to the Curie point for ferromagnetic substances given by

$$T_c = \frac{2J_0}{K(1-\sqrt{1-8/z})}.$$

Van Vleck [3], on the other hand, has laid much stress on the fact that Heisenberg's "exchange forces" play only a minor rôle in giving rise to Δ in paramagnetic salts, where there is considerable magnetic dilution. He has pointed out that the alignment of the spin of a given atom having a non-vanishing spin is not influenced by the interaction with atoms having a closed shell of electrons (in ^1S states). Though the exchange effect does not disappear entirely between a pair of atoms one of which is in a ^1S state, the additive exchange term obtained in this case does not involve the spin and is of no significance for magnetic considerations; according to Van Vleck and his collaborators the major part of Δ in paramagnetic salts of the iron group arises mainly from the distortion effects involving the orbital angular momentum. They have shown that the relation between

χ and T is expressed by a power series development in T^{-1}, viz.,

$$\frac{1}{\chi} = \frac{T}{c} - n + \frac{A}{T} + \frac{B}{T^2} + \cdots$$

The Weiss formula is obtained when the series is broken at the second term, Δ then appearing as the ratio of the coefficient of the second term to that of the first. For substances of sufficient magnetic dilution for interactions not to matter Δ arises from the second term of a T^{-1} series development, when the ground state consists of a number of levels with separation small compared to kT. The investigations of Bethe [4], Kramers [5], Van Vleck and his collaborators have shown that inhomogeneous crystalline fields cause a decomposition of the ground state of the free ion into a number of levels; the magnitude of the separation $h\nu_{sep.}$ may be (i.) small, (ii.) of the same order of magnitude, or (iii.) large compared to kT. For (ii.) the Boltzmann distribution over these levels gives rise to Weiss formula with fairly large Δ value, where Δ is pretty nearly constant over a considerable range of temperature. If $h\nu_{sep.} > kT$ and the lowest state is non-degenerate, the substance shows a constant paramagnetism independent of temperature. If the degeneracy arises from the presence of an odd number of electrons the magnetization obeys a hyperbolic tangent law.

If the fine structure of the ground state arises from the effect of external electric fields on the spin-orbit coupling exact calculations show that for cubic crystals, crystal powders, and solutions Δ must vanish to a first approximation [6]. The considerably large values of Δ in the case of anhydrous crystal powders must then be due to exchange forces, which may be acting either between the paramagnetic ions themselves or between the paramagnetic ions and the immediately surrounding anions. That exchange forces play a part in giving rise to Δ in this class of salts is also evident from the fact that even in the case of Mn^{++} ion [7], which is in the ^6S state (so that orbital moment is zero and no question of distortion of the same comes in), there is a perceptible though comparatively small value of Δ, whose origin can only be attributed to the exchange forces. As we pass on to the hydrated or other complex salts, owing to the interposition of the polarizable H_2O or other dipole molecules,

the distance between the interacting ions increase, and consequently there is a diminution of the exchange forces between them. The small value of Δ in these cases represents the residual effect of the exchange forces. Solutions also should, according to the theory of Van Vleck, and his collaborators, behave like cubic crystals or crystal powders, and the value of Δ should not be appreciably different from zero. The values of Δ given in Table II. show that at the lower temperature ranges they are small and of the same order of magnitude as for the hydrated salts. In an earlier paper, from a study of the absorption and Raman spectra, as well as of the magnetic behaviour of the above solutions, it has been concluded that at the low temperature ranges the paramagnetic carriers are complexes of the ions with the surrounding dipole molecules of water or alcohol, so that their behaviour is similar to that of the hydrated crystal powders of the same salts *. It is quite in conformity with the above view that the Δ values should be of the same order. For the higher range of temperature it is shown in Table II. that the Δ values for the acid and alcohol solutions of $CoCl_2$ and $NiCl_2$ increase in value and approach those for the corresponding anhydrous salts. From evidence given in the previous paper it is concluded that for this range of temperature the salts exist in these solutions as undissociated molecules. The increase in the value of Δ cannot be attributed to the interaction between the paramagnetic ions, since the concentration of the latter remains unchanged. The origin of this large value of Δ must therefore be sought in the interchange interaction effect between the paramagnetic Co or Ni atoms and the Cl atoms with which they form homopolar molecules. As stated before, according to Van Vleck no interchange effect can arise due to interaction between paramagnetic ions and their diamagnetic neighbours (ions or molecules). But the objection does not hold in the case of the undissociated molecules under consideration, whose constituent atoms are held together partly by quantum mechanical forces. The interaction integrals are due to the latter type of forces, which can therefore give rise to large values of Δ if the molecules are paramagnetic. In a recent report, published in the 'Review of Modern

* Our remarks are confined to fairly concentrated solutions, where the paramagnetic salts may not be completely dissociated.

Physics,' on the theory of strong electrolytes Falkenhagen [8] has drawn attention to the necessity of taking into consideration not only electrostatic forces between the ions (*i. e.*, coulomb forces and forces of polarization). but also the quantum mechanical forces and the inter-ionic dispersion forces. The chlorides, with which we are dealing, probably do not belong to the class of strong electrolytes, as most of them can be volatilized, and therefore in them the interaction forces are in still greater evidence.

Moreover, the above objection of Van Vleck may be strictly valid only in the case of ferromagnetic media, since his conclusions are deduced from the fact that the exchange terms in such cases do not involve the spin at all, which alone is of significance in the case of ferromagnetics. But in the case of paramagnetic salts of the type under consideration we have to consider partly the orbital moment in addition to the spin, and the exchange effect, being orbital in nature, may perhaps influence the magnetic moment even if one of the interacting ions contains a closed shell. It is very likely that even in the anhydrous salts, *e. g.*, the paramagnetic chlorides, Δ arises mainly from the exchange forces between the paramagnetic ions and the surrounding anions, and this explains the very remarkable dependence of the sign of Δ on the nature of the anion, whatever may be the state of aggregation in which the cation exists.

Summary.

In the present paper the results of the temperature variation of susceptibility of a number of Co^{++} and Ni^{++} compounds containing the ions in different states of aggregation, viz., as powdered crystals of anhydrous, hydrated, and other complex salts, as well as solutions of their chlorides, in different types of solvent have been recorded, and the causes of the origin of the term Δ have been discussed in relation to the two types of theories developed by Weiss and Heisenberg, and Van Vleck and his collaborators. The results indicate that the values of Δ are much smaller in powdered crystals of the hydrated and other complex salts than for corresponding anhydrous powdered crystals, in the latter case the value of Δ being fairly large. Also the sign of Δ is found

to remain constant for the same anion, only the absolute value changing with the state of aggregation. In the acid and alcohol solutions of the paramagnetic chlorides different values of Δ are obtained for different temperature ranges, the magnetic dilution remaining the same throughout. At the low temperature range the value of Δ is small and comparable to that for hydrated crystal powder, whereas at higher temperature range the Δ values are greater and approach nearly the values for the corresponding anhydrous crystal powder. It is shown that Van Vleck's theory of the origin of Δ due to the distortion of the orbital moment of the paramagnetic ion is not sufficient to explain the above results. From evidence cited in a previous paper it was made probable that for this range of temperature the paramagnetic salts exist as undissociated molecules in the solution, and the large value of Δ observed is to be attributed to some form of interchange interaction effect between the electrons attached to the paramagnetic atom and its halogen neighbours. The large value of Δ in the anhydrous salt is also atributed to the same interchange effect.

In conclusion, the writer desires to express his grateful thanks to Prof. D. M. Bose for his kind interest and helpful suggestions.

References.

(1) P. Weiss, *Journ. de Phys.* vi. p. 667 (1907); i. p. 166 (1930).
(2) W. Heisenberg, *Zeits. f. Phys.* xlix. p. 619 (1928).
(3) J. H. Van Vleck, 'Theory of Electric and Magnetic Susceptibilities,' p. 321 (1932).
(4) H. Bethe, *Ann. der Phys.* iii. p. 133 (1929); *Zeits. f. Phys.* lx. p 218 (1930).
(5) H. A. Kramers, Proc. Amst. Acad. xxxii. p. 1176 (1929); xxxiii. p. 959 (1930).
(6) C. J. Gorter, *Phys. Zeits.* xxxiii. p. 546 (1932).
(7) B. Cabrera and A. Duperier, *Journ. de Phys.* vi. p. 121 (1925).
(8) H. Falkenhagen, Rev. Mod. Phys. iii. p. 412 (1932).

Ghosh Physical Laboratory,
University College of Science,
Calcutta.

XCVIII. *The Behaviour of Electrons in Nitric Oxide.*

By V. A. Bailey, *M.A., D.Phil.* (*Oxon*), *F.Inst.P., Associate Professor of Physics, University of Sydney, and* J. M. Somerville, *Deas Thomson Scholar, University of Sydney* *.

1. *Introduction.*

IT has been shown in recent publications † that the motions of slow electrons in polyatomic gases bear an interesting relation to the corresponding infra-red absorption spectra. The results obtained by Skinker and White ‡ for nitric oxide were not given, as it appeared from their published results that the presence of notable

Fig. 1.

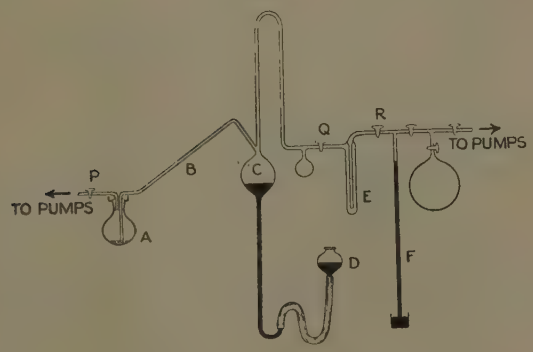

numbers of negative ions had reduced the accuracy of the observations made on electrons whose velocities corresponded to the strongest infra-red absorption band.

In the course of an examination of their data for traces of a relation to this absorption band it was found that the authors had apparently made a clerical error, since the values of W shown in their Table V. are quite different from the values indicated by the curve in their figure 1.

* Communicated by the Authors.

† V. A. Bailey and W. E. Duncanson, Phil. Mag., July 1930, p. 145 ; V. A. Bailey, Phil. Mag., May 1932, p. 993 ; V. A. Bailey and J. B. Rudd, Phil. Mag., December 1932, p. 1033.

‡ M. F. Skinker and J. V. White, Phil. Mag., October 1923, p. 630.

For this reason, and also because it was desirable to obtain more accurate data for the lower velocities, it was decided to investigate nitric oxide by means of the methods developed in Sydney which are specially designed to eliminate any errors due to the presence of negative ions.

2. *Preparation of Pure NO.*

The gas was prepared by allowing a 4 per cent. solution of KNO_2 in concentrated H_2SO_4 to react with mercury *in vacuo*.

Fig. 2.

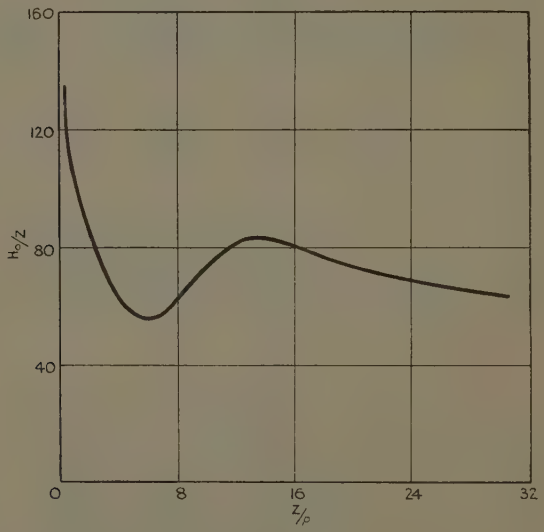

It is necessary frequently to renew the surface of mercury in contact with the solution in order to maintain the interaction, so the apparatus shown in fig. 1 was used.

The vessel A contains the solution, and the vessels C and D contain the mercury, D being left open to the atmosphere. The vessels A and C are pumped out simultaneously through the taps P and Q, until all the air is removed. With the tap Q shut, air is admitted slowly through the tap P until most of the solution is displaced through B into the vessel C, care being taken

that no air gets past the vessel A. The latter is then re-exhausted and the tap P closed. Gas is generated by moving the reservoir D up and down slowly, thus bringing fresh surfaces of mercury into contact with the solution in C.

The gas was then condensed in the trap E by means of liquid air, the tap Q closed, and any uncondensed gas

Fig. 3.

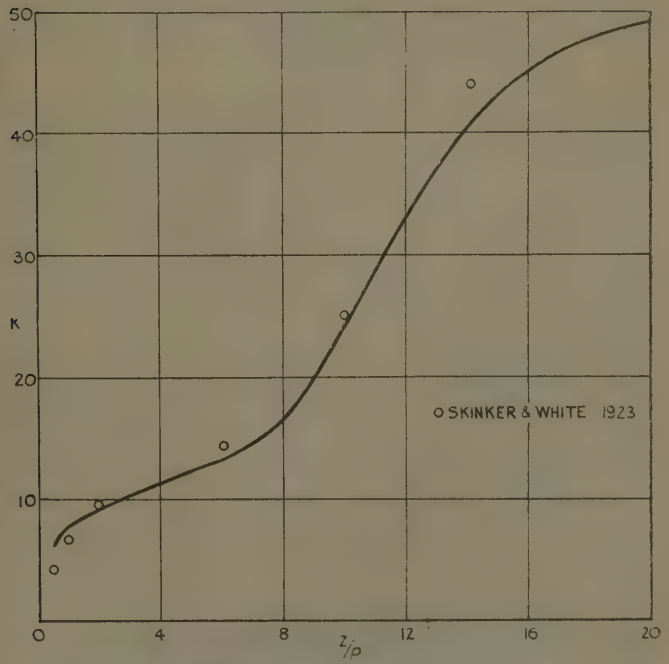

pumped off through R. The vapour pressure of the condensed gas was observed with the mercury column F and found to be about 3·5 mm. The liquid air around E was replaced by a freezing mixture of petrol ether and liquid air, whose temperature was adjusted to be slightly lower than the boiling-point of NO, as observed by means of the gauge F. Some of the gas in E was pumped off and most of the remainder admitted into a gas reservoir containing P_2O_5, and left for use.

Three different samples of the gas were prepared, of which one was subjected to extra fractional distillation. The results obtained with the different samples were found to be in good agreement.

3. *The Observations.*

The principles of the methods of observation used are

Fig. 4.

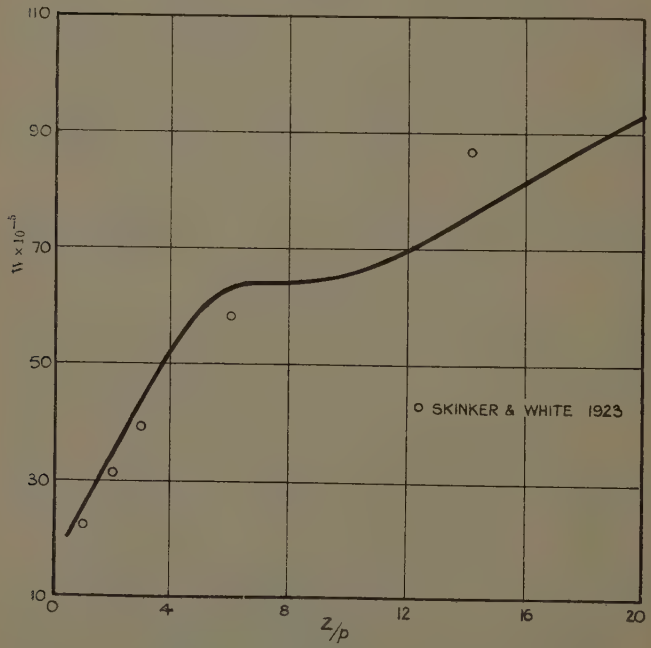

sufficiently described in the publication * on the properties of nitrous oxide, and so need not be given here.

Some modifications of the procedure were also made to suit the special properties of nitric oxide.

Before describing the results obtained it is convenient to tabulate here the symbols used and their definitions :—

* V. A. Bailey and J. B. Rudd, Phil. Mag., December 1932, p. 1033.

p = Pressure of the gas in mm. of Hg.

Z = The electric force in volts/cm.

k = The Townsendian factor, *i. e.*, the factor by which the mean energy of an electron exceeds that of a molecule at 15° C.

W = Drift-velocity of the electrons under the influence of Z.

H_0 = The magnetic force, parallel to Z, which causes the electronic stream to spread exactly like a stream of ions in the same electric field.

Fig. 5.

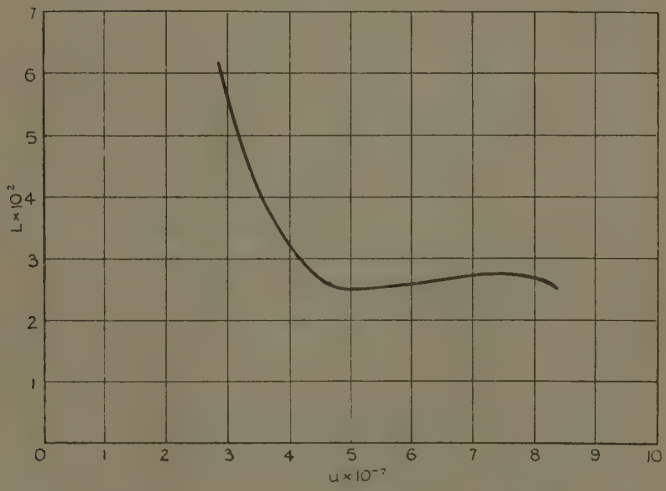

u = The mean velocity of agitation of an electron.

L = Mean free path of an electron at 1 mm. pressure of gas.

λ = Mean proportion of its own energy which an electron loses at a collision with a molecule.

The quantities H_0/Z, k, and W are functions of the ratio Z/p alone, and so may be represented in terms of Z/p by means of curves.

The curves obtained with NO are shown in figs. 2 to 4. In figs. 3 and 4 values obtained by Skinker and White are also shown by means of small circles for comparison.

It will be seen that there is a fair agreement between their results and ours, and it may also be concluded that their clerical error consists in giving the values of W wrongly in their Table V.

Also in agreement with their observations, we found that negative ions were present in larger quantities with the lower values of Z/p than with the higher.

The conditions were such that no very accurate values of h, the probability of attachment, could be obtained, so

Fig. 6.

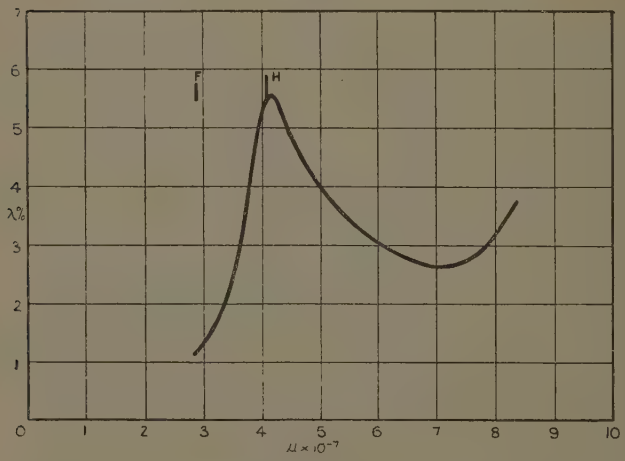

we need only mention that h was found to diminish notably as the velocity u increased.

4. *Discussion.*

The values of the mean free path L and the proportion of energy lost λ, deduced from the curves in figs. 2 and 3, are represented in terms of the velocity u by means of curves in figs. 5 and 6.

It will be seen that the mean free path decreases considerably as the velocity increases from $2{\cdot}8\times10^7$ to 5×10^7 cm./sec. As already mentioned, the probability of attachment h also diminishes as u increases in this range. In these respects therefore NO resembles O_2.

We thus have another example of a generalization published previously *, namely :—

An electron is the more likely to remain attached the further it penetrates into the molecule. This rule is true of all the gases for which the probabilities of attachment have been determined, namely :—O_2, NO, C_2H_4, C_5H_{12}, N_2O, NH_3, H_2O, and HCl.

In the first four gases L and h both diminish on the whole as u increases, but both increase with u in the last four.

The first three gases are paramagnetic † and the remainder are diamagnetic, so it appears that where negative ions are formed the attachment and deflexion of the electrons may be influenced by the magnetic properties of the molecules.

With regard to these points it is proposed in the future to examine by our methods other paramagnetic gases.

In fig. 6 the short vertical lines marked by F and H indicate respectively the values of u corresponding to the fundamental vibration absorption band ‡ $5{\cdot}3\,\mu$ and its harmonic $2{\cdot}6\,\mu$, as determined by Einstein's relation. The fundamental F is known to be much more intense than the harmonic H. Nevertheless, the approximate coincidence of F with the peak of the λ-curve, previously found to occur with polyatomic molecules, is not even approached with the molecule NO. On the contrary it is the much weaker harmonic H which appears to coincide with the peak.

This anomalous behaviour of NO is not altogether surprising if it be noted that this molecule is already regarded as anomalous, on different grounds, by chemists and spectroscopists §.

Summary.

The methods developed in Sydney for the study of the motions of electrons in gases are applied to the gas NO, and information is obtained about the mean free path L,

* V. A. Bailey and W. E. Duncanson, *loc cit.* p. 159.

† The evidence regarding C_2H_4 is conflicting. According to Faraday and Quicke it is paramagnetic and according to Jefimow (*Journ. de Phys.* (2) vii. p. 494) and Bitter (Phys. Rev. (11) xxxiii. p. 389 (1929)) diamagnetic.

‡ The data are those given by Rawlins, Snow, and Rideal in Proc. Roy. Soc. cxxiv. A, p. 453, and cxxvi. A, p. 355 (1929).

§ Jevons, 'Molecular Spectra,' p. 245.

the probability of attachment h, and the proportion λ of its own energy lost by an electron at a collision.

The following conclusions are reached :—

1. A generalization previously published is also true of NO, viz. : an electron is the more likely to remain attached the further it penetrates into the molecule.

2. The magnetic properties of a molecule appear partly to influence the attachment of electrons.

3. The peak of the λ-curve for NO corresponds to the first harmonic vibration absorption band in the infra-red region, instead of corresponding to the fundamental band as with other gases.

XCIX. *Nuclear Changes in the Atoms of Radioactive Substances. By* HAROLD J. WALKE, *B.Sc., Mardon Research Scholar, Washington Singer Laboratories, University College, Exeter* *.

1. *Introduction.*

LANDÉ †, following Heisenberg ‡, has developed a nuclear scheme by means of which he explains many facts about the existence and stability of isotopes, by assuming that the building stones of the nucleus consist of α-particles, zero or one loose proton, and neutrons. He, however, stressed more than Heisenberg, the rôle that the α-particle plays in nuclear structure, and from isotopic considerations, was able to support this model throughout the periodic table.

In this scheme the rules of Harkins concerning the relative abundance of the stable elements and their isotopes read :—Elements with a free proton (odd atomic number) are much rarer, and therefore less stable, than elements without a free proton in their nuclei (even atomic number). Furthermore, if at first only even elements are considered, it is found that isotopes with an even number of nuclear neutrons are much more frequent than those with an odd number of neutrons. In most

* Communicated by Prof. F. H. Newman, D.Sc.

† Landé, Phys. Rev. xliii. p. 620 (1933).

‡ W. Heisenberg, *Zeit. für Physik*, lxxviii. p. 150 (1932).

cases missing isotopes would possess odd neutron arrangements, and further elements with an odd atomic number have no isotopes with an odd number of neutrons. In general therefore we would expect that nuclei with odd neutron arrangements would be unstable, and that in cases where a proton and odd neutron arrangements occur in nuclei these will be very unstable.

Landé only applied this model to the elements of atomic number 1 to 54. It is the purpose of this paper to show that the scheme is applicable to the radioactive elements, and that it describes qualitatively the relative stability of many of the radioactive isotopes.

2. *Radioactive Disintegration.*

In this scheme Landé does not make use of free electrons as nuclear components, and it is not necessary to consider these particles as existing within the nuclei of radioactive substances to discuss disintegration involving β-ray emission, as these electrons may be considered as due to the formation within the negative field of the nucleus of a pair of electrons, as in the Dirac Theory of the Electron, by the materialization of energy in the form of γ radiation (that is, by the materialization of energy released by changes in α-particle states within the nucleus). The positive electron of the pair so formed remains within the nucleus, being in a negative potential field, while the negative electron is expelled and appears as a disintegration electron.

The experiments of Kurie * and considerations of the spins of the lighter nuclei, as discussed by Chadwick † in the Bakerian Lecture for 1933, support the idea that the neutron is the fundamental unit of matter, the proton accordingly being complex and consisting of a neutron and positron in close combination. The recent experiments of Auger ‡ lend additional weight to the hypothesis, for he is able to explain the high energy γ radiation obtained from paraffin bombarded by neutrons, and first noted by Lea §, by assuming that the mass of the neutron is 1·009—1·011 (mean values obtained from all the known cases of transmutation). The proton is thus considered to have

* Kurie, Phys. Rev. xliv. p. 463 (1933).
† Chadwick, Proc. Roy. Soc. A, xiv. p. 1 (1933).
‡ Auger, *Comptes Rendus*, cxcviii. p. 365 (1934).
§ Lea, ' Nature,' cxxxiii. p. 24 (1934).

a mass defect of $2—4\times10^6$ e.v.*, and may release energy of this amount when formed by the union of a positive electron and a neutron.

By using these views of the constitution of the proton and neutron we can extend Landé's theory to the radioactive nuclei. In β-ray disintegrations we assume that, owing to the inability of α-particles to pass through the potential barrier, they emit energy in passing to lower energy states, this energy being internally converted in the potential field within the barrier, and giving rise to a positive electron within the nucleus, as well as the disintegrating β-ray. The positron unites with a neutron and forms a proton within the nucleus where none existed before. In consequence a less stable nucleus is formed, so that we should expect that the nucleus resulting from an initial β-ray disintegration would have a smaller half period than the parent nucleus. This is true throughout all the radioactive series except for the C″ bodies and for the β-ray disintegration of UY, but these are explicable, as will be shown later.

The formation of the proton as a result of the p-ray emission produces excitation energy of the resultant nucleus equal to the mass defect of the proton, viz., $2—4\times10^6$ e.v. If we assume that the excitation energy is in general given to α-particles, which are thereby raised to higher states, then we should naturally expect γ radiation to accompany β-ray emission, though we should not expect γ-ray quanta of energy greater than this amount. It is significant that the highest energy γ-ray quantum emitted by the radioactive elements is $2{\cdot}65\times10^6$ e.v.

As the first β-ray emitting nucleus has generally an even neutron configuration, the product nucleus has a structure containing a proton and an odd number of neutrons. We should expect in these cases that a second β-ray disintegration would follow, as by this means a second proton will be formed within the nucleus, which will unite with two neutrons and the first proton to produce an α-particle, with an even neutron arrangement. The energy set free by such a process will be very great and will leave a highly unstable nucleus. In consequence we should expect the emission of swift α-particles from the products of the second β-ray disintegration, the products

* e.v. indicates electron-volts.

having a comparatively short life. This is shown by the C′ bodies of all the radioactive series, as will be indicated later. With the ejection of this newly formed α-particle a nucleus results in which there is an even number of neutrons. We should therefore expect a comparatively stable nucleus to be produced. This is so with the C→C′→D transformations, as Th D and Ac D are stable, being isotopes of lead, and Ra D has a half period of twenty-five years.

Thus within radioactive nuclei we may have neutrons, a proton, and α-particles, but no free electrons. Disintegration in some cases therefore involves the formation of new units inside the nucleus itself.

In what follows we shall denote α-particles by α, neutrons by n, and protons by p. Where a number precedes α or n it denotes the number of these particles considered to be present in the nucleus.

3. *The Uranium Series.*

Let us first consider the uranium series as far as ionium. The disintegration processes may be indicated schematically thus :—

Element.	Atomic no.	Mass no.	Constitution (following Landé).	Half period.
UI	92	238	$46\alpha+54n$	$4{\cdot}5\times10^9$ yrs.
			↓	
UX_1	90	234	$45\alpha+54n$	24·5 days.
		(99·65 %) β ↙	↘ β(0·35%).	
		UX_2	UZ	

Considering first the more usual disintegration, we have

UX_1	90	234	$45\alpha+54n$	24·5 days.
			↓ β & γ	
UX_2	91	234	$45\alpha+p+53n$	1·14 min.
			↓ β	
UII	92	234	$45\alpha+p+p+52n$	10^6 yrs.
			$45\alpha+\alpha+50n$	
			↓ α	
Io	90	230	$45\alpha+50n$	$7{\cdot}6\times10^4$ yrs.

There are several interesting points in this series which illustrate the general ideas expressed in this application of Landé's scheme. It can be seen that the least stable product UX_2 has a proton in the nucleus and an odd number of neutrons. Both factors, according to the

nuclear scheme adopted, lead to instability. In addition the first β-ray disintegration produces the most unstable product, which disintegrates by a second β-ray emission, as this leads to a return to the even neutron grouping, as shown by U II, which should be, therefore, comparatively stable. The stability of this even neutron grouping is shown by the fact that the formation of the α-particle does not lead to instability as it does with the C′ bodies. This may be because the α-particle so formed can be used to fill in an empty place in some shell system, as we may expect that in the looser structure surrounding the very tightly bound core of α-particles there are α-particle shells as well as neutron shells. Further, as a result of the formation of the proton the uranium X_1 nucleus is excited, and in consequence emits γ radiation.

The second branch product formed from uranium X_1 is uranium Z. This product, of the same constitution as uranium X_2 on this scheme, is also very unstable compared with the other members of the uranium series, and is more unstable than uranium X_1, as is shown by its half period of 6·07 hours. Moreover, this product disintegrates by β-ray emission, supporting the statements already made. It is, however, difficult to understand why the branching occurs, unless two conversions of γ-ray energy are concerned, resulting in the formation of positive electrons of different energy, these forming protons in different neutron shells and producing two products of different stabilities.

4. *The Radium Series.*

The product ionium gives rise to the radium series, successive disintegrations by α-particle emission giving rise to the products radon, radium A, and radium B, in which the neutron arrangement remains the same. It may be significant that each succeeding α-ray product as far as radium A is less and less stable, as shown by the fact that the half period values get smaller and smaller. It is possible that there is some shell system for some of the less tightly bound α-particles, such a shell being emptied by successive transformations, the shell being completely free of α-particles in radium B, which then loses no more α-particles but gives rise to radium C by β-ray emission.

We may represent the series as we did the uranium series as follows :—

Io.....	90	230	$45\alpha+50n$	$7{\cdot}6\times10^4$ yrs.
			$\downarrow\alpha$	
Ra.....	88	226	$44\alpha+50n$	1600 yrs.
			$\downarrow\alpha$	
Radon	86	222	$43\alpha+50n$	3·825 days.
			$\downarrow\alpha$	
RaA.....	84	218	$42\alpha+50n$	3·05 min.
			$\downarrow\alpha$	
RaB.....	82	214	$41\alpha+50n$	26·8 min.
			$\downarrow\beta\ \&\ \gamma$	
RaC	83	214	$41\alpha+p+49n$	19·7 min.

With RaC we get branching of the series, the unstable nucleus resulting from the first β-ray disintegration breaking up in two different ways. It is to be noted that here we have another example of the product resulting from the β-ray disintegration being more unstable than the parent product and accompanying γ-rays due to the excitation of the nucleus in the formation of the proton.

Of the RaC atoms 99·96 per cent. follow the disintegration process we should expect, with the emission of β-rays and returning to the even neutron arrangement. The remaining atoms 0·04 per cent. disintegrate by α-ray emission. The series may be shown as follows :—

RaC	83	214	$41\alpha+p+49n$	19·7 min.
		99·96%	$\downarrow\beta\ \&\ \gamma$ (high energy).	
RaC′	84	214	$41\alpha+p+p+48n$	10^{-6} sec.
			$41\alpha+\alpha+46\,n$	
			$\downarrow\alpha$ (high energy).	
RaD	82	210	$41\alpha+46\,n$	25 years.
			$\downarrow\beta\ \&\ \gamma$	
RaE	83	210	$41\alpha+p+45n$	5·0 days.
			$\downarrow\beta$	
RaF	84	210	$41\alpha+p+p+44n$	136·3 days.
			$41\alpha+\alpha+42n$	
			$\downarrow\alpha$ (high energy).	
RaG	82	206	$41\alpha+42n$	Stable.

The second type of disintegration of RaC is:

RaC	83	214	$41\alpha+p+49n$	19·7 min.
			$\downarrow\beta$	
RaC″	81	210	$40\alpha+p+49n$	1·32 min.
			$\downarrow\beta$	
RaD	82	210	$40\alpha+p+p+48n$	25 years.
			$40\alpha+\alpha+46n$	

This series illustrates very well the points which have been mentioned. It would be expected that the majority

of the RaC atoms would disintegrate by β-ray emission, as is the case. The result of this transformation leads to the production of an α-particle in the nucleus, and the release of energy is so great that the RaC′ nucleus, though forming an even neutron configuration, disintegrates rapidly, producing a swift α-particle, which is probably the particle newly formed. This particle probably crosses the potential barrier and does not leak through it as with the other α-ray transformations. If, moreover, we assume that β-ray disintegration occurs when the α-particles are not able to penetrate the potential barrier producing γ-ray energy which is internally converted in the nucleus, then the fact that a β-ray disintegration occurs following the return to the even neutron arrangement of RaD would seem to support the idea that the α-particle emitted is not already present in the RaB nucleus, but is actually formed in the nucleus of RaC′.

On account of the even neutron arrangement in the nucleus RaC′ should be more stable than RaC″, but the release of energy due to the formation of the α-particle makes the reverse true. The high energy of the α-rays from polonium is probably due to the same cause, as we note with RaE—RaF an α-particle is again formed in the nucleus. It is interesting to note that in considering the disintegration of RaB→RaC no α-particles are emitted in the main disintegration, which cannot be accounted for as formed within the nucleus. This seems to support the idea that a shell of α-particles is completely emptied at RaB. It would thus seem that RaD formed by the disintegration RaC→C″→D should be different from the RaD formed by the more usual transformation RaC→C′→D. Certainly we should expect the nucleus formed to be highly excited as a result of the formation of the α-particle. Perhaps for this 0·03 per cent. of the atoms one α-particle from the completed shell leaks out through barrier, so that when the new α-particle is formed by RaC″→RaD this particle fills the empty place, and the complete shell is again formed. In this disintegration therefore the newly formed α-particle would not be emitted as a swift α-ray, the energy set free by the formation of the particle being partly used up in binding it in the incomplete shell. As exactly similar results are obtained in considering all the series, we conclude that

RaB, RaC, RaD; ThB, ThC, ThD; AcB, AcC, and AcD, with nuclei containing 41 α-particles, represent a system of closed α-particle shells surrounding the tightly bound nuclear core, the α-particle emission from the heavier nuclei being due to the incompleteness of the additional shell formed around this system. The great stability of thorium may mean that within the nucleus of this element an additional shell of four α particles is completed. It is certainly noteworthy that each α-particle emission leaves a more unstable nucleus in all the series, and, further, that the α-particle constitution of the elements above do not alter except in the way that has been accounted for by the formation of a new particle.

5. *The Thorium Series.*

Similar results are to be observed in the thorium series, as follows :—

Th	90	232	$45\alpha+52n$	$1{\cdot}63\times10^{10}$ yrs.
			↓ α	
MsTh I	88	228	$44\alpha+52n$	6·7 yrs.
			↓ β & γ	
MsTh II	89	228	$44\alpha+p+51n$	6·13 hrs.
			↓ β & γ	
RdTh	90	228	$44\alpha+p+p+50n$	6·7 yrs.
			$44\alpha+\alpha+48n$	
			↓ α	
ThX	88	224	$44\alpha+48n$	3·64 days.
			↓ α	
Thoron.....	86	220	$43\alpha+48n$	54·5 secs.
			↓ α	
ThA	84	216	$42\alpha+48n$	0·145 sec.
			↓ α	
ThB	82	212	$41\alpha+48n$	10·6 hrs.

Thorium B gives rise to thorium C by β-ray emission, as in the radium series. There is some difference owing to the β-ray disintegration of mesothorium I. Here, however, we have another example of two succeeding β-ray changes, the product nucleus of the first transformation being much more unstable than the parent nucleus; also γ-rays are omitted in each case as a result of excitation of the product nuclei by the mass defect energy set free in the formation of the new particles. In addition return to the even neutron arrangement results in an increase in stability, as shown by the increased half period of radiothorium. Further, as the resultant nucleus has the same number of α-particles as thorium, it is probable that the α-particle formed fills in and completes

a further shell of α-particles, the greater instability as compared with thorium being due to the additional excitation energy resulting from the formation of the α-particle. The successive α-particle disintegrations, each succeeding product being more unstable than the preceding, the α-particle configuration changing from 45α to 41α, lend support to the idea that with the stable neutron arrangement emission of α-particles occurs until a complete shell is emptied, resulting in a stable α-particle configuration which is the same as that of the lead isotope closing the whole series of disintegration processes.

The remaining nuclear transformations may be represented thus :—

ThB	82	212	$41\alpha+48n$	10·6 hrs.
			$\downarrow \beta \,\&\, \gamma$	
ThC	83	212	$41\alpha+p+47n$	60·5 min.
		65%	$\downarrow \beta$	
ThC′	84	212	$41\alpha+p+p+46n$	10^{-11} sec.
			$41\alpha+\alpha+44n$	
			$\downarrow \alpha$	
ThD	82	208	$41\alpha+44n$	Stable.

and for the second branch:

ThC	83	212	$41\alpha+p+47n$	60·5 min.
		35%	$\downarrow \alpha$	
ThC″	81	208	$40\alpha+p+47n$	3·20 min.
			$\downarrow \beta \,\&\, \gamma$	
			$40\alpha+p+p+46n$	
ThD	82	208	$41\alpha+44n$	Stable.

With this series all the remarks applied to the radium branch transformations can be confirmed. The points to be emphasized are the double β-ray transformations, the production of γ-radiation due to the energy set free in the formation of the proton, and α-particle, the instability of the C′ product resulting in the expulsion of the newly formed particle. The α-ray emission of ThC″ can be explained, as can the non α-ray disintegration of ThD formed by the C—C″—D branch, by considering the α-ray configuration 41α to represent a closed system of shells. The vacant place in the shell caused by the α-ray emission of ThC is filled by the α-particle produced by the β-ray disintegration of ThC″ in the same manner as was indicated with the radium series. However, there is excess energy which is set free in the form of the strong nuclear γ-radiation of ThC′. Again, it is probable that

the newly born α-particle crosses the potential barrier of the ThC′ nucleus.

6. *The Actinium Series.*

The actinium series is perhaps the most interesting, as the separate products are in general less stable than the corresponding radium and thorium products. This, as will be seen, is due to the persistence of an odd number of nuclear neutrons throughout the series. In considering the origin of actinium the following transformations are imagined to occur :—

AcUr.....	92	235	$46\alpha+51n$	..
			$\downarrow \alpha$	
U.Y.....	90	231	$45\alpha+51n$	24·6 hrs.
			$\downarrow \beta$	
Pa	91	231	$45\alpha+p+50n$	$1{\cdot}25\times10^4$ yrs.

In this connexion it is significant that actino-uranium is not found in uranium ores (indicating relative instability) and that uranium Y has such a short half period. Both these elements are therefore comparatively unstable because of the odd neutron configuration, and in consequence a single β-ray disintegration of uranium Y results in the return to the comparatively stable even neutron arrangement of protactinium, as shown by the half period of $1{\cdot}25\times10^4$ years. Consequently this β-ray disintegration is not followed by a second one, the comparatively stable product disintegrating by emitting an α-particle to form actinium. The series may be shown as follows :—

Pa	91	231	$45\alpha+p+50n$	$1{\cdot}25\times10^4$ yrs.
			$\downarrow \alpha$	
Ac	89	227	$44\alpha+p+50n$	13·4 yrs.
			$\downarrow \beta$ & γ	
RdAc	..	..	$44\alpha+p+p+49n$	18·9 days.
			$44\alpha+\alpha+47n$	
			$\downarrow \alpha$	
AcX	88	223	$44\alpha+47n$	11·2 days.
			$\downarrow \alpha$	
Actinon....	86	219	$43\alpha+47n$	3·92 sec.
			$\downarrow \alpha$	
AcA.	84	215	$42\alpha+47n$	$2{\cdot}0\times10^{-3}$ sec.
			$\downarrow \alpha$	
AcB.	82	211	$41\alpha+47n$	36·0 min.

Here we notice the loss in stability after β-ray emission, the γ-rays of radio-actinium being due to the excitation

energy emitted in the disintegration of actinium with the formation of an α-particle. However, as this α-particle is not emitted, there is probably again a filling up of an empty position to form the complete α-particle shell with the 45α configuration. Thus the β-ray disintegration of actinium, while causing the disappearance of the proton and the completion of the α-particle shell, leaves the odd neutron arrangement, which is unstable, as is shown by the shorter decay periods of all the actinium products. However, the series of α-ray disintegrations again seems to confirm the existence of the shell of four α-particles, formed above the 41α stable configuration.

The AcB product disintegrates by β-ray emission as follows :—

AcB	82	211	$41\alpha+47n$	36·0 min.
			$\downarrow\beta$	
AcC	83	211	$41\alpha+p+46n$	2·16 min.
			99·97% $\downarrow\alpha$	
AcC″.....	81	207	$40\alpha+p+46n$	4·76 min.
			$\downarrow\beta$	
AcD	82	207	$40\alpha+p+p+45n$	Stable.
			$41\alpha+43n$	

the second branch being:

AcC	83	211	$41\alpha+p+46n$	2·16
			0·03% $\downarrow\beta$	
AcC′.....	84	211	$41\alpha+p+p+45n$	5×10^{-3} sec.
			$41\alpha+\alpha+43n$	
			$\downarrow\alpha$	
AcD	82	207	$41\alpha+43n$	Stable.

Here we notice that the main disintegration of actinium C is in the form of α-particle emission. This is to be expected on account of the even neutron arrangement which persists with α-particle emission. In the other series the main disintegration is by β-ray emission, as by this means an odd neutron arrangement is transformed into an even configuration. However, the C′ product is again of short life, on account of the formation of the α-particle. With AcC″—AcD the α-particle formed is not emitted, as it completes the stable α-particle shell grouping. The difference in the C C′ C″ change in the actinium series, as well as the comparative instability of the actinium products, are thus readily explained on Landé's structural scheme.

7. *Radioactive Isotopes.*

Several of these facts can be better appreciated by comparing the individual isotopes, as follows :—

Atomic no.	Mass no.	Chemical symbol.	Structure.	Half period.
92	238	UI	$46\alpha+54n$	$4{\cdot}5\times10^{9}$ yrs.
	235	AcU	$46\alpha+51n$	?
	234	UII	$46\alpha+50n$	10^{6} yrs.

As actino-uranium is not found in uranium ores, it seems certain that it is much less stable than the other two uranium isotopes, so that in this group comparative instability is shown by the odd neutron arrangement :—

91	234	UX_2	$45\alpha+p+53n\rightarrow\beta$	1·14 min.
	234	UZ	$45\alpha+p+53n\rightarrow\beta$	6·7 hrs.
	231	Pa	$45\alpha+p+50n\rightarrow\alpha$	$1{\cdot}25\times10^{4}$ yrs.

The greater instability of UX_2 and UZ and the β-ray disintegration of these isotopes is to be expected, as their nuclei contain a proton and an odd number of neutrons. Protactinium, with an even neutron configuration, is stabler and α-particle emission occurs, as by this transformation the resultant nucleus contains an even number of neutrons.

90	234	UX_1	$45\alpha+54n$	24·5 days.
	232	Th	$45\alpha+52n$	$1{\cdot}65\times10^{10}$ yrs.
	231	UY	$45\alpha+51n$	24·6 hours.
	230	Io	$45\alpha+50n$	$7{\cdot}6\times10^{4}$ yrs.
	228	RdTh	$45\alpha+48n$	6·7 yrs.
	227	RdAc	$45\alpha+47n$	18·9 days.

In this range of isotopes the two most unstable nuclei have odd neutron arrangements in their nuclei.

89	228	MsTh2	$44\alpha+p+51n$	6·13 hours.
	227	Ac	$44\alpha+p+50n$	13·4 yrs.

Here we have further evidence of the greater stability of the nuclei with an even number of neutrons.

88	228	MsThI	$44\alpha+52n$	6·7 yrs.
	226	Ra	$44\alpha+50n$	1600 yrs.
	224	ThX	$44\alpha+48n$	3·64 days.
	223	AcX	$44\alpha+47n$	11·2 days.

In this group we have apparently an even neutron grouping which is less stable than the odd arrangement of actinium X.

86	222	Radon	$43\alpha+50n$	3·825 days.
	220	Thoron	$43\alpha+48n$	54·5 sec.
	219	Actinon	$43\alpha+47n$	3·92 sec.
84	218	RaA	$42\alpha+50n$	3·05 min.
	216	ThA	$42\alpha+48n$	0·145 sec.
	215	AcA	$42\alpha+47n$	$2{\cdot}0\times10^{-3}$ sec.
	210	RaF	$42\alpha+42n$	136·3 days.

In these two sets of isotopes we have further examples to show that in general those nuclei with an odd neutron configuration are less stable than those in which the number of neutrons is even. The C, C′, and C″ products will be considered separately, as they show several interesting points.

82	214	RaB	$41\alpha+50n$	26·8 min.
	212	ThB	$41\alpha+48n$	10·6 hrs.
	211	AcB	$41\alpha+47n$	36·0 min.
	210	RaD	$41\alpha+46n$	25 yrs.

The isotope in the nucleus of which there is an odd number of neutrons in this grouping is very unstable, but RaB is apparently less stable. It is possible, however, as the periods of decay are not very different, that this difference is due to some experimental error.

In the case of the C bodies it is interesting to note that with RaC and ThC the majority of the atoms disintegrate by β-ray emission, whereas with AcC the main transformation results in the expulsion of an α-particle. The nuclei are thought of as :

83	214	RaC	$41\alpha+p+49n$	$\rightarrow\beta$ 99·96%	$\rightarrow\alpha$ 0·04%
	212	ThC	$41\alpha+p+47n$	$\rightarrow\beta$ 68%	$\rightarrow\alpha$ 35%
	211	AcC	$41\alpha+p+46n$	$\rightarrow\beta$ 0·03%	$\rightarrow\alpha$ 99·97%

It is significant that the first two nuclei contain an odd number of neutrons and that by the main disintegration the resultant nuclei contain an even neutron arrangement. In the case of AcC with an even number of nuclear neutrons the β-ray product contains an odd number of neutrons, whereas with α-ray disintegration the even neutron arrangement persists. The difference in the branching of the actinium series is thus to be attributed to the different neutron configuration of AcC.

The great instability of the C′ products, as has already been mentioned, is thought of as due to the formation of an α-particle within their nuclei by the second β-ray transformations.

Finally, it is to be noted that in the case of the C″ products AcC″ has an even number of neutrons, and with this group of isotopes of atomic number 81 that of actinium C″ is more stable than the radium and thorium bodies. As can be seen the actinium products with the odd neutron configurations persisting throughout the series are, in general, less stable than the radium and thorium products which possess an even number of nuclear neutrons. With the change to even neutron arrangement the actinium product becomes the more stable as shown :

81	210	RaC″	$40\alpha+p+49n$	1·32 min.
	208	ThC″	$40\alpha+p+47n$	3·20 min.
	207	AcC″	$40\alpha+p+46n$	4·76 min.

It can thus be seen that the Landé nuclear scheme, together with the ideas formulated respecting the formation of nuclear particles and of possible α-particle shells, can be applied with some success to the radioactive atoms, and although certain points are not quite clear, it would appear that the neutron constitution of such nuclei is an important factor in determining their relative stability. The determination of the exact arrangement of α-particle and neutron shells within these nuclei would probably bring to light important information regarding the cause of the instability of the atoms concerned.

This work was carried out under the direction of Professor Newman.

C. *Notices respecting New Books.*

The Principles of Geometry.—Vol. V. *Theory of Curves.* By Professor H. F. Baker, F.R.S. [Pp. 247.] (Cambridge : University Press. Price 15*s.*)

The mathematical world, and in particular the section of Geometry, owes a deep debt of gratitude to Professor H. F. Baker for his extended set of treatises on the Principles of Geometry.

The subject-matter is vast, and the methods of attack include those of Algebra, Pure Synthetic Geometry, Invariants, and Abelian Integrals. The great contributors extending over nearly a century and a half have belonged to diverse nationalities and have used many tongues. The results of their researches lie hidden in multifarious learned journals. The result is that the mathematician with general interests or with specialized interests other than those of geometry, finds it all but impossible to obtain a bird's-eye view of the territory conquered during this long period by the pure geometer. The feeling that these properties should be made more generally known is evidenced by the fact that not only has Professor Baker attempted to meet the general need, but Professor Julian Lowell Coolidge, of Harvard University, issued in 1931 a treatise on Algebraic Plane Curves dealing with the same field in a much more circumscribed compass. It still remains for someone to deal with the same subject-matter from the standpoint of its historical development, and to present the lives, work, and careers of the great contributors, together with the age and historical setting under which their work was produced.

The present issue is the fifth volume of Professor Baker's great work. In Vol. I. he deals with "Foundations," in Vol. II. with "Plane Geometry," in Vol. III. with "Solid Geometry," in Vol. IV. with "Higher Geometry." The volume under review treats of the "Theory of Curves." There is the promise of one further volume at least.

Vol. V. contains eight chapters dealing respectively with :—

Chap. I. "Introductory Account of Rational and Elliptic Curves."

„ II. "The Elimination of the Multiple Points of a Plane Curve."

„ III. "The Branches of an Algebraic Curve; the Order of a Rational Function; Abel's Theorem."

„ IV. "The Genus of a Curve. Fundamentals of the Theory of Linear Series."

„ V. "The Periods of Algebraic Integrals. Loops in a Plane Riemann Surface."

„ VI. "The Various Kinds of Algebraic Integrals. Relations among Periods."

„ VII. "The Modular Expression of Rational Functions and Integrals."

„ VIII. "Enumerative Properties of Curves."

It is needless to say that throughout the treatment of the above subject-matter Professor Baker's wide and profound knowledge is conspicuous on every page. The subjects dealt with are in essence frequently difficult and abstract, but throughout the book concrete examples are introduced and worked out so as to clarify the mind and bring the particular general property under discussion down to earth.

In general terms, one may say that the subject-matter of the book is the geometrical development of Abel's Theorem and the exposition of those geometrical properties that proceed directly therefrom. Geometrical results that depend on the properties of the Theta Functions—such as the properties of Contact Curves—are not dealt with in any detail, though they are mentioned. A concise account, from the very beginnings, is given of the Abelian Integrals and their periods. This opens up a vast geometrical field. Linear series of curves and the sets of points they cut out on a given curve receive detailed treatment; the Riemann-Roch theorem is deduced and its consequences developed in great detail. The treatment embraces curves in higher space as well as those in a plane. The reduction of multiple points and kindred matters receives a very thorough algebraic discussion.

There are very approximately 250 pages in the book, all filled with concise material. No more can be done therefore than to give the above general idea of the contents. It remains only to add that the general viewpoint governing the selection of the subject-matter as a whole is of the utmost importance and could hardly be improved upon. The exposition is excellent, and Professor Baker's reputation is a sufficient guarantee for the quality of the book as a contribution to geometrical theory.

1. *Données numériques de Spectroscopie.* Rédigées par P. Auger, L. Brunninghaus, V. Henri, et F. Wolfers. Extraits des Volumes VIII. (Années 1927–1928) et IX. (Année 1929). Gauthier Villars et Cie (Paris); Dépositaire pour les Etats Unis et le Canada; McGraw Hill Book Co. Inc. (New York), 1932.

These tremendous volumes of about 1500 pages make a most formidable book when bound in one cover and represent a very great deal of painstaking work of abstraction.

The constants and numerical data collected refer to spectroscopy and are collected under four main headings: (1) Emission spectra; (2) Absorption spectra; (3) Electro-magneto optics; (4) Scattering of light.

II. *Données numériques de physique du globe.* Par Ch. Mauriam, C. E. Brazier, L. Eble, H. Labrouste, Ed. Salles. Extrait du Volume VIII. (Années 1927–1928).

Numerical constants and data having reference to Geophysics, under which general heading the following sub-headings are comprised :—

1. Figure of the earth, density, &c. ;
2. Seismology ;
3. Terrestrial magnetism and earth currents ;
4. Atmospheric electricity ;
5. Polar lights ;
6. Radioactivity ;
7. Radiations, solar, atmospheric and terrestrial ;
8. Meteorology ;

and about three hundred pages of abstracts on these topics.

III. *Données numériques d'électricité, magnétisme et électrochimie.* Rédigées par P. Auger, L. Durand, G. Foex, L. Néel, N. Marinesco, A. Schnorf, N. Thon, F. Wolfers. Extraits des Volumes VIII. (Années 1927–1928) et IX. (Année 1929).

The numerical data and constants under the headings of these two volumes include under electricty such matters as piezo-electrictiy, thermo electricity, the Volta effect; metallic conductivity, electro-technics, dielectric constants. There is a full section on magnetism and one on ionization of gases. The section of electrochemistry deals in the main with conductivity of electrolytes.

The two volumes are bound in one and run to over 220 pages.

The three volumes noticed above are further instalments of the well-known and much appreciated annual tables of constants and numerical data—chemical, physical, biological, and technological. Printed in English and French, in parallel columns where necessary, they have an international appeal and utility which cannot be denied.

They are, as usual, excellently produced, printed and bound, while the high standing of the individual abstractors gives a feeling of confidence and security in the accuracy and value of the abstracts.

The difficulties of condensing the matter contained in the various papers have been admirably surmounted, but the present writer feels that even the briefest reference to publications by authors in the lesser known journals would really enhance the present high value of these publications.

[*The Editors do not hold themselves responsible for the views expressed by their correspondents.*]

FIG. 2.

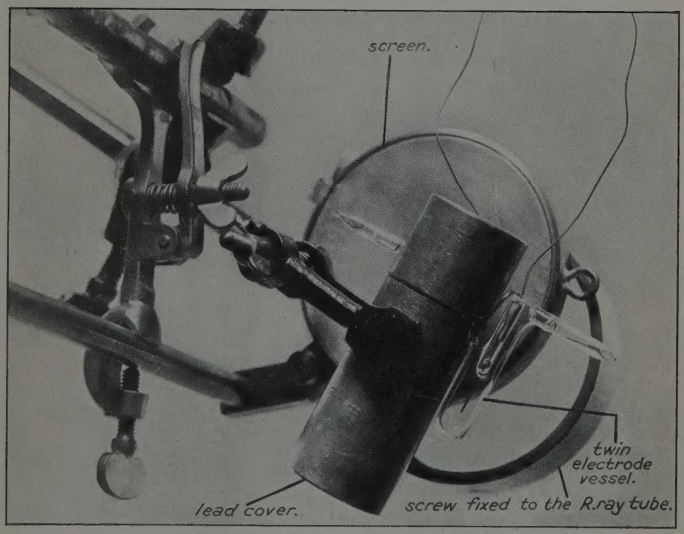
screen.
twin electrode vessel.
lead cover.
screw fixed to the R.ray tube.

FIG. 3.

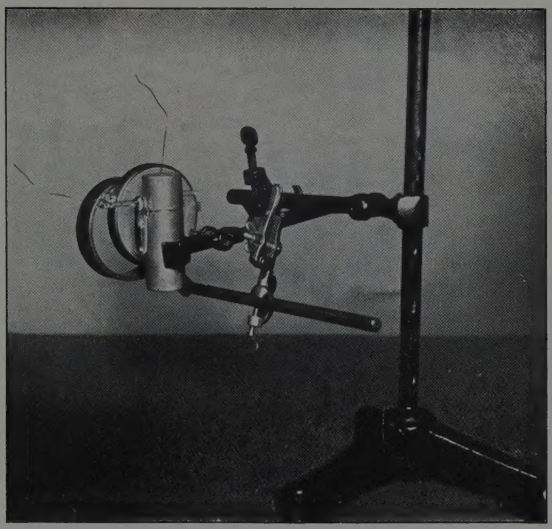

FIG. 4.